Intestinal Barrier Function in Response to *Cryptosporidium parvum*, Inflammation, and Hyperglycemia: Intestinal Organoids as a Model System

By

Charles Kikutaro Crawford

DISSERTATION

Submitted in partial satisfaction of the requirements for the degree of

DOCTOR OF PHILOSOPHY

in

Molecular, Cellular, and Integrative Physiology

in the

OFFICE OF GRADUATE STUDIES

of the

UNIVERSITY OF CALIFORNIA, DAVIS

Approved:

_____

Amir Kol, DVM, Ph.D., Chair

_____

Helen E. Raybould, Ph.D.

_____

Jeroen P. Saeij, Ph.D.

Committee in Charge

2023

Dedication

To my Mima, **Emiko Sato Coffey**. I could never have done this without you. I love you forever.

Acknowledgments

I thank **my wife**, Taylor Scartozzi for being my loving partner in all endeavors.

I thank **my son**, Percy Crawford Scartozzi for being the light of my life.

I thank **pets**, Loki and Bruce Banner, for sparking joy in my life every day.

I thank **my Principal Investigator and mentor**, Amir Kol, for your patience, guidance, and genuine care for my growth and well-being.

I thank **my family**, Mimi Coffey Sr., David Crawford, Spartacus Crawford, Spencer Crawford, Mimi Ann Coffey, Mitchell Crawford, Julie Crawford, Tony Mancil, Melvin Pete Crawford, Dorothy Crawford, Joseph Coffey, Emiko K. Coffey, Miyako Coffey, and Lisha Coffey, for your unending support and love.

I thank **my best friend**, Tyler Finzel, for always being there for me, near or far.

I thank **my friends made in Davis**, Megan Hyler, Forrest Hyler, Dee Shorty, Robert Duffy, Ian Salveson, Dana Hartman, Linnea Dolph, and Jake Dalton, for bringing fun, warmth, and sincerity to my time in Davis.

I thank **my Dissertation Committee members**, Helen Raybould and Jeroen Saeij for your essential advice and perspective.

I thank **my lab mates**, Veronica Lopez Cervantes, María Questa, Diego Castillo, Aeelin Beltran, Mary Quilici, Maryam Moshref, Patrawin Wanakumjorn, Mimo Uehara, Leon Huynh, Muhammad Matloob, Yihong Chen, Benjamin Goodwin, and Akshita Kaparaboyna for your immense scientific and personal support.

I thank **my teaching mentors**, Arik Davidyan and Lauren Liets for helping me to cultivate my passion for teaching.

Abstract

The intestinal barrier separates the gut lumen from the internal tissues of the body. It is comprised of a layer of mucus, a monolayer of intestinal epithelial cells adjoined and maintained by junctional protein complexes, and a lamina propria which contains specialized immune cells. This barrier is responsible for the absorption of nutrients, preventing the entry of harmful pathogens and substances, and is a critical component of the innate immune system. This dissertation presents a comprehensive review of the role of the intestinal barrier and innate immune response to the apicomplexan parasite, *Cryptosporidium parvum*, and the use of intestinal organoids as a model of study (Chapter 1) and the effects of both inflammation and Diabetes mellitus on the function of the intestinal epithelium (Chapter 2). It shows that inflammatory cytokines directly increase the permeability of the bovine intestinal epithelium while altering tight junction morphology and reducing cellular turnover, using bovine intestinal organoids as a model (Chapter 3). Finally, this work uses feline intestinal organoids to show that hyperglycemia-like conditions directly increase the permeability of feline intestinal epithelium while altering tight junctional morphology, as mediated through the activation of protein kinase C-α (PKCα); the drug fenofibrate prevents hyperglycemia-induced barrier dysfunction and restores PKCα activity to baseline levels (Chapter 4).

Table of Contents

Chapter 1: The Mucosal Innate Immune Response to *Cryptosporidium parvum*, a Global One Health Issue

Charles K. Crawford, Amir Kol

Abstract

Cryptosporidium parvum is an apicomplexan parasite that infects the intestinal epithelium of humans and livestock animals worldwide. Cryptosporidiosis is a leading cause of diarrheal-related deaths in young children and a major cause of economic loss in cattle operations. The disease is especially dangerous to infants and immunocompromised individuals, for which there is no effective treatment or vaccination. As human-to-human, animal-to-animal and animal-to-human transmission play a role in cryptosporidiosis disease ecology, a holistic ‘One Health’ approach is required for disease control. Upon infection, the host's innate immune response restricts parasite growth and initiates the adaptive immune response, which is necessary for parasite clearance and recovery. The innate immune response involves a complex communicative interplay between epithelial and specialized innate immune cells. Traditional models have been used to study innate immune responses to *C. parvum* but cannot fully recapitulate natural host-pathogen interactions. Recent shifts to human and bovine organoid cultures are enabling deeper understanding of host-specific innate immunity response to infection. This review examines recent advances and highlights research gaps in our understanding of the host-specific innate immune response to *C. parvum*. Furthermore, we discuss evolving research models used in the field and potential developments on the horizon.

Introduction

Cryptosporidium parvum is an apicomplexan parasite that causes potentially life-threatening infectious diarrhea in infants and neonate calves with no available FDA-approved vaccine [1, 2]. Nitazoxanide is approved for use in adult, immunocompetent patients, but is not effective or approved for use in the most vulnerable populations: infants and immunocompromised patients [2]. Infected hosts (humans and cows) shed billions of highly infectious and environmentally stable parasites [3, 4]. The parasite is transmitted zoonotically and between humans worldwide [5-7], and it contaminates drinking water sources [8], recreational swimming sites [9], soils [10], and aquaculture environments [11]. Wildlife is further impacted by cryptosporidiosis [12]. As such, a comprehensive and interdisciplinary research approach is required to eliminate this significant source of global disease burden. Cryptosporidiosis is one of three etiologies responsible for the most global diarrheal deaths in children younger than five years of age [13-17]. In the U.S. *C. parvum* caused the largest waterborne pathogen outbreak in American history [18], and 444 outbreaks of cryptosporidiosis were reported from 2009-2017, leading to an estimated 750,000 individual cases per year [19, 20]. *Cryptosporidium* has even been included as a relevant biological threat agent by the CDC [21].

While the role of $CD4^+$ T cells in clearing infection is well studied, the role of the innate immune response within the parasite's natural hosts (i.e. human and cattle) is not fully understood. We will succinctly review current advances in our understanding of the mucosal innate immune response to *C. parvum*, and innovative models that have the

potential to elucidate such responses within clinically relevant hosts. We will highlight key knowledge gaps and future research opportunities.

Innate Immune Response

The intestinal innate immune system, comprised of the gut epithelium and specialized innate immune cells, is the first line of defense against *C. parvum* infection. Innate immunity restricts the expansion and growth of the parasite and initiates the adaptive response. Understanding the innate immune response to *C. parvum* infection in its native hosts is critical in building a 'One Health' strategy to limit *Cryptosporidium's* devastating impact on global health, agriculture, and the environment [12, 22, 23].

Intestinal Epithelial Cells that line the gut epithelium create a physical barrier between luminal content and internal tissues. Because *C. parvum* infects intestinal epithelial cells and does not invade deeper tissues, the epithelium is particularly important regarding the immune response to *C. parvum*.

Primary bovine intestinal epithelial cell infection by *C. parvum* leads to activation of the inflammatory transcription factor NF-κB; this increases expression of the long noncoding RNA NR_045064 [24] and induces the transcription of numerous inflammatory mediators, primarily CXCL8 (aka IL-8) and TNFα, a response primarily mediated by Toll-like receptor-2 (TLR2) and TLR4 [25]. *C. parvum* infection induces an increase in TLR4 expression, regulated by suppression of the noncoding miRNA, *let-7i* [26]. TLR2 and TLR4 activation by *C. parvum* and subsequent NF-κB nuclear translocation induces the release of antimicrobial peptides LL-37 and β-defensin-2 [27]. Despite this, TLR2 and TLR4 deficiency did not increase parasite load in neonatal mice;

however, direct comparisons are difficult given the different models and experimental designs [28].

Evidence suggests that intracellular recognition of *C. parvum* via NOD-like receptors (NLR) and subsequent activation of the inflammasome complex is an important innate response to infection. IL-18, a product of the inflammasome complex, is elevated in human epithelial cell lines following *C.* parvum infection [29]; moreover, IL-18 knockout and inflammasome components caspase-1 or ASC knockout mice are more susceptible to *Cryptosporidium* infection than control mice [30-32]. IL-1β, the second key product of inflammasome activation, was not increased post-infection, nor was there an effect on infection susceptibility in IL-1β knockout mice [31]. The latter findings are corroborated by the fact that parasite shedding was strongly increased in mice lacking NLRP6, which induces IL-18 secretion, but not in mice lacking other inflammasome-forming NLRs including NLRP3, NLRP1b, Aim2, and NLRc4 that primarily induce IL-1β secretion [32].

Antimicrobial peptides include small positively charged polypeptides that elicit antimicrobial effects against a variety of pathogens including bacteria, fungi, viruses, and protozoan parasites [33]. Phospholipases [34] and the antimicrobial peptides β-defensin-1, β-defensin-2, and LL-37 can kill *C. parvum* [35]. Part of the TLR signal response by epithelial cells includes the release of LL-37 and β-defensin-2, and these antimicrobial peptides bind to free *C. parvum* to directly enact their effects [27]. LL-37 and α-defensin-2 are increased in response to the rise in the inflammasome product, IL-18, in human cell lines [29]. However, *C. parvum* influences epithelial cells by inhibiting

the production of other antimicrobial peptides including β-defensin-1 by an undiscovered mechanism [36], and CCL20 by a *C. parvum*-induced rise in miR21 [37].

C. parvum infection is restricted to a parasitophorous vacuole on the apical side of the intestinal epithelium, therefore chemokine and cytokine release from infected epithelial cells is critical in the recruitment of specialized immune cells that facilitate parasite clearance [38]. Activation of TLRs by *C. parvum* induces the NF-κB signaling pathway causing the basolateral release of Growth Regulated Oncogene-α (GRO-α) [25] and CXCL8, which are key neutrophil chemoattractant molecules [39]. Additionally, in the neonatal mouse model, several chemokines including CCL2, CCL5, CXCL10, and CXCL9 are released, which recruit various immune cells to the infection site [40-42]. Chemokine-induced immune cell recruitment is critical in the response to *C. parvum*, as evidenced by the increased susceptibility to infection of mice deficient in chemokine receptors, even in spite of redundancy in immune cell recruitment processes [42, 43].

Another defense against intracellular pathogens is apoptosis of the host cell, and infection by *C. parvum* initiates apoptosis of infected and surrounding epithelial cells through Fas and Fas-L interactions [44]. However, within hours post-infection, *C. parvum* in one life stage, the trophozoite, inhibits apoptosis, likely to facilitate growth within the host cell, by inducing the production of anti-apoptotic factors BCL-2 [45], survivin [46], and osteoprotegerin [47, 48]. Later in infection, in a different part of the *C. parvum* life cycle known as the sporozoite and merozoite life stages, inhibition is removed and apoptosis of the host cell is promoted [45, 46].

Interferons (IFNs) are an essential component to the host response to *C. parvum*. The importance of IFN-γ is shown by an increased susceptibility to *C. parvum*

infection in IFN-γ$^{-/-}$ mice [41, 49] and wild-type neonate mice treated with anti-IFN-γ-antibodies [50]. Adult mice with a disrupted IFN-γ gene shed more parasites, experience extensive damage to the intestinal mucosa, and die within weeks of infection [51]. Severe combined immunodeficiency (SCID) mice, which are deficient in T and B cells, experience reduced *C. parvum* infection compared to SCID IFN-γ$^{-/-}$ mice, showing that protective IFN-γ during *C. parvum* infection is derived, at least in part, from non-T or B cells [52]. In addition to increased IFN-γ, *in vivo* piglet infection and *in vitro* experiments show that intestinal epithelial cells secrete abundant IFN-λ3 (a type-III IFN) independently of specialized immune cells [53]. Historically, type III IFNs have been associated with local epithelial defense from viruses [54]. More recently, IFN-λ was shown to mediate the gut epithelium defense against non-viral pathogens via TLRs [55]. Neutralization of IFN-λ3 leads to increased villus blunting and fecal shedding of infective *C. parvum* in neonate mice, and when intestinal epithelial cells are primed with recombinant IFN-λ3 they show reduced barrier disruption and increased cellular defense against *C. parvum* [53].

Specialized Immune Cells

Natural killer (NK) cells contribute to the innate immune response to *C. parvum* through IFN-γ production and cytolysis of infected epithelial cells. *In vivo*, treating immunocompetent or immunodeficient mice with the NK cell activator, IL-12, leads to a protective effect against *C. parvum* associated with a concomitant rise in intestinal IFN-γ [56]; *in vitro*, human NK cells lyse infected intestinal epithelial cells in response to IL-15 and presentation of MHC class I-related protein A and B [57]. Mice lacking NK cells experience increased severity of infection and excrete more oocysts compared to mice

with NK cells, but when treated with anti-IFN-γ antibodies the infection of NK positive mice was heavily exacerbated, thus implying a protective role of NK cells that is connected to IFN-γ [58]. Despite the increased morbidity in mice without NK cells, they produced IFN-γ after infection, meaning that NK cells are one, but not the only source of IFN-γ in response to *C. parvum*. The number of NK cells localized in the gut is increased within days following *C. parvum* exposure in lambs [59]. Activation of the NK cell receptor, NKG2D, is involved in NK cell-mediated protection, via its ligand, MICA, which is upregulated in the intestinal epithelium of infected humans [57]. The role that other innate-like lymphocytes play during *C. parvum* infection is poorly understood and future investigations are warranted.

Dendritic cells (DCs) exposed to *C. parvum* secrete numerous cytokines including IL-6, IL-1β, IL-12, IL-18, TNFα, and type I interferons via TLR4 receptor activation [60-62]. DCs also capture *C. parvum* antigens in the gut mucosa and migrate to draining lymph nodes where they present these antigens and facilitate the adaptive immune response [40, 62]. DCs may acquire such antigens by directly capturing luminal organisms or phagocytizing apoptotic infected epithelial cells [63]. Macrophages may further engulf free *C. parvum* and transfer the parasite to DCs for migration [64]. One hypothesis for the increased infection susceptibility of neonatal mice compared to adults is that neonates have fewer intestinal DCs, and injecting neonates with Flt3L – which induces DC differentiation from progenitor cells – increases the number of DCs as well as resistance to infection [42]. Furthermore, adult mice devoid of DCs are more susceptible to infection and excrete more parasites, and adoptive transfer of DCs pre-exposed to *C. parvum* reduces the parasite load [65].

Macrophages develop from the same bone marrow precursor cells as DCs and are found in most organ systems and epithelial barriers, including the gut [66, 67]. Following *C. parvum* infection in neonatal mice, macrophages accumulate in the lamina propria [68] and are associated with intact and digested parasites in Payer's patches in guinea pigs [64]. Macrophages' contribution to *C. parvum* clearance appears to be primarily as a secondary source of IFN-γ. Infected $Rag2^{-/-}\gamma_c^{-/-}$ mice, which lack T and B lymphocytes and NK cells, still produce IFN-γ, suggesting an IFN-γ source alternative to T cells and NK cells [58]. When treated with clodronate-liposomes to deplete macrophages, the mice were less resistant to *C. parvum* and could not produce IFN-γ [58]. IFN-γ production by macrophages is promoted by IL-18 when $Rag2^{-/-}\gamma_c^{-/-}$ mice are infected by *C. parvum* [69], and IFN-$\gamma^{-/-}$ mice have fewer macrophages and T cells recruited to the gut accompanying an inability to recover from infection [41].

Neutrophils infiltrate the intestinal mucosa during *C. parvum* infection [70], and preventing mucosal recruitment of neutrophils increases *C. parvum*-related barrier dysfunction as measured by transepithelial electrical resistance [71]. Inhibiting neutrophil recruitment does not influence mortality or infection severity, nor does it affect *C. parvum*-mediated villous atrophy and diarrhea [71]. With no influence on mortality or infection severity, it does not appear that neutrophils are directly protective in the context of *C. parvum.*

As research models advance, the multi-dimensional innate immune response grows more complex but better understood (Fig. 1). However, questions regarding the relevancy of these data to the natural hosts of *C. parvum* remain, provided the use of models that do not fully recapitulate the environment of human or ruminant intestines.

New biotechnological advances, such as the development of bovine and human organoids, may provide the models necessary to confirm what is currently inferred about the innate immune response to *C. parvum* in these hosts.

Cryptosporidium Research Models

The potential to fully understand *C. parvum*'s pathogenesis and develop therapeutics is dependent on the models used to research the host-pathogen interactions it induces within its natural and clinically relevant hosts (i.e. human and cattle). Traditional *in vitro C. parvum* infection models can only be maintained for several days at a time and do not fully recapitulate native intestinal tissue, and *In vivo* mouse models are sub-optimal, as mice are not a natural host of *C. parvum*. Innovative models and advancing technologies are necessary to advance this field.

***In vivo* Models:** *In vivo* animal models are foundational to host-pathogen interaction research, but the nature of *C. parvum* complicates the application of traditional animal models. The natural and clinically relevant hosts for *C. parvum* are humans and ruminants; mice can sustain *C. parvum* infection but only when severely immunocompromised [72-74]. Given that humans and ruminants are the primary natural hosts, calves, lambs, and non-human primates have been used to investigate cryptosporidiosis in naturally infected species [75]. However, housing and maintaining large animal species requires significant funds and specialized facilities, equipment, and training. Moreover, many of the genetic and molecular research tools that are available for mice models are not available for large animal models such as cows or sheep.

Adult mice, a preferred animal model in terms of costs and availably of reagents, are resistant to *C. parvum* but are susceptible to infection by the related species, *C. muris*; however, *C. muris* differs from *C. parvum* in phylogeny, biochemical nature of infection, and infection site (*C. muris* infects the stomach mucosa) [76]. Mice can become susceptible to *C. parvum* through chemical or genetic immunosuppression, such as the previously discussed SCID [73], IFN-$\gamma^{-/-}$ [72], and Rag2$^{-/-}$ mice, which, in addition to neonate mice, have provided established murine platforms for *C. parvum* research [74]. Unfortunately, mouse models have limited translatability for natural hosts such as humans and cattle. This has been elucidated through bovine-specific responses to *C. parvum* that are absent in mice, such as differences in NK cell receptor activation [77], recruitment of γδ T cells [78], and developed resistance in adulthood [76]. More recently, *C. tyzzeri* was identified as a natural mouse pathogen that mirrors aspects of *C. parvum's* pathogenesis and host response in mice [76].

***In vitro* Models:** The allure of primary intestinal epithelium cells lies in the morphological and species-specific accuracy compared to immortalized cell lines. Primary human [79] and bovine intestinal epithelial cells have been successfully infected with *C. parvum* [80]. Unfortunately, primary intestinal cells have limitations involving their availability, obsoletion, and difficulty in long-term propagation [81].

Most *in vitro* models for *C. parvum* host-pathogen interaction research include cancer-derived transformed or immortalized human cell lines including HCT-8, Caco-2, and HT29 cells, which are all derived from colorectal adenocarcinomas [82]. Other non-colorectal cancer cell lines have also been used: RL95-2 (human endometrial carcinoma) [83], Madin-Darby bovine kidney cells [84], MRC-5 (lung fibroblast) [85],

FHs 74 Int cells (non-cancer, immortalized human small intestinal epithelium) [81], and BS-C-1 (African green monkey kidney) cells [86]. None of these lines maintained infection longer than six days except for HT29 cells, which could maintain infection for thirteen days but only for the asexual life stages of *C. parvum*. One non-intestinal cell line, COLO-680N, is human esophageal squamous carcinoma-derived and can propagate infective parasites continually for eight weeks, but applications to host-pathogen interaction are questionable given that the esophagus is not the natural niche for *C. parvum* [87].

Early attempts to utilize three-dimensional structures for *C. parvum* research involved low-shear microgravity cultures where HCT-8 cells seeded onto submucosa grafts formed structures that maintained *C. parvum* infection; however, parasites decreased after 48 hours [88]. Later, a hollow fiber bioreactor system was used to infect three-dimensional HCT-8 cell structures for over six months, which is far longer than two-dimensional HCT-8 infection, while producing significantly more oocysts/day/mL [89]. Silk fiber scaffolding has also been utilized to induce three-dimensional culture of Caco-2 and HT29 cells, maintaining infection for two weeks [90].

While these cell lines are useful tools, they are susceptible to genetic variation, most cannot maintain all phases of the *C. parvum* life cycle, and most cannot maintain and propagate *C. parvum* infection for extended periods of time [91]. This, in addition to the fact that these cell lines do not recapitulate the native intestinal epithelial tissue of *C. parvum* hosts, encourages the search for increasingly accurate models of study.

Enteroids: Intestinal organoids (aka enteroids) circumvent shortcomings exhibited by cell lines and primary epithelial cells while also introducing a three-

dimensional culture model. Enteroids are composed of a polarized single layer of epithelium with crypt and villus domains containing the various intestinal epithelial cells such as stem cells, enterocytes, enteroendocrine cells, goblet cells, etc., thus recapitulating the microanatomy and functionality of native intestinal epithelial tissue (Fig. 2) [92].

Stem cell-derived organoids allow long-term three-dimensional culture while maintaining the morphological relevance of native tissue. Isolated crypts from neonatal and immunocompromised mice were exposed to *C. parvum* upon plating, resulting in inhibited organoid propagation and budding, decreased expression of intestinal stem cell markers, and increased cell senescence [93]. In another study, human enteroids were infected with *C. parvum* by microinjection and the parasite was able to complete its entire life cycle within these organoids [94]. Though bovine enteroids have been described, they have not yet been used to study *C. parvum* infection [95-97].

Organoid technology for *C. parvum* research is in its relative infancy, but the benefits of the culture model are enticing and allow questions that were not possible to investigate with previous models.

Discussion

C. parvum is a parasite of international clinical importance across human and animal healthcare. Because of its high infectivity, resistance to water treatment, and the danger it poses to immunocompromised individuals, understanding the responses it induces in its host is a high priority endeavor to allow the creation of effective preventative measures and therapies. The innate immune response is multifaceted and

involves the intestinal epithelium, innate immune cells, and a complex interplay of cytokine signaling. To discover this, various models have been utilized. These include natural host species such as calves as well as more specialized models like immunocompromised mice, and *in vitro* models such as primary cell explants and immortalized cell lines. A relatively recent shift to three-dimensional cultures and the expanding use of organoids opens new avenues to study the parasite and its host-pathogen interaction.

As research in the field continues, attention must be brought to handling *C. parvum* from a ‘One Health’ perspective. New models must increase the relevant understanding of the parasite in bovine and human hosts and drive the discovery of innate mechanisms of resistance that can be utilized for management. Improved knowledge of the innate defenses against *C. parvum* in both ruminant and human hosts will hopefully lead to treatments to augment host natural innate defense and act as transient preventative measures to reduce environmental transmission of *C. parvum* between and within host species.

Figures

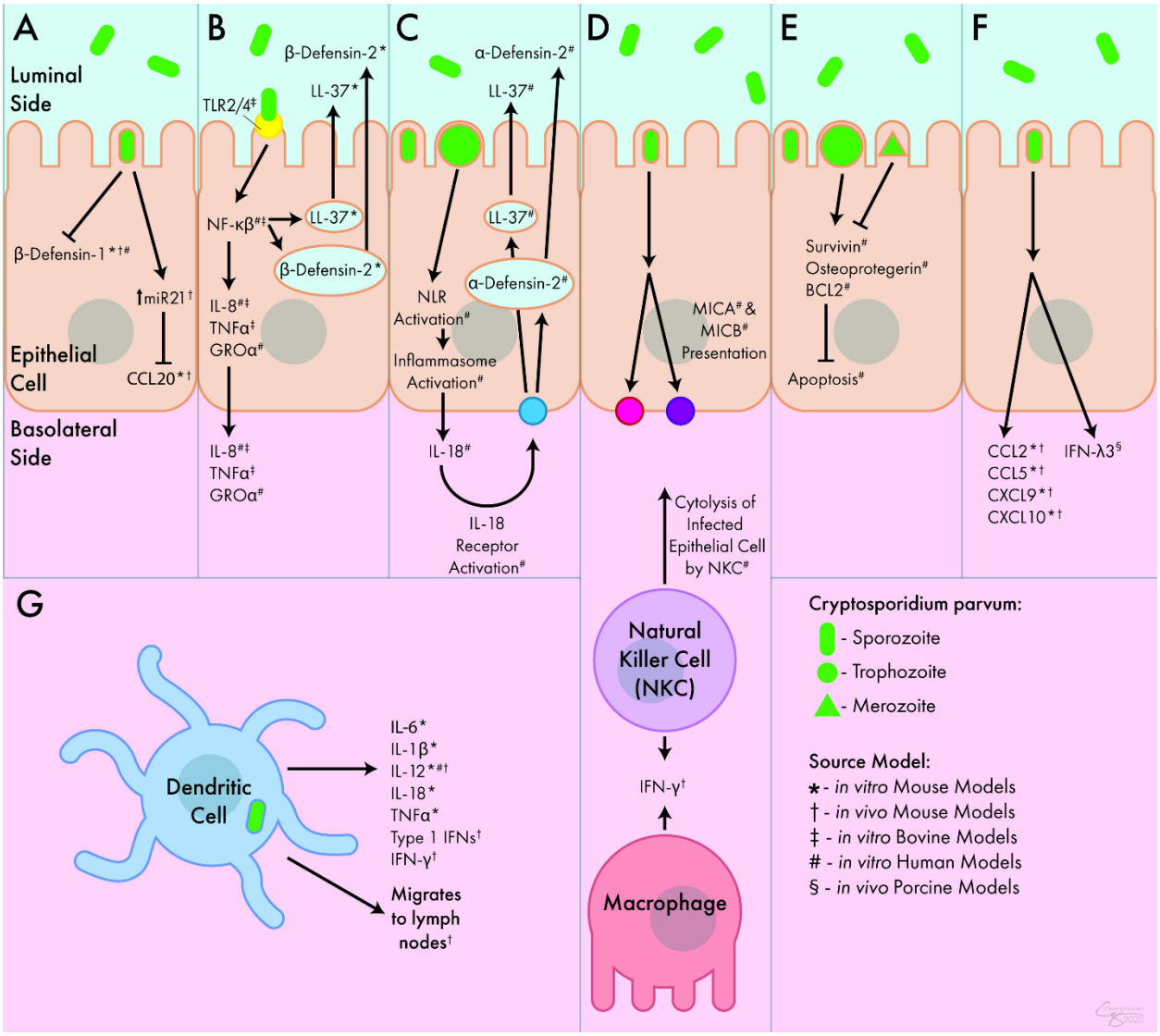

Figure 1. Innate Immune Response to *C. parvum*. **A)** *C. parvum* inhibits the release of the antimicrobial peptides β-defensin-1 and CCL20. **B)** Activation of TLR receptors by *C. parvum* leads to the luminal secretion of antimicrobial peptides β-defensin-2 and LL-37 as well as the basolateral secretion of IL-8, TNFα, and GROα. **C)** Inflammasome activation by *C. parvum* leads to the basolateral release of IL-18, which causes the luminal secretion of α -defensin-2 and LL-37. **D)** *C. parvum*-mediated presentation of MICA and MICB lead to cytolysis of infected epithelial cells by NK cells. NK cells and macrophages both act as sources of IFN-γ during infection. **E)** *C. parvum* trophozoites stimulate apoptosis, but merozoites inhibit apoptosis, mediated through survivin, osteoprotegerin, and BCL2. **F)** In response to *C. parvum*, intestinal epithelial cells release numerous chemokines and cytokines including CCL2, CCL5, CXCL9, CXCL10, and IFN-λ3. **G)** DCs respond to *C. parvum* by releasing IL-6, IL-1β, IL-12, IL-18, TNFα, and type I interferons. They can also migrate to lymph nodes following parasite

exposure. Abbreviation used: Interferon (IFN), Interleukin (IL-), Tumor Necrosis Factor (TNF), C-C Chemokine Ligand (CCL), C-X-C Chemokine Ligand (CXCL), Growth Regulated Oncogene (GRO), Toll-Like Receptor (TLR), Nod-Like Receptor (NLR), MicroRNA 21 (miR21), Nuclear Factor (NF), Cathelicidin (LL-37), Major Histocompatibility Complex Class I Chain-Related Protein (MIC), B-Cell Lymphoma 2-Apoptosis Regulator (BCL2), Natural Killer Cell (NKC)

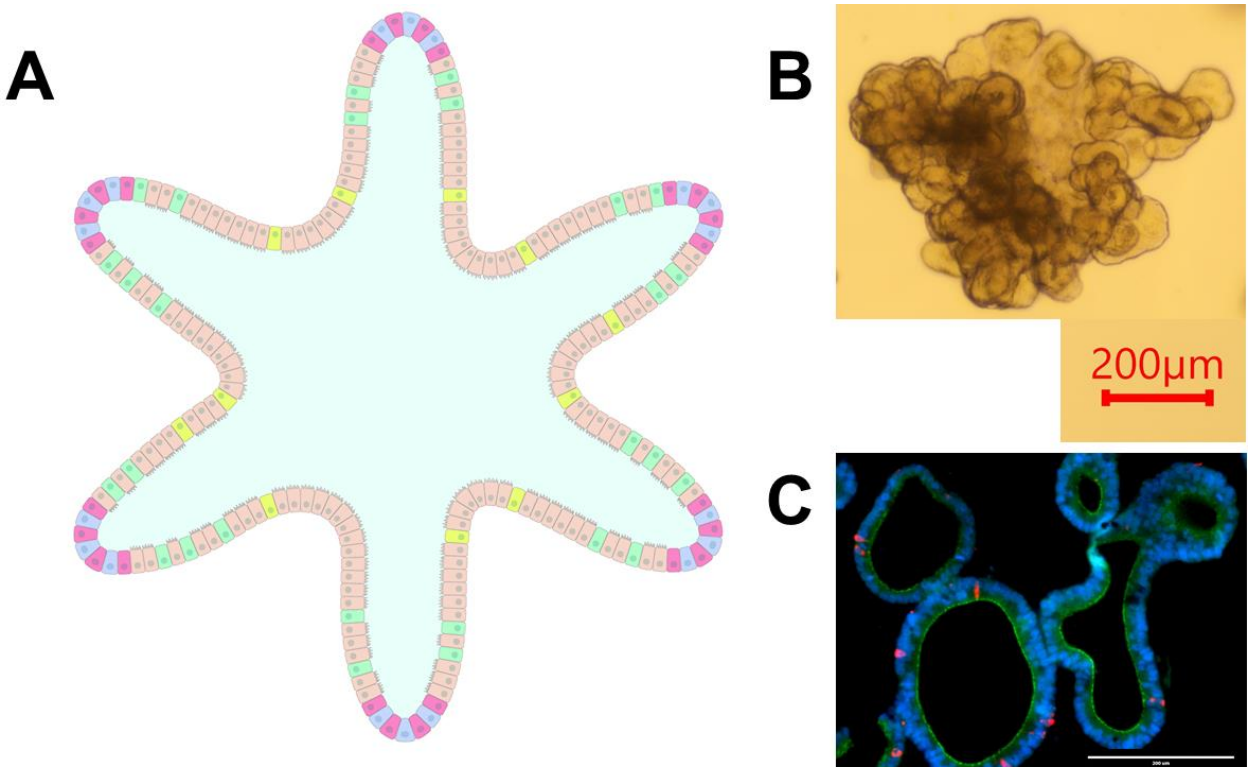

Figure 2. Intestinal Organoids. **A)** graphical representation of an intestinal organoid. The inside of the organoid corresponds to the luminal side, and the outside of the organoid corresponds to the basolateral side. Blue: intestinal stem cells, Red: Paneth cells, Tan: enterocytes, Green: goblet cells, Yellow: enteroendocrine cells. **B)** Bovine intestinal organoid 6 days post-plating. Numerous folds and budding structures are noted, indicating crypt and villi-like domains. **C)** Sectioned ovine intestinal organoid illustrating nuclei (DAPI), apical junctional protein ZO-1 (green), and chromogranin-A (red) indicating enteroendocrine cell differentiation.

Conflict of Interest

The authors declare that the research was conducted in the absence of any commercial or financial relationships that could be construed as a potential conflict of interest.

Funding

The work presented here was supported by funding from The Center for Food and Animal Health of The National Institute of Food and Agriculture, grant number: CALV-RIVAS-0060

Acknowledgments

We thank Chrisoula Toupadakis Skouritakis, PhD for assistance in the development of figures 1 and 2.

References

1. Abrahamsen, M.S., et al., *Complete genome sequence of the apicomplexan, Cryptosporidium parvum.* Science, 2004. **304**(5669): p. 441-5.
2. Abubakar, I., et al., *Prevention and treatment of cryptosporidiosis in immunocompromised patients.* Cochrane Database Syst Rev, 2007(1): p. CD004932.
3. Nydam, D.V., et al., *Number of Cryptosporidium parvum oocysts or Giardia spp cysts shed by dairy calves after natural infection.* Am J Vet Res, 2001. **62**(10): p. 1612-5.
4. Zambriski, J.A., et al., *Cryptosporidium parvum: determination of ID(5)(0) and the dose-response relationship in experimentally challenged dairy calves.* Vet Parasitol, 2013. **197**(1-2): p. 104-12.
5. Bouzid, M., et al., *Cryptosporidium pathogenicity and virulence.* Clin Microbiol Rev, 2013. **26**(1): p. 115-34.
6. Hatam-Nahavandi, K., et al., *Cryptosporidium infections in terrestrial ungulates with focus on livestock: a systematic review and meta-analysis.* Parasit Vectors, 2019. **12**(1): p. 453.
7. Ryan, U., A. Zahedi, and A. Paparini, *Cryptosporidium in humans and animals-a one health approach to prophylaxis.* Parasite Immunol, 2016. **38**(9): p. 535-47.
8. Chique, C., et al., *Cryptosporidium spp. in groundwater supplies intended for human consumption - A descriptive review of global prevalence, risk factors and knowledge gaps.* Water Res, 2020. **176**: p. 115726.
9. Li, X., et al., *Microbiological safety of popular recreation swimming sites in Central California.* Environ Monit Assess, 2019. **191**(7): p. 456.
10. Nag, R., et al., *Ranking hazards pertaining to human health concerns from land application of anaerobic digestate.* Sci Total Environ, 2020. **710**: p. 136297.
11. Marquis, N.D., N.R. Record, and J.A. Robledo, *Survey for protozoan parasites in Eastern oysters (Crassostrea virginica) from the Gulf of Maine using PCR-based assays.* Parasitol Int, 2015. **64**(5): p. 299-302.
12. Ziegler, P.E., et al., *Prevalence of Cryptosporidium species in wildlife populations within a watershed landscape in southeastern New York State.* Vet Parasitol, 2007. **147**(1-2): p. 176-84.
13. Checkley, W., et al., *Asymptomatic and symptomatic cryptosporidiosis: their acute effect on weight gain in Peruvian children.* Am J Epidemiol, 1997. **145**(2): p. 156-63.
14. Gormley, F.J., et al., *Zoonotic cryptosporidiosis from petting farms, England and Wales, 1992-2009.* Emerg Infect Dis, 2011. **17**(1): p. 151-2.
15. Khalil, I.A., et al., *Morbidity, mortality, and long-term consequences associated with diarrhoea from Cryptosporidium infection in children younger than 5 years: a meta-analyses study.* Lancet Glob Health, 2018. **6**(7): p. e758-e768.
16. Kotloff, K.L., et al., *Burden and aetiology of diarrhoeal disease in infants and young children in developing countries (the Global Enteric Multicenter Study, GEMS): a prospective, case-control study.* Lancet, 2013. **382**(9888): p. 209-22.
17. Ong, C.S., et al., *Enzyme immunoassay of Cryptosporidium-specific immunoglobulin G antibodies to assess longitudinal infection trends in six*

communities in British Columbia, Canada. Am J Trop Med Hyg, 2005. **73**(2): p. 288-95.
18. Corso, P.S., et al., *Cost of illness in the 1993 waterborne Cryptosporidium outbreak, Milwaukee, Wisconsin.* Emerg Infect Dis, 2003. **9**(4): p. 426-31.
19. Gharpure, R., et al., *Cryptosporidiosis Outbreaks - United States, 2009-2017.* MMWR Morb Mortal Wkly Rep, 2019. **68**(25): p. 568-572.
20. Scallan, E., et al., *Foodborne illness acquired in the United States--major pathogens.* Emerg Infect Dis, 2011. **17**(1): p. 7-15.
21. Rotz, L.D., et al., *Public health assessment of potential biological terrorism agents.* Emerg Infect Dis, 2002. **8**(2): p. 225-30.
22. Laurent, F. and S. Lacroix-Lamande, *Innate immune responses play a key role in controlling infection of the intestinal epithelium by Cryptosporidium.* Int J Parasitol, 2017. **47**(12): p. 711-721.
23. Ivanova, D.L., et al., *Innate Lymphoid Cells in Protection, Pathology, and Adaptive Immunity During Apicomplexan Infection.* Front Immunol, 2019. **10**: p. 196.
24. Li, M., et al., *Induction of a Long Noncoding RNA Transcript, NR_045064, Promotes Defense Gene Transcription and Facilitates Intestinal Epithelial Cell Responses against Cryptosporidium Infection.* J Immunol, 2018. **201**(12): p. 3630-3640.
25. Yang, Z., et al., *Bovine TLR2 and TLR4 mediate Cryptosporidium parvum recognition in bovine intestinal epithelial cells.* Microb Pathog, 2015. **85**: p. 29-34.
26. Chen, X.M., et al., *A cellular micro-RNA, let-7i, regulates Toll-like receptor 4 expression and contributes to cholangiocyte immune responses against Cryptosporidium parvum infection.* J Biol Chem, 2007. **282**(39): p. 28929-28938.
27. Chen, X.M., et al., *Multiple TLRs are expressed in human cholangiocytes and mediate host epithelial defense responses to Cryptosporidium parvum via activation of NF-kappaB.* J Immunol, 2005. **175**(11): p. 7447-56.
28. Lantier, L., et al., *Poly(I:C)-induced protection of neonatal mice against intestinal Cryptosporidium parvum infection requires an additional TLR5 signal provided by the gut flora.* J Infect Dis, 2014. **209**(3): p. 457-67.
29. McDonald, V., et al., *A potential role for interleukin-18 in inhibition of the development of Cryptosporidium parvum.* Clin Exp Immunol, 2006. **145**(3): p. 555-62.
30. Ehigiator, H.N., et al., *Mucosal cytokine and antigen-specific responses to Cryptosporidium parvum in IL-12p40 KO mice.* Parasite Immunol, 2005. **27**(1-2): p. 17-28.
31. McNair, N.N., et al., *Inflammasome components caspase-1 and adaptor protein apoptosis-associated speck-like proteins are important in resistance to Cryptosporidium parvum.* Microbes Infect, 2018. **20**(6): p. 369-375.
32. Sateriale, A., et al., *The intestinal parasite Cryptosporidium is controlled by an enterocyte intrinsic inflammasome that depends on NLRP6.* Proc Natl Acad Sci U S A, 2021. **118**(2).
33. Mahlapuu, M., et al., *Antimicrobial Peptides: An Emerging Category of Therapeutic Agents.* Front Cell Infect Microbiol, 2016. **6**: p. 194.

34. Carryn, S., et al., *Phospholipases and cationic peptides inhibit Cryptosporidium parvum sporozoite infectivity by parasiticidal and non-parasiticidal mechanisms.* J Parasitol, 2012. **98**(1): p. 199-204.
35. Giacometti, A., et al., *In-vitro activity of polycationic peptides against Cryptosporidium parvum, Pneumocystis carinii and yeast clinical isolates.* J Antimicrob Chemother, 1999. **44**(3): p. 403-6.
36. Zaalouk, T.K., et al., *Differential regulation of beta-defensin gene expression during Cryptosporidium parvum infection.* Infect Immun, 2004. **72**(5): p. 2772-9.
37. Guesdon, W., et al., *CCL20 Displays Antimicrobial Activity Against Cryptosporidium parvum, but Its Expression Is Reduced During Infection in the Intestine of Neonatal Mice.* J Infect Dis, 2015. **212**(8): p. 1332-40.
38. Laurent, F., et al., *Pathogenesis of Cryptosporidium parvum infection.* Microbes Infect, 1999. **1**(2): p. 141-8.
39. Laurent, F., et al., *Cryptosporidium parvum infection of human intestinal epithelial cells induces the polarized secretion of C-X-C chemokines.* Infect Immun, 1997. **65**(12): p. 5067-73.
40. Auray, G., et al., *Involvement of intestinal epithelial cells in dendritic cell recruitment during C. parvum infection.* Microbes Infect, 2007. **9**(5): p. 574-82.
41. Lacroix-Lamande, S., et al., *Role of gamma interferon in chemokine expression in the ileum of mice and in a murine intestinal epithelial cell line after Cryptosporidium parvum infection.* Infect Immun, 2002. **70**(4): p. 2090-9.
42. Lantier, L., et al., *Intestinal CD103+ dendritic cells are key players in the innate immune control of Cryptosporidium parvum infection in neonatal mice.* PLoS Pathog, 2013. **9**(12): p. e1003801.
43. Lacroix-Lamande, S., et al., *CCR5 is involved in controlling the early stage of Cryptosporidium parvum infection in neonates but is dispensable for parasite elimination.* Microbes Infect, 2008. **10**(4): p. 390-5.
44. Chen, X.M., et al., *Cryptosporidium parvum induces apoptosis in biliary epithelia by a Fas/Fas ligand-dependent mechanism.* Am J Physiol, 1999. **277**(3): p. G599-608.
45. Mele, R., et al., *Cryptosporidium parvum at different developmental stages modulates host cell apoptosis in vitro.* Infect Immun, 2004. **72**(10): p. 6061-7.
46. Liu, J., et al., *Biphasic modulation of apoptotic pathways in Cryptosporidium parvum-infected human intestinal epithelial cells.* Infect Immun, 2009. **77**(2): p. 837-49.
47. Castellanos-Gonzalez, A., et al., *Cryptosporidium infection of human intestinal epithelial cells increases expression of osteoprotegerin: a novel mechanism for evasion of host defenses.* J Infect Dis, 2008. **197**(6): p. 916-23.
48. McCole, D.F., et al., *Intestinal epithelial cell apoptosis following Cryptosporidium parvum infection.* Infect Immun, 2000. **68**(3): p. 1710-3.
49. Mead, J.R. and X. You, *Susceptibility differences to Cryptosporidium parvum infection in two strains of gamma interferon knockout mice.* J Parasitol, 1998. **84**(5): p. 1045-8.
50. McDonald, V., et al., *Innate immune responses against Cryptosporidium parvum infection.* Parasite Immunol, 2013. **35**(2): p. 55-64.

51. Theodos, C.M., et al., *Profiles of healing and nonhealing Cryptosporidium parvum infection in C57BL/6 mice with functional B and T lymphocytes: the extent of gamma interferon modulation determines the outcome of infection.* Infect Immun, 1997. **65**(11): p. 4761-9.
52. Hayward, A.R., K. Chmura, and M. Cosyns, *Interferon-gamma is required for innate immunity to Cryptosporidium parvum in mice.* J Infect Dis, 2000. **182**(3): p. 1001-4.
53. Ferguson, S.H., et al., *Interferon-lambda3 Promotes Epithelial Defense and Barrier Function Against Cryptosporidium parvum Infection.* Cell Mol Gastroenterol Hepatol, 2019. **8**(1): p. 1-20.
54. Zhou, J.H., et al., *Type III Interferons in Viral Infection and Antiviral Immunity.* Cell Physiol Biochem, 2018. **51**(1): p. 173-185.
55. Odendall, C., A.A. Voak, and J.C. Kagan, *Type III IFNs Are Commonly Induced by Bacteria-Sensing TLRs and Reinforce Epithelial Barriers during Infection.* J Immunol, 2017. **199**(9): p. 3270-3279.
56. Urban, J.F., Jr., et al., *IL-12 protects immunocompetent and immunodeficient neonatal mice against infection with Cryptosporidium parvum.* J Immunol, 1996. **156**(1): p. 263-8.
57. Dann, S.M., et al., *Interleukin-15 activates human natural killer cells to clear the intestinal protozoan cryptosporidium.* J Infect Dis, 2005. **192**(7): p. 1294-302.
58. Barakat, F.M., et al., *Roles for NK cells and an NK cell-independent source of intestinal gamma interferon for innate immunity to Cryptosporidium parvum infection.* Infect Immun, 2009. **77**(11): p. 5044-9.
59. Olsen, L., et al., *The early intestinal immune response in experimental neonatal ovine cryptosporidiosis is characterized by an increased frequency of perforin expressing NCR1(+) NK cells and by NCR1(-) CD8(+) cell recruitment.* Vet Res, 2015. **46**: p. 28.
60. Barakat, F.M., et al., *Cryptosporidium parvum infection rapidly induces a protective innate immune response involving type I interferon.* J Infect Dis, 2009. **200**(10): p. 1548-55.
61. Bedi, B. and J.R. Mead, *Cryptosporidium parvum antigens induce mouse and human dendritic cells to generate Th1-enhancing cytokines.* Parasite Immunol, 2012. **34**(10): p. 473-85.
62. Perez-Cordon, G., et al., *Interaction of Cryptosporidium parvum with mouse dendritic cells leads to their activation and parasite transportation to mesenteric lymph nodes.* Pathog Dis, 2014. **70**(1): p. 17-27.
63. Farache, J., et al., *Luminal bacteria recruit CD103+ dendritic cells into the intestinal epithelium to sample bacterial antigens for presentation.* Immunity, 2013. **38**(3): p. 581-95.
64. Marcial, M.A. and J.L. Madara, *Cryptosporidium: cellular localization, structural analysis of absorptive cell-parasite membrane-membrane interactions in guinea pigs, and suggestion of protozoan transport by M cells.* Gastroenterology, 1986. **90**(3): p. 583-94.
65. Bedi, B., N.N. McNair, and J.R. Mead, *Dendritic cells play a role in host susceptibility to Cryptosporidium parvum infection.* Immunol Lett, 2014. **158**(1-2): p. 42-51.

66. Kumar, V., *Macrophages: The Potent Immunoregulatory Innate Immune Cells*, in *Macrophage Activation - Biology and Disease*, K.H. Bhat, Editor. 2019, IntechOpen.
67. Verschoor, C.P., A. Puchta, and D.M. Bowdish, *The macrophage.* Methods Mol Biol, 2012. **844**: p. 139-56.
68. de Sablet, T., et al., *Cryptosporidium parvum increases intestinal permeability through interaction with epithelial cells and IL-1beta and TNFalpha released by inflammatory monocytes.* Cell Microbiol, 2016. **18**(12): p. 1871-1880.
69. Choudhry, N., et al., *A protective role for interleukin 18 in interferon gamma-mediated innate immunity to Cryptosporidium parvum that is independent of natural killer cells.* J Infect Dis, 2012. **206**(1): p. 117-24.
70. Goodgame, R.W., et al., *Intestinal function and injury in acquired immunodeficiency syndrome-related cryptosporidiosis.* Gastroenterology, 1995. **108**(4): p. 1075-82.
71. Zadrozny, L.M., et al., *Neutrophils do not mediate the pathophysiological sequelae of Cryptosporidium parvum infection in neonatal piglets.* Infect Immun, 2006. **74**(10): p. 5497-505.
72. Griffiths, J.K., et al., *The gamma interferon gene knockout mouse: a highly sensitive model for evaluation of therapeutic agents against Cryptosporidium parvum.* J Clin Microbiol, 1998. **36**(9): p. 2503-8.
73. Mead, J.R., et al., *Chronic Cryptosporidium parvum infections in congenitally immunodeficient SCID and nude mice.* J Infect Dis, 1991. **163**(6): p. 1297-304.
74. Petry, F., H.A. Robinson, and V. McDonald, *Murine infection model for maintenance and amplification of Cryptosporidium parvum oocysts.* J Clin Microbiol, 1995. **33**(7): p. 1922-4.
75. Tzipori, S., *Cryptosporidiosis: laboratory investigations and chemotherapy.* Adv Parasitol, 1998. **40**: p. 187-221.
76. Sateriale, A., et al., *A Genetically Tractable, Natural Mouse Model of Cryptosporidiosis Offers Insights into Host Protective Immunity.* Cell Host Microbe, 2019. **26**(1): p. 135-146 e5.
77. Allan, A.J., et al., *Cattle NK Cell Heterogeneity and the Influence of MHC Class I.* J Immunol, 2015. **195**(5): p. 2199-206.
78. Guzman, E., et al., *Bovine gammadelta T cells: cells with multiple functions and important roles in immunity.* Vet Immunol Immunopathol, 2012. **148**(1-2): p. 161-7.
79. Castellanos-Gonzalez, A., et al., *Human primary intestinal epithelial cells as an improved in vitro model for Cryptosporidium parvum infection.* Infect Immun, 2013. **81**(6): p. 1996-2001.
80. Hashim, A., et al., *Interaction of Cryptosporidium hominis and Cryptosporidium parvum with primary human and bovine intestinal cells.* Infect Immun, 2006. **74**(1): p. 99-107.
81. Varughese, E.A., et al., *A new in vitro model using small intestinal epithelial cells to enhance infection of Cryptosporidium parvum.* J Microbiol Methods, 2014. **106**: p. 47-54.
82. Karanis, P. and H.M. Aldeyarbi, *Evolution of Cryptosporidium in vitro culture.* Int J Parasitol, 2011. **41**(12): p. 1231-42.

83. Rasmussen, K.R., N.C. Larsen, and M.C. Healey, *Complete development of Cryptosporidium parvum in a human endometrial carcinoma cell line.* Infect Immun, 1993. **61**(4): p. 1482-5.
84. Upton, S.J., M. Tilley, and D.B. Brillhart, *Comparative development of Cryptosporidium parvum (Apicomplexa) in 11 continuous host cell lines.* FEMS Microbiol Lett, 1994. **118**(3): p. 233-6.
85. Dawson, D.J., et al., *Survival of Cryptosporidium species in environments relevant to foods and beverages.* J Appl Microbiol, 2004. **96**(6): p. 1222-9.
86. Deng, M.Q. and D.O. Cliver, *Cryptosporidium parvum development in the BS-C-1 cell line.* J Parasitol, 1998. **84**(1): p. 8-15.
87. Miller, C.N., et al., *A cell culture platform for Cryptosporidium that enables long-term cultivation and new tools for the systematic investigation of its biology.* Int J Parasitol, 2018. **48**(3-4): p. 197-201.
88. Alcantara Warren, C., et al., *Detection of epithelial-cell injury, and quantification of infection, in the HCT-8 organoid model of cryptosporidiosis.* J Infect Dis, 2008. **198**(1): p. 143-9.
89. Morada, M., et al., *Continuous culture of Cryptosporidium parvum using hollow fiber technology.* Int J Parasitol, 2016. **46**(1): p. 21-9.
90. DeCicco RePass, M.A., et al., *Novel Bioengineered Three-Dimensional Human Intestinal Model for Long-Term Infection of Cryptosporidium parvum.* Infect Immun, 2017. **85**(3).
91. Bhalchandra, S., D. Cardenas, and H.D. Ward, *Recent Breakthroughs and Ongoing Limitations in Cryptosporidium Research.* F1000Res, 2018. **7**.
92. Zachos, N.C., et al., *Human Enteroids/Colonoids and Intestinal Organoids Functionally Recapitulate Normal Intestinal Physiology and Pathophysiology.* J Biol Chem, 2016. **291**(8): p. 3759-66.
93. Zhang, X.T., et al., *Cryptosporidium parvum infection attenuates the ex vivo propagation of murine intestinal enteroids.* Physiol Rep, 2016. **4**(24).
94. Heo, I., et al., *Modelling Cryptosporidium infection in human small intestinal and lung organoids.* Nat Microbiol, 2018. **3**(7): p. 814-823.
95. Derricott, H., et al., *Developing a 3D intestinal epithelium model for livestock species.* Cell Tissue Res, 2019. **375**(2): p. 409-424.
96. Hamilton, C.A., et al., *Development of in vitro enteroids derived from bovine small intestinal crypts.* Vet Res, 2018. **49**(1): p. 54.
97. Powell, R.H. and M.S. Behnke, *WRN conditioned media is sufficient for in vitro propagation of intestinal organoids from large farm and small companion animals.* Biol Open, 2017. **6**(5): p. 698-705.

Chapter 2: The Effects of Inflammation and Diabetes on Intestinal Epithelial Barrier Function

Charles K. Crawford, Amir Kol

Abstract

The intestinal epithelium is a monolayer of epithelial cells that comprises a major component of the intestinal barrier which separates the gut lumen from sterile internal tissues. These cells are adjoined by tight junctions, which are protein complexes that regulate paracellular transport of molecules across the barrier. Dysfunction of the intestinal epithelial barrier can increase permeability of the barrier and increase the risk of systemic infection. Both inflammation and Diabetes mellitus (DM) are associated with dysfunction of the intestinal barrier. Inflammatory cytokines negatively influence the intestinal epithelial barrier by increasing permeability and altering the morphology and expression of tight junction proteins, as well as inducing cellular death. The expression of myosin light chain kinase (MLCK) and subsequent phosphorylation of the MLCK target, myosin light chain (MLC), is highly associated with inflammation-induced dysfunction of the barrier and is a likely causative mechanism. DM, which can often be accompanied by inflammation, is also shown to increase permeability of the intestinal epithelial barrier and alter tight junction expression. Works to isolate the effects of glucose from inflammation have shown that luminal glucose directly induces dysfunction of the intestinal epithelial barrier and increases actomyosin tension. Altogether, both inflammation and DM reduce the function of the intestinal epithelial barrier, though the specific mechanisms separating the effects of inflammation and DM, specifically, are not yet fully elucidated.

Intestinal Epithelial Barrier Function

The intestines form a barrier that separates the intestinal lumen from the internal compartments of the body [1, 2]. The barrier consists of a layer of mucus that covers a monolayer of epithelial tissue, followed by the lamina propria, a layer of connective tissue that houses immune cells [3]. The epithelial portion of the barrier consists of a single layer of epithelial cells that form a polarized monolayer with the apical portion facing the lumen and the basolateral portion facing internal tissues [2]. the epithelium is folded to form protruding villi and concave crypts [2]. Adult intestinal stem cells reside in the crypts and undergo proliferation causing upward migration of cells [4]. As cells migrate toward the villus tip, they differentiate into specialized epithelial cells including enterocytes that are responsible for nutrient absorption and brush border enzyme production, enteroendocrine cells that synthesize and release gut hormones, and goblet cells that secrete mucus [2]. This intestinal epithelium is semipermeable and allows the uptake of nutrients, electrolytes, and water, while preventing the entry of intraluminal pathogens [5-9]. Movement of substances across the epithelium involves transcellular transport via selective transporter proteins or paracellular transport in between epithelial cells [6-8, 10].

Cells of the intestinal epithelium are adjoined by a series of protein complexes including desmosomes, adherens junctions, and tight junctions [11]. Desmosomes and adherens junctions are more basolateral than tight junctions; they are linked to intracellular cytoskeletal filaments and their primary function in the intestinal epithelium is to maintain cell to cell adhesion [12-15]. Tight junctions are the most apical of the protein complexes and they form a ring around the apical border connecting adjacent

epithelial cells [11]. They are comprised of the transmembrane proteins occludin, claudins, junctional adhesion molecules, and tricellulin, and are connected to cytoskeletal fibers by zonula occludens proteins including ZO-1, ZO-2, and ZO-3 [16-18]. Tight junctions are the primary regulators of paracellular transport and permeability, as mediated through interactions with cytoskeletal structures [19].

The intestinal epithelium plays a key role in regulating intestinal homeostasis. Dysfunction of this epithelial barrier can lead to increased intestinal permeability and increased risk of infection and paracellular movement of pathogens or pathogen products and toxins into the systemic circulation [20]. Intestinal barrier dysfunction is associated with numerous systemic and intestinal pathologies including Celiac disease, ulcerative colitis, obesity, and diabetes [21-28]. In these diseases it is not fully determined if barrier dysfunction plays a causative role in pathology, is a consequence of the primary disease, or both in a positive feedback loop [29]. Damage to this barrier can come from a multitude of factors including diet, genetic susceptibility, pathogens, stress, and drugs [29]. Two factors that contribute to barrier dysfunction include inflammation and hyperglycemia [30, 31], and will be further reviewed.

The Effects of Inflammation on Intestinal Epithelial Barrier Function

The inflammatory response is a defense mechanism resulting from the immune system responding to a harmful stimulus [32, 33]. It involves the activation of immune signaling pathways in immune cells and tissue resident cells and is induced by pro-inflammatory cytokines including interleukins (ILs), tumor necrosis factors (TNFs),

interferons (IFNs), transforming growth factors (TGFs), and chemokines [34, 35]. Excessive and chronic production of pro-inflammatory cytokines can induce damage to tissues, organ failure, and even death [36, 37]. Chronic intestinal inflammation and systemic inflammation are associated with intestinal barrier dysfunction [38-49].

The mechanisms by which inflammation induces intestinal barrier dysfunction are multifactorial. Intestinal cell line monolayers (CACO-2) and intestinal organoids treated with the pro-inflammatory cytokine TNFα, which is primarily produced by monocytes and macrophages [50], display an increased permeability, altered tight junctional morphology as shown through tight junction tortuosity, and reduced tight junction protein expression [51-55]. Intestinal organoids and organoid-derived monolayers exposed to TNFα also show an increase in programmed cell death (apoptosis and necroptosis) [52, 53]. Additionally, exposure of CACO-2 cells and intestinal organoids to TNFα increases the expression of Myosin Light Chain Kinase (MLCK) and phosphorylation of the MLCK target, Myosin Light Chain (MLC) [53, 56, 57]. Transgenic upregulation of MLCK increases intestinal permeability in mice [58]. Increased activation of MLCK is known to induce perijunctional myosin II motor activity resulting in actomyosin cytoskeletal contractility which physically induces tight junctional disassembly, resulting in epithelial barrier dysfunction [57, 59-64]. Interleukin 6 (IL-6), another pro-inflammatory cytokine produced by monocytes and macrophages, induced a decrease in the expression of occludin and claudin-1 in intestinal organoids and CACO-2 cells [65, 66]. Intestinal organoids and CACO-2 cells treated with IFNγ, a pro-inflammatory cytokine produced by adaptive immune cells, also displayed increased barrier permeability and reduced levels of ZO-1 and occludin [59, 67-69]. IFNγ also induces apoptosis in intestinal

epithelial cell lines (HT-29 and CACO-2) [70]. Inhibition of TNFα and IFNγ in intestinal epithelial cell lines (T84 and CACO-2) reduces MLC phosphorylation and restores barrier function [57]. Thus, the pro-inflammatory cytokines appear to reduce intestinal barrier function through several mechanisms including the alteration of tight junction function via cytoskeletal contraction and reduced tight junction protein expression, as well as an increase in epithelial cell death.

Anti-inflammatory cytokines may counter the negative effects of pro-inflammatory cytokines on the barrier function of the intestinal epithelium. Interleukin 10 (IL-10) is an anti-inflammatory cytokine produced by monocytes and some lymphocytes [71]. IL-10 exposure opposes the effects of IFNγ and prevents IFNγ-induced barrier dysfunction in T84 epithelial monolayers [72-74]. While this suggests that IL-10 may inhibit the effects of IFNγ, it is not clear if anti-inflammatory cytokines improve intestinal barrier function independently of the pro-inflammatory-induced reduction in function.

Taken together, the inflammatory response exposes the intestinal epithelial barrier to numerous inflammatory cytokines that induce alterations of tight junction morphology, reduction in the expression of tight junction proteins, activation of MLCK, and increased cell death, ultimately resulting in dysfunction of the intestinal barrier.

The Effects of Diabetes on Intestinal Epithelial Barrier Function

Diabetes mellitus (DM) is a metabolic disease defined by compromised glucose regulation and persistent hyperglycemia; it influences many organ systems across the body [75]. DM is associated with dysfunction of the intestinal epithelial barrier in the

form of increased permeability, though the specific mechanisms are multifactorial and not well understood [21, 27, 76, 77]. Obesity, which is commonly associated with DM, can result in chronic systemic inflammation with elevated levels of inflammatory cytokines such as TNFα and IFNγ [78-81]. Additionally, enteric neurons are susceptible to damage by inflammation, hyperglycemia, vascular impairment, and oxidative stress during diabetes, resulting in altered neuronal signaling to intestinal tissue contributing to diabetic enteropathy [82-86]. Altogether, the multitude of factors contributing to DM-induced intestinal barrier dysfunction make it less clear what direct effect hyperglycemia may have on the intestinal epithelial barrier and its role in DM-induced barrier dysfunction.

The effects of hyperglycemia on the intestinal barrier are difficult to parse from other contributing factors on barrier dysfunction in DM and have been studied in diabetic and hyperglycemic models. Mice induced with diabetes by streptozotocin, a compound that is toxic to the insulin-producing cells of the pancreas [87], have increased intestinal permeability and a reduction in immunoreactivity for the adherens junction protein, E-Cadherin [31]. A high-carbohydrate diet was shown to induce intestinal barrier dysfunction and reduce protein expression of tight junction proteins ZO-1 and occludin, but this was seen in conjunction with an increase in pro-inflammatory cytokines [88]. Glucose-fed mice displayed an increase in paracellular permeability and both glucose or fructose-fed mice showed an increase in intestinal MLCK levels, although this was accompanied by an increase in TNFα and IFNγ [89]. These data demonstrate that increasing dietary simple sugars can alter intestinal permeability, but the concomitant increase in inflammatory cytokines makes it difficult to interpret this as a primary effect.

However, some strides have been made in models that allow the isolation of the effects of glucose. Exposure to glucose on the luminal side induces an expansion of lateral intercellular spaces observed via electron microscopy, described as ‘tight junctional dilation’, in isolated segments of hamster small intestine that increase paracellular transport of a heme-conjugated peptide tracer, increase actomyosin ring tension, and additionally increase clearance of solutes in rat intestines [90-92]. Mucosal glucose exposure in Ussing chambers showed that tight junction dilation is triggered by activation of sodium/glucose transporters [93]. Intestinal epithelial cell lines have been used to further examine the mechanisms behind glucose-induced alterations of intestinal permeability; apical exposure of glucose to CACO-2 cells induces an increase in the tortuosity of tight junctions [31, 94]. These studies show an effect of high glucose concentration on the intestinal barrier when exposed via the luminal side, however, these models do not accurately depict the effects of hyperglycemia on intestinal barrier function; in diabetic patients it is the basolateral side of the epithelial cells that are exposed to high glucose concentrations. Deletion of GLUT2 transporters or inhibition of glucose metabolism in hyperglycemic mice was found to repair function of the intestinal epithelial barrier by reducing pathogen entry through the intestines, implying a mechanistic dependence of GLUT2-dependent retrograde transport of glucose into epithelial cells and the metabolism of glucose in hyperglycemia [31]. More work is needed to fully elucidate the mechanisms driving the effects of hyperglycemia-induced intestinal barrier dysfunction.

Conclusions

Both inflammation and hyperglycemia influence the function of the intestinal epithelial barrier. Inflammatory cytokines and glucose exposure increase paracellular permeability and alter the morphology and function of tight junctions. Some models of diabetes do display reduced expression of tight junction proteins, and increased expression of MLCK, however these *in-vivo* models do not necessarily separate the effects of glucose from the effects of DM-associated inflammation. The molecular mechanisms driving inflammation-induced barrier dysfunction have been further investigated and cytoskeletal alterations appear to be a driving factor, which is also seen in some models of DM but not those that isolate hyperglycemia from inflammation.

Acquiring a comprehensive understanding of the factors that influence the intestinal epithelial barrier in both inflammatory diseases and DM and the causative mechanisms behind these driving forces may provide the necessary tools to combat the barrier dysfunction associated with these pathologies and provide symptomatic relief to patients across the world.

Figures

Table 1. The effects of inflammation on intestinal epithelial barrier function

Model	Insult	Effect on the Intestinal Barrier	References
CACO-2 cell line & Intestinal organoids	TNFα exposure	↑Permeability ↑Tight junction tortuosity ↓Tight junction protein expression ↑MLCK expression ↑MLC phosphorylation	51-57
Intestinal organoids & Organoid-derived monolayers	TNFα exposure	↑Programmed cell death	52,53
CACO-2 cell line & Intestinal organoids	IFNγ exposure	↑Permeability ↓Tight junction protein expression	59,67-69
CACO-2 & HT-29 cell lines	IFNγ exposure	↑Apoptosis	70
CACO-2 & T84 cell lines	Inhibition of TNFα & IFNγ	↓MLC phosphorylation ↑Permeability ↓Transepithelial Electrical Resistance (TEER)	57
T84 cell line	IL-10 exposure	Prevents the IFNγ-induced ↑in TEER and permeability	72-74
CACO-2 cell line & Intestinal organoids	IL-6 exposure	↓Tight junction protein expression	65,66
Mice	Transgenic upregulation of MLCK	↑Intestinal permeability	58
CACO-2 & T84 cell lines	Inhibition of MLCK	↓MLC phosphorylation ↑TEER ↑Permeability Prevention of TNFα & IFNγ-induced ↓ in TEER and permeability	57,59,63
T84 cell line	IFNγ exposure	Endocytosis of tight junction proteins via non-myosin II motor activity	59, 62

Table 2. The effects of diabetes on intestinal epithelial barrier function

Model	Insult	Effect on the Intestinal Barrier	References
Mice	Diabetes induction (STZ)	↑Intestinal permeability ↓Adherens junction protein immunoreactivity	31
Mice	High-carbohydrate diet	↓Tight junction protein expression ↑Intestinal permeability ↑Inflammation	88
Mice	15% glucose in drinking water	↑Intestinal permeability ↑MLCK expression ↑TNFα & IFNγ	89
Rats	Recirculated glucose perfusion in intestinal lumen	↑Paracellular permeability (directly proportional to glucose concentration)	92
Isolated segments of hamster intestine	Glucose infusion	↓TEER Expansion of lateral intracellular spaces Tight junction dilation ↑actomyosin ring tension ↑Paracellular permeability	90,91
CACO-2 cell line	Apical glucose exposure	↑Tight junction tortuosity	31,94
Mice	Diabetes induction (STZ) & GLUT2 deletion	GLUT2 deletion prevented glucose-induced ↓Tight junction immunoreactivity, ↑permeability	31

References

1. Barrett, K.E., *New ways of thinking about (and teaching about) intestinal epithelial function.* Adv Physiol Educ, 2008. **32**(1): p. 25-34.
2. Collins, J.T., A. Nguyen, and M. Badireddy, *Anatomy, Abdomen and Pelvis, Small Intestine*, in *StatPearls*. 2021: Treasure Island (FL).
3. Vancamelbeke, M. and S. Vermeire, *The intestinal barrier: a fundamental role in health and disease.* Expert Rev Gastroenterol Hepatol, 2017. **11**(9): p. 821-834.
4. van der Flier, L.G. and H. Clevers, *Stem cells, self-renewal, and differentiation in the intestinal epithelium.* Annu Rev Physiol, 2009. **71**: p. 241-60.
5. Blikslager, A.T., et al., *Restoration of barrier function in injured intestinal mucosa.* Physiol Rev, 2007. **87**(2): p. 545-64.
6. Broer, S., *Amino acid transport across mammalian intestinal and renal epithelia.* Physiol Rev, 2008. **88**(1): p. 249-86.
7. Ferraris, R.P. and J. Diamond, *Regulation of intestinal sugar transport.* Physiol Rev, 1997. **77**(1): p. 257-302.
8. Kunzelmann, K. and M. Mall, *Electrolyte transport in the mammalian colon: mechanisms and implications for disease.* Physiol Rev, 2002. **82**(1): p. 245-89.
9. Podolsky, D.K., *Mucosal immunity and inflammation. V. Innate mechanisms of mucosal defense and repair: the best offense is a good defense.* Am J Physiol, 1999. **277**(3): p. G495-9.
10. Van Itallie, C.M. and J.M. Anderson, *Claudins and epithelial paracellular transport.* Annu Rev Physiol, 2006. **68**: p. 403-29.
11. Farquhar, M.G. and G.E. Palade, *Junctional complexes in various epithelia.* J Cell Biol, 1963. **17**(2): p. 375-412.
12. Delva, E., D.K. Tucker, and A.P. Kowalczyk, *The desmosome.* Cold Spring Harb Perspect Biol, 2009. **1**(2): p. a002543.
13. Meng, W. and M. Takeichi, *Adherens junction: molecular architecture and regulation.* Cold Spring Harb Perspect Biol, 2009. **1**(6): p. a002899.
14. Saito, M., et al., *Classical and desmosomal cadherins at a glance.* J Cell Sci, 2012. **125**(Pt 11): p. 2547-52.
15. Thomason, H.A., et al., *Desmosomes: adhesive strength and signalling in health and disease.* Biochem J, 2010. **429**(3): p. 419-33.
16. Bauer, H., et al., *Astrocytes and neurons express the tight junction-specific protein occludin in vitro.* Exp Cell Res, 1999. **250**(2): p. 434-8.
17. Blank, F., et al., *Macrophages and dendritic cells express tight junction proteins and exchange particles in an in vitro model of the human airway wall.* Immunobiology, 2011. **216**(1-2): p. 86-95.
18. Umeda, K., et al., *ZO-1 and ZO-2 independently determine where claudins are polymerized in tight-junction strand formation.* Cell, 2006. **126**(4): p. 741-54.
19. Horowitz, A., et al., *Paracellular permeability and tight junction regulation in gut health and disease.* Nat Rev Gastroenterol Hepatol, 2023: p. 1-16.
20. Ghosh, S.S., et al., *Intestinal Barrier Dysfunction, LPS Translocation, and Disease Development.* J Endocr Soc, 2020. **4**(2): p. bvz039.
21. Bosi, E., et al., *Increased intestinal permeability precedes clinical onset of type 1 diabetes.* Diabetologia, 2006. **49**(12): p. 2824-7.

22. Braun, A., et al., *Alterations of phospholipid concentration and species composition of the intestinal mucus barrier in ulcerative colitis: a clue to pathogenesis.* Inflamm Bowel Dis, 2009. **15**(11): p. 1705-20.
23. Cani, P.D., et al., *Changes in gut microbiota control metabolic endotoxemia-induced inflammation in high-fat diet-induced obesity and diabetes in mice.* Diabetes, 2008. **57**(6): p. 1470-81.
24. Fasano, A., et al., *Zonulin, a newly discovered modulator of intestinal permeability, and its expression in coeliac disease.* Lancet, 2000. **355**(9214): p. 1518-9.
25. Genser, L., et al., *Increased jejunal permeability in human obesity is revealed by a lipid challenge and is linked to inflammation and type 2 diabetes.* J Pathol, 2018. **246**(2): p. 217-230.
26. Larsson, J.M., et al., *Altered O-glycosylation profile of MUC2 mucin occurs in active ulcerative colitis and is associated with increased inflammation.* Inflamm Bowel Dis, 2011. **17**(11): p. 2299-307.
27. Sapone, A., et al., *Zonulin upregulation is associated with increased gut permeability in subjects with type 1 diabetes and their relatives.* Diabetes, 2006. **55**(5): p. 1443-9.
28. Szakal, D.N., et al., *Mucosal expression of claudins 2, 3 and 4 in proximal and distal part of duodenum in children with coeliac disease.* Virchows Arch, 2010. **456**(3): p. 245-50.
29. Chelakkot, C., J. Ghim, and S.H. Ryu, *Mechanisms regulating intestinal barrier integrity and its pathological implications.* Exp Mol Med, 2018. **50**(8): p. 1-9.
30. Crawford, C.K., et al., *Inflammatory cytokines directly disrupt the bovine intestinal epithelial barrier.* Sci Rep, 2022. **12**(1): p. 14578.
31. Thaiss, C.A., et al., *Hyperglycemia drives intestinal barrier dysfunction and risk for enteric infection.* Science, 2018. **359**(6382): p. 1376-1383.
32. Medzhitov, R., *Inflammation 2010: new adventures of an old flame.* Cell, 2010. **140**(6): p. 771-6.
33. Nathan, C. and A. Ding, *Nonresolving inflammation.* Cell, 2010. **140**(6): p. 871-82.
34. Lawrence, T., *The nuclear factor NF-kappaB pathway in inflammation.* Cold Spring Harb Perspect Biol, 2009. **1**(6): p. a001651.
35. Turner, M.D., et al., *Cytokines and chemokines: At the crossroads of cell signalling and inflammatory disease.* Biochim Biophys Acta, 2014. **1843**(11): p. 2563-2582.
36. Czaja, A.J., *Hepatic inflammation and progressive liver fibrosis in chronic liver disease.* World J Gastroenterol, 2014. **20**(10): p. 2515-32.
37. Liu, Z., et al., *Dexmedetomidine attenuates inflammatory reaction in the lung tissues of septic mice by activating cholinergic anti-inflammatory pathway.* Int Immunopharmacol, 2016. **35**: p. 210-216.
38. Abuajamieh, M., et al., *Inflammatory biomarkers are associated with ketosis in periparturient Holstein cows.* Res Vet Sci, 2016. **109**: p. 81-85.
39. Hamilton, I., et al., *Small intestinal permeability in dermatological disease.* Q J Med, 1985. **56**(221): p. 559-67.

40. Harris, C.E., et al., *Intestinal permeability in the critically ill.* Intensive Care Med, 1992. **18**(1): p. 38-41.
41. Koch, F., et al., *Heat stress directly impairs gut integrity and recruits distinct immune cell populations into the bovine intestine.* Proc Natl Acad Sci U S A, 2019. **116**(21): p. 10333-10338.
42. Madara, J.L. and J. Stafford, *Interferon-gamma directly affects barrier function of cultured intestinal epithelial monolayers.* J Clin Invest, 1989. **83**(2): p. 724-7.
43. Muehler, A., et al., *Clinical relevance of intestinal barrier dysfunction in common gastrointestinal diseases.* World J Gastrointest Pathophysiol, 2020. **11**(6): p. 114-130.
44. Pate, R.T., et al., *Immune and metabolic effects of rumen-protected methionine during a heat stress challenge in lactating Holstein cows.* J Anim Sci, 2021. **99**(12).
45. Smyth, D., et al., *Interferon-gamma-induced increases in intestinal epithelial macromolecular permeability requires the Src kinase Fyn.* Lab Invest, 2011. **91**(5): p. 764-77.
46. Ukabam, S.O., R.J. Mann, and B.T. Cooper, *Small intestinal permeability to sugars in patients with atopic eczema.* Br J Dermatol, 1984. **110**(6): p. 649-52.
47. Wallaert, B., et al., *Increased intestinal permeability in active pulmonary sarcoidosis.* Am Rev Respir Dis, 1992. **145**(6): p. 1440-5.
48. Yang, R., et al., *IL-6 is essential for development of gut barrier dysfunction after hemorrhagic shock and resuscitation in mice.* Am J Physiol Gastrointest Liver Physiol, 2003. **285**(3): p. G621-9.
49. Zhang, S., et al., *Short-term feed restriction impairs the absorptive function of the reticulo-rumen and total tract barrier function in beef cattle.* J Anim Sci, 2013. **91**(4): p. 1685-95.
50. Spriggs, D.R., S. Deutsch, and D.W. Kufe, *Genomic structure, induction, and production of TNF-alpha.* Immunol Ser, 1992. **56**: p. 3-34.
51. Grosheva, I., et al., *High-Throughput Screen Identifies Host and Microbiota Regulators of Intestinal Barrier Function.* Gastroenterology, 2020. **159**(5): p. 1807-1823.
52. Hosic, S., et al., *Cholinergic Activation of Primary Human Derived Intestinal Epithelium Does Not Ameliorate TNF-alpha Induced Injury.* Cell Mol Bioeng, 2020. **13**(5): p. 487-505.
53. Lee, C., et al., *TNFalpha Induces LGR5+ Stem Cell Dysfunction In Patients With Crohn's Disease.* Cell Mol Gastroenterol Hepatol, 2022. **13**(3): p. 789-808.
54. Ma, T.Y., et al., *TNF-alpha-induced increase in intestinal epithelial tight junction permeability requires NF-kappa B activation.* Am J Physiol Gastrointest Liver Physiol, 2004. **286**(3): p. G367-76.
55. Tak, L.J., et al., *Superoxide Dismutase 3-Transduced Mesenchymal Stem Cells Preserve Epithelial Tight Junction Barrier in Murine Colitis and Attenuate Inflammatory Damage in Epithelial Organoids.* Int J Mol Sci, 2021. **22**(12).
56. Ma, T.Y., et al., *Mechanism of TNF-alpha modulation of Caco-2 intestinal epithelial tight junction barrier: role of myosin light-chain kinase protein expression.* Am J Physiol Gastrointest Liver Physiol, 2005. **288**(3): p. G422-30.

57. Zolotarevsky, Y., et al., *A membrane-permeant peptide that inhibits MLC kinase restores barrier function in in vitro models of intestinal disease.* Gastroenterology, 2002. **123**(1): p. 163-72.
58. Su, L., et al., *Targeted epithelial tight junction dysfunction causes immune activation and contributes to development of experimental colitis.* Gastroenterology, 2009. **136**(2): p. 551-63.
59. Boivin, M.A., et al., *Mechanism of interferon-gamma-induced increase in T84 intestinal epithelial tight junction.* J Interferon Cytokine Res, 2009. **29**(1): p. 45-54.
60. Bruewer, M., et al., *Interferon-gamma induces internalization of epithelial tight junction proteins via a macropinocytosis-like process.* FASEB J, 2005. **19**(8): p. 923-33.
61. Cunningham, K.E. and J.R. Turner, *Myosin light chain kinase: pulling the strings of epithelial tight junction function.* Ann N Y Acad Sci, 2012. **1258**(1): p. 34-42.
62. Utech, M., et al., *Mechanism of IFN-gamma-induced endocytosis of tight junction proteins: myosin II-dependent vacuolarization of the apical plasma membrane.* Mol Biol Cell, 2005. **16**(10): p. 5040-52.
63. Wang, F., et al., *Interferon-gamma and tumor necrosis factor-alpha synergize to induce intestinal epithelial barrier dysfunction by up-regulating myosin light chain kinase expression.* Am J Pathol, 2005. **166**(2): p. 409-19.
64. Xu, P., et al., *Corticosteroid enhances epithelial barrier function in intestinal organoids derived from patients with Crohn's disease.* J Mol Med (Berl), 2021. **99**(6): p. 805-815.
65. Al-Sadi, R., et al., *Interleukin-6 modulation of intestinal epithelial tight junction permeability is mediated by JNK pathway activation of claudin-2 gene.* PLoS One, 2014. **9**(3): p. e85345.
66. Wiley, J.W., et al., *Histone H3K9 methylation regulates chronic stress and IL-6-induced colon epithelial permeability and visceral pain.* Neurogastroenterol Motil, 2020. **32**(12): p. e13941.
67. Han, X., et al., *Lactobacillus rhamnosus GG prevents epithelial barrier dysfunction induced by interferon-gamma and fecal supernatants from irritable bowel syndrome patients in human intestinal enteroids and colonoids.* Gut Microbes, 2019. **10**(1): p. 59-76.
68. Schroder, K., et al., *Interferon-gamma: an overview of signals, mechanisms and functions.* J Leukoc Biol, 2004. **75**(2): p. 163-89.
69. Youakim, A. and M. Ahdieh, *Interferon-gamma decreases barrier function in T84 cells by reducing ZO-1 levels and disrupting apical actin.* Am J Physiol, 1999. **276**(5): p. G1279-88.
70. Schuhmann, D., et al., *Interfering with interferon-gamma signalling in intestinal epithelial cells: selective inhibition of apoptosis-maintained secretion of anti-inflammatory interleukin-18 binding protein.* Clin Exp Immunol, 2011. **163**(1): p. 65-76.
71. Said, E.A., et al., *Programmed death-1-induced interleukin-10 production by monocytes impairs CD4+ T cell activation during HIV infection.* Nat Med, 2010. **16**(4): p. 452-9.

72. Madsen, K.L., et al., *Interleukin 10 prevents cytokine-induced disruption of T84 monolayer barrier integrity and limits chloride secretion.* Gastroenterology, 1997. **113**(1): p. 151-9.
73. Varma, T.K., et al., *Cellular mechanisms that cause suppressed gamma interferon secretion in endotoxin-tolerant mice.* Infect Immun, 2001. **69**(9): p. 5249-63.
74. Yanagawa, Y., K. Iwabuchi, and K. Onoe, *Co-operative action of interleukin-10 and interferon-gamma to regulate dendritic cell functions.* Immunology, 2009. **127**(3): p. 345-53.
75. Inzucchi, S.E., *Diagnosis of diabetes.* N Engl J Med, 2013. **368**(2): p. 193.
76. Paroni, R., et al., *Lactulose and mannitol intestinal permeability detected by capillary electrophoresis.* J Chromatogr B Analyt Technol Biomed Life Sci, 2006. **834**(1-2): p. 183-7.
77. Secondulfo, M., et al., *Ultrastructural mucosal alterations and increased intestinal permeability in non-celiac, type I diabetic patients.* Dig Liver Dis, 2004. **36**(1): p. 35-45.
78. Dallmeier, D., et al., *Metabolic syndrome and inflammatory biomarkers: a community-based cross-sectional study at the Framingham Heart Study.* Diabetol Metab Syndr, 2012. **4**(1): p. 28.
79. DeFronzo, R.A., *Pathogenesis of type 2 diabetes mellitus.* Med Clin North Am, 2004. **88**(4): p. 787-835, ix.
80. Feuerer, M., et al., *How punctual ablation of regulatory T cells unleashes an autoimmune lesion within the pancreatic islets.* Immunity, 2009. **31**(4): p. 654-64.
81. Tsalamandris, S., et al., *The Role of Inflammation in Diabetes: Current Concepts and Future Perspectives.* Eur Cardiol, 2019. **14**(1): p. 50-59.
82. Bagyanszki, M. and N. Bodi, *Diabetes-related alterations in the enteric nervous system and its microenvironment.* World J Diabetes, 2012. **3**(5): p. 80-93.
83. Bodi, N., et al., *Gut region-specific diabetic damage to the capillary endothelium adjacent to the myenteric plexus.* Microcirculation, 2012. **19**(4): p. 316-26.
84. Chandrasekharan, B., et al., *Colonic motor dysfunction in human diabetes is associated with enteric neuronal loss and increased oxidative stress.* Neurogastroenterol Motil, 2011. **23**(2): p. 131-8, e26.
85. Furlan, M.M., S.L. Molinari, and M.H. Miranda Neto, *Morphoquantitative effects of acute diabetes on the myenteric neurons of the proximal colon of adult rats.* Arq Neuropsiquiatr, 2002. **60**(3-A): p. 576-81.
86. Zanoni, J.N., et al., *Morphological and quantitative analysis of the neurons of the myenteric plexus of the cecum of streptozotocin-induced diabetic rats.* Arq Neuropsiquiatr, 1997. **55**(4): p. 696-702.
87. Graham, M.L., et al., *The streptozotocin-induced diabetic nude mouse model: differences between animals from different sources.* Comp Med, 2011. **61**(4): p. 356-60.
88. Do, M.H., et al., *High-Glucose or -Fructose Diet Cause Changes of the Gut Microbiota and Metabolic Disorders in Mice without Body Weight Change.* Nutrients, 2018. **10**(6).

89. Zhang, X., et al., *Glucose but Not Fructose Alters the Intestinal Paracellular Permeability in Association With Gut Inflammation and Dysbiosis in Mice.* Front Immunol, 2021. **12**: p. 742584.
90. Atisook, K. and J.L. Madara, *An oligopeptide permeates intestinal tight junctions at glucose-elicited dilatations. Implications for oligopeptide absorption.* Gastroenterology, 1991. **100**(3): p. 719-24.
91. Madara, J.L. and J.R. Pappenheimer, *Structural basis for physiological regulation of paracellular pathways in intestinal epithelia.* J Membr Biol, 1987. **100**(2): p. 149-64.
92. Pappenheimer, J.R. and K.Z. Reiss, *Contribution of solvent drag through intercellular junctions to absorption of nutrients by the small intestine of the rat.* J Membr Biol, 1987. **100**(2): p. 123-36.
93. Atisook, K., S. Carlson, and J.L. Madara, *Effects of phlorizin and sodium on glucose-elicited alterations of cell junctions in intestinal epithelia.* Am J Physiol, 1990. **258**(1 Pt 1): p. C77-85.
94. Crakes, K.R., et al., *Fenofibrate promotes PPARalpha-targeted recovery of the intestinal epithelial barrier at the host-microbe interface in dogs with diabetes mellitus.* Sci Rep, 2021. **11**(1): p. 13454.

Chapter 3: Inflammatory Cytokines Directly Disrupt the Bovine Intestinal Epithelial Barrier

Charles K. Crawford, Veronica Lopez Cervantes, Mary L. Quilici, Aníbal G. Armién, María Questa, Muhammad S. Matloob, Leon D. Huynh, Aeelin Beltran, Sophie J. Karchemskiy, Katti R. Crakes, and Amir Kol

Abstract

The small intestinal mucosa constitutes a physical barrier separating the gut lumen from sterile internal tissues. Junctional complexes between cells regulate transport across the barrier, preventing water loss and the entry of noxious molecules or pathogens. Inflammatory diseases in cattle disrupt this barrier; nonetheless, mechanisms of barrier disruption in cattle are poorly understood. We investigated the direct effects of three inflammatory cytokines, TNFα, IFNγ, and IL-18, on the bovine intestinal barrier utilizing intestinal organoids. Flux of fluorescein isothiocyanate (FITC)-labeled dextran was used to investigate barrier permeability. Immunocytochemistry and transmission electron microscopy were used to investigate junctional morphology, specifically tortuosity and length/width, respectively. Immunocytochemistry and flow cytometry were used to investigate cellular turnover via proliferation and apoptosis. Our study shows that 24-hour cytokine treatment with TNFα or IFNγ significantly increased dextran permeability and tight junctional tortuosity, and reduced cellular proliferation. TNFα reduced the percentage of G2/M phase cells, and IFNγ treatment increased cell apoptotic rate. IL-18 did not directly induce significant changes to barrier permeability or cellular turnover. Our study concludes that the inflammatory cytokines, TNFα and IFNγ, directly induce intestinal epithelial barrier dysfunction and alter the tight junctional morphology and rate of cellular turnover in bovine intestinal epithelial cells.

Introduction

The gastrointestinal (GI) tract comprises an extensive interface between an organism's internal and external environments; it is responsible for various functions including nutrient digestion and absorption, hormone production, and it plays a primary role as a physical barrier between the luminal content of the GI tract and internal, sterile, tissues [1]. As a selective barrier with a primary goal of facilitating nutrient and water absorption, the GI tract must also prevent the entry of harmful substances/organisms, while also preventing the loss of water and beneficial solutes (ions, macromolecules etc.) [2]. The integrity of this barrier and the resulting permeability is influenced by numerous factors, one of note being inflammation. Human patients with varied inflammatory diseases such as eczema, psoriasis, pulmonary sarcoidosis, pancreatitis, and shock were found to have intestinal barrier disruption shown by differential sugar or 51Cr-EDTA absorption tests [3-6]. These clinical observations are supported by experimental data in mice [7, 8] and in human cell lines [9-12] that indicate a direct role of inflammatory cytokines in intestinal barrier dysfunction. Systemic inflammation commonly affects cattle in modern dairy operations, and inflammatory diseases such as metritis, ruminitis, and mastitis as well as metabolic diseases, such as ketosis, negatively influence the health and wellbeing of the animals and result in reduced milk output, weight gain, reproduction, and survivorship [13-16]. Furthermore, there is a monetary cost of potentially up to $500 per affected animal including veterinary, labor, and reduced production costs [14]. Inflammatory diseases and other inflammatory stressors in cattle, such as heat stress and reduced feeding, coincide with disruption to the intestinal barrier [17-21]. While there is extensive focus on the inflammation caused

by these diseases, it is not fully understood if the concomitant systemic inflammation induces intestinal barrier dysfunction in these cattle – a potentially underappreciated consequence that may be addressed to improve the livelihood and production of these agricultural animals.

The intestinal mucosa contains a continuous monolayer of specialized columnar epithelial cells that form a critical component of the barrier [22]. A pool of intestinal stem cells in the intestinal crypts proliferates and differentiates into specialized cell types to maintain the barrier as older cells slough off into the intestinal lumen [23]. The integrity of the epithelial cell surface is maintained by the junctional complexes, tight junctions, adherens junctions, and desmosomes which altogether regulate paracellular permeability [24]. Adherens junctions and desmosomes are more basolateral than tight junctions and form adhesive bonds that maintain the epithelial layer [25]. Tight junctions seal the intercellular space and are the most apical of the complexes; they contain the transmembrane proteins claudins and occludins, as well as regulatory proteins and the peripheral membrane proteins zonula occludens-1 (ZO-1) and zonula occludens-2 (ZO-2) [25].

The mechanisms by which systemic inflammation may induce disruption of the intestinal barrier are multifaceted but not well understood in cattle. We have chosen to investigate the direct effects of three prototypical pro-inflammatory cytokines that are synthesized by three different cellular sources: epithelial cells (Interleukin-18), innate immune cells (tumor necrosis factor-α), and adaptive immune cells (interferon-γ) [26-28]. Interleukin-18 (IL-18) is produced by epithelial cells following inflammasome

activation [29] and induces the production of tumor necrosis factor-α (TNFα) and interferon-γ (IFNγ) in specialized immune cells [30]. It also acts as an autocrine/paracrine signal influencing intestinal goblet cell development, and inhibition of IL-18 signaling reduces mucus production and induces resultant mucosal damage in mice [31]. TNFα is a potent pro-inflammatory cytokine primarily produced by activated monocytes and macrophages [28]. IFNγ is produced by T lymphocytes and other specialized immune cells to aid in the adaptive immune response, especially in response to viral infection [27]. High levels of plasma TNFα and/or IFNγ have been recorded in multiple bovine inflammatory disorders such as metritis and rumenitis [15, 32-35]. In *in vitro* epithelial monolayers – Caco2 and T84 human cell lines – treatment with TNFα and/or IFNγ disrupts the epithelial barrier as measured by transepithelial electrical resistance, bacterial translocation, or molecular flux [9-12]. Coinciding with the increased epithelial permeability, treatment with these two cytokines also altered the integrity and morphology of tight junction proteins [9, 10]. Altogether, these three cytokines are tightly linked during the inflammatory process *in vivo*, and we utilized isolated *in vitro* treatments to determine their individual effects and contributions to inflammation-induced barrier disruption in the bovine gut.

We hypothesized that inflammatory cytokines directly disrupt the bovine intestinal barrier by altering tight junction structure and cell cycle. To further investigate these direct effects of inflammatory cytokines on intestinal barrier permeability in cattle, we utilize intestinal organoids (enteroids) derived from primary intestinal tissue as a relevant *in vitro* model [36]. We found that inflammatory cytokine treatment, specifically

TNFα or IFNγ, increases the barrier permeability, increases junctional tortuosity, and disrupts epithelial cell cycle in bovine enteroids.

Materials and Methods

Animals and Enteroid Generation: Tissue samples were obtained from cows according to a protocol approved by the Institutional Animal Care and Use Committee (IACUC) at UC Davis (protocol #21553). Tissues were collected from animals sacrificed for a separate study (IACUC protocol #21553) in accordance with American Veterinary Medical Association guidelines for the human slaughter of animals. No experiments in this study were conducted on live animals. Approximately 10cm-long segments of jejunum and ileum were harvested from cows immediately post-mortem and placed in cold PBS with 25µg/mL gentamicin (Thermo Fisher) and 100U/mL penicillin/streptomycin (Gibco) and processed as previously described, with slight modifications described as follows [37, 38]. The intestine was cut longitudinally and washed in PBS with gentamicin and penicillin/streptomycin. The mucosa was separated with a glass slide, minced with scissors, and placed into a 50mL Falcon tube with cold PBS, gentamicin, and penicillin/streptomycin. The tube was shaken, and tissue fragments were allowed to settle before the supernatant was removed. This process was repeated until the supernatant was clear. Tubes were then centrifuged for 2 minutes at 200g, the supernatant was removed, and tissue was placed in a new 50mL Falcon tube in 0.8mM EDTA solution and incubated for 30 minutes at 4°C with agitation to liberate intestinal crypts. After incubation, the tube was vigorously shaken, then centrifuged for 2 mins at 400g. Supernatant was discarded, and the pellet was reconstituted in 25mL of PBS, gentamicin, and penicillin/streptomycin. The tube was

shaken, allowed to settle, and supernatant was passed through a 70µm strainer into a new collection tube. This step was repeated. Tubes were centrifuged for 3 mins at 100g, supernatant was removed, and crypts were reconstituted in DMEM/F12 media containing 1X B27 Supplement minus Vitamin A, 25µg/mL gentamicin, and 100U/mL penicillin/streptomycin. Crypts were then counted via a hemocytometer. The appropriate volume was extracted to plate 300 crypts per well. 20µL of crypt solution was combined with 30µL of ice-cold Matrigel™ (Corning) per well. 50µL droplets were set in the center of a well of a pre-warmed 24 well plate. These domes were incubated at 37°C for 10 mins. 700µL of Intesticult™ (Stemcell Technologies) growth media supplemented with 100U/mL penicillin/streptomycin, 25µg/mL gentamicin (only for primary culture), 100mM Y-27632 (Tocris Bioscience), and 3µM CHIR99021 (Tocris Bioscience) . Y-27632 and CHIR99021 were used during initial organoid propagation and for the first 2-3 days after each passage. Media was changed every 3 days and organoids passaged mechanically every 7-10 days.

Cytokine Treatment: Enteroids were treated with 100ng/mL of recombinant bovine TNFα (Invitrogen), IFNγ (Thermo Scientific), or IL-18 (Kingfisher Biotech) in Intesticult growth media on the fourth day following passage for a duration of 24 hours. Following treatment, cytokine-treated growth media was removed, and organoids were prepared for downstream analysis.

Immunofluorescence (IF): Organoids were cultured in 8-well chamber slides (Thermo Scientific) for immunocytochemical staining. Media was removed and organoids were fixed in 4% paraformaldehyde (PFA) for 20 minutes at room temperature. Afterwards,

organoids were permeabilized in PBS containing 0.5% Triton X-100 for 20 minutes at room temperature. Wells were washed in IF buffer (PBS containing 0.2% Triton X-10 and .05% Tween) and then blocked in IF buffer containing 1% BSA for 30 mins at room temperature. After blocking, organoids were incubated in IF buffer containing 1% bovine serum albumin (BSA) with primary antibodies overnight at 4°C. Organoids were then washed in IF buffer, then incubated in blocking solution with secondary antibodies for 1 hour at room temperature. The following primary antibodies were used in this study: ZO-1 (Zo1-1A12, Invitrogen), Occludin (Polyclonal REF#71-1500, Invitrogen), Ki67 (SP6, Invitrogen) and Cleaved Caspase-3 (D175, Cell Signaling). Organoids were washed, then incubated in 0.1% DAPI in IF buffer for 10 mins at room temperature. The gasket of the chamber slide was then removed, one drop of ProLong Gold antifade reagent (Invitrogen) was placed into well sections, and the slide was covered with a coverslip and allowed to cure for 24 hours before being placed in 4°C protected from light until imaging.

FITC Dextran Permeability Assay: Enteroids cultured in 8-well chamber slides were cultured in Intesticult growth media supplemented with 5µg/mL 4kDa or 70kDa fluorescein isothiocyanate-dextran (FITC) for 1 hour, then washed in PBS and imaged with a EVOS M5000 fluorescent microscope (Thermo Fisher), as modified from previous whole-enteroid FITC dextran permeability experiments [39, 40]. FITC intensity inside of the enteroids (three data points per enteroid) was measured and normalized to FITC intensity outside of the enteroids (three data points averaged per enteroid) using an image analysis software (ImageJ).

Cell Cycle Analyses: Enteroids were dissociated into a single cell suspension using TrypLE™ Express (Thermo Fisher) and a 40µm cell strainer (Fisher Scientific). Cells were fixed in 70% ethanol and stained with the Muse Cell Cycle Kit according to the manufacturer's instructions (Millipore, Hayward, CA). After staining, data was captured with a Muse Cell Analyzer (Millipore, Hayward, CA).

Tortuosity Analysis: Following immunofluorescent staining for the tight junction proteins, ZO-1 or Occludin, images were acquired using a TCS SP8 STED 3X confocal microscope (Leica Microsystems). Images were then processed utilizing the image analysis software (ImageJ) via a morphological segmentation plug-in, allowing for tortuosity calculation: the ratio of segment length and the Euclidian distance between the 2 points that define that given segment [41].

Electron Microscopy: Enteroids were gently removed from wells using a cell scraper and cut P1000 micropipette tip and placed in Karnovsky's fixative (3% glutaraldehyde and 2% formaldehyde in 0.1M phosphate buffer, pH 7.4.; all reagents were obtained from Electron Microscopy Sciences, Hatfield, PA, USA). Samples were submitted to the California Animal Health & Food Safety Laboratory (Davis, CA) for transmission electron microscopy processing, as previously described [42]. Briefly, organoids were postfixed with 1% osmium tetroxide in 0.1M sodium cacodylate buffer and were dehydrated using a 25%–100% ethyl alcohol gradient. Organoids were then infiltrated with 2:1 ethanol: EMbed 812 resin for 1 hour and subsequently transferred to a 1:2 ethanol: EMbed 812 resin mixture for 1 hour. Organoids were further infiltrated with 100% resin and were embedded and incubated at 58˚C for 24 hours to polymerize the resin. Embedded

samples were trimmed and sectioned on a Leica UC6 ultramicrotome (Leica Microsystems, Vienna, Austria). Thin sections (60–70nm) were obtained and collected on a 200 mesh Nickle grid (Electron Microscopy Sciences, Hatfield, PA, USA). Grids were contrasted with 5% uranyl acetate for 20 minutes and Sato's lead citrate for 6 minutes.All samples were visualized using a JEOL 1400 transmission electron microscope (JEOL LTD, Tokyo, Japan). Images were obtained and analyzed using a OneView camera system Model 1095, 16 megapixels with the Gatan Microscope Suite (GMS3.0) (Gatan Inc, Pleasanton, CA, USA). Tight junctions were identified via morphology, location, and electron density as described previously [43, 44].

Statistical Analysis: Experiments were conducted in three enteroid lines: C1, C2, and C3. Data collected from 4kDa FITC imaging (N=2505), Ki67 staining (N=536), and Cleaved Caspase-3 staining (N=653) for three different enteroid lines were nested and analyzed via nested ANOVA (α=0.05) utilizing Holm- Šídák post hoc analysis. 70kDa FITC (N=5409) data were acquired from experiments conducted on two enteroid lines and analyzed via nested ANOVA (α=0.05) utilizing Holm- Šídák post hoc analysis. Data from the 4kDa FITC positive control experiment (untreated n=120, EGTA n=180) were analyzed via a one-tailed Mann-Whitney non-parametric test (α=0.05). Data from ZO-1 (N=3306) and Occludin (N=2562) tortuosity analysis for one enteroid line were analyzed via Kruskal-Wallis non-parametric ANOVA (α=0.05) utilizing Dunn's post hoc analysis. Data from cell cycle analysis (N=72) from three enteroid lines were aggregated and analyzed via two-way ANOVA (α=0.05) utilizing Dunnet post hoc analysis. Values of tight junction lengths (N=223) and widths (N=237) collected via electron microscopy for two enteroid lines were aggregated and analyzed via Kruskal-Wallis non-parametric

ANOVA (α=0.05) utilizing Dunn's post hoc analysis. Every experiment was conducted at least two times each.

Results

TNFα and IFNγ treatment disrupts normal enteroid morphology

Our bovine enteroids replicate the native gut micro-anatomy and display crypt-like domains with a central lumen (Fig 1A). Low magnification (Fig 1B) and high magnification (Fig 1C) transmission electron microscopy (TEM) images of a bovine enteroid show microvilli protruding from enteroid cells towards to enteroid lumen confirming enterocyte cell identity. TEM further demonstrates apical tight junctions (Fig 1C). ZO-1 staining (Fig 1D) and 3D image analysis further demonstrates the apical positioning of the tight junctions (Fig 1E and F).

Bovine enteroids that were generated from 3 different cows, were treated with the inflammatory cytokine TNFα, IFNγ, or IL-18 at a concentration of 100ng/mL for 24 and 48 hours. Over the course of 48 hours, untreated and IL-18-treated enteroids displayed unremarkable morphology consistent with extended enteroid culture: increased enteroid density, increased budding of enteroids, and slight darkening of the lumen (Fig 2). However, enteroids treated with 100ng/mL of TNFα or IFNγ displayed an increased darkening of the enclosed lumen, and enteroids treated with IFNγ also displayed irregular and ruffled basolateral margins. These morphological changes suggest an increased rate of dead cell accumulation within the enteroid lumen.

TNFα and IFNγ treatment induces increased barrier permeability in bovine enteroids

We hypothesized that these deleterious morphologic changes are associated with increased permeability. To test our hypothesis and determine the underpinning mechanisms we determined the direct impact these inflammatory cytokines have on organoid dextran permeability utilizing a FITC dextran permeability assay (Fig 3). 24-hour cytokine treatment did induce a significant effect on 4kDa barrier permeability ($p=0.0097$); treatment of either TNFα or IFNγ increased the enteroid permeability to 4kDa dextran and induced a significant increase in normalized FITC intensity relative to untreated enteroids ($p=0.0257$, $p=0.0132$, respectively) (Fig 3G). 24-hour cytokine treatment also induced a significant effect on 70kDa barrier permeability ($p=0.039$); TNFα or IFNγ trended towards inducing an effect ($p=0.053$ $p=0.063$, respectively) (Fig 3H). There was no apparent effect of IL-18 treatment on 4kDa or 70kDa dextran permeability.

TNFα and IFNγ treatment induces altered tight junction conformation

As tight junctions are the primary structure that regulates paracellular movement of water and solutes, we set to determine how inflammatory cytokines impact tight junction structure and spatial conformation. The tortuosity of tight junctions was determined and analyzed through ZO-1 and Occludin immunocytochemistry and image analysis. 24-hour treatment of either TNFα or IFNγ induced a significant increase in junctional tortuosity of ZO-1 ($p<0.0001$ for each treatment) (Fig 4). There was no significant effect of IL-18 treatment on junctional tortuosity. 24-hour treatment of IFNγ induced a significant increase in Occludin tortuosity ($p<0.0001$).

To further investigate the morphology of tight junctions following cytokine treatment, TEM was utilized to measure junctional width and length. Ultrastructure analysis of tight junctions following 24-hour cytokine treatment was determined by TEM. Tight junctions were identified by morphology, location, and electron density as guided by previous work [43, 44], and the length width of the tight junctions were measured. No apparent change in tight junction length or width was induced by cytokine treatment (Fig 5).

TNFα and IFNγ treatment reduces cellular proliferation in bovine enteroids

Changes in cellular turnover may lead to junctional morphological changes as cytoskeletal tension may be altered, leading to a more severe barrier injury, as suggested by the increase in 70kDa permeability. To investigate this, we analyzed cellular proliferation in our organoids and measured the proportion of Ki67-positive cells. Treatment with TNFα (100ng/mL) (0.0703 ± 0.006, Mean ± SEM) or IFNγ (100ng/mL) (0.121 ± 0.009) significantly reduced the proportion of Ki67-positive cells in bovine enteroids ($p=0.0031$, $p=0.0072$, respectively) relative to untreated enteroids (0.349 ± 0.01), thus indicating a reduction in cellular proliferation in these treated enteroids (Fig 6). Enteroids treated with IL-18 (100ng/mL) (0.3352 ± 0.01) did not exhibit any significant changes in Ki67+ cell fraction.

Cell cycle analysis indicated that TNFα treatment significantly increased the percentage of cells in the G0/G1 phase ($p=0.0003$) and significantly decreased the percentage of cells in the G2/M phase ($p=0.0379$) relative to untreated enteroids (Fig 6).

IFNγ and IL-18-treated cells did not display a significant change in cell cycle phase percentages.

IFNγ treatment increases apoptosis in bovine enteroids

Further investigating the effects of cytokine treatment on cellular turnover, we also investigated the apoptotic cell rate in our organoids. IFNγ (100ng/mL) treatment induced a significant increase in Cleaved Caspase-3 positive cells relative to untreated enteroids ($p=0.0325$). TNFα treatment trended towards increasing apoptotic cell rate but was not significant ($p=0.1190$). IL-18 treatment did not cause any effect on apoptotic cell rate.

Discussion

'Leaky gut' and downstream metabolic derangements due to intestinal barrier dysfunction are recognized in multiple common diseases of cattle such as rumen acidosis, heat stress, reduced feed intake, and ketosis, though the mechanism of action is poorly understood [17-21]. Inflammation is a shared pathway in all of these pathologies and is known to directly contribute to gut barrier dysfunction in murine models and human intestinal cell lines. Generating comprehensive insight into these cow-specific molecular and cellular pathways may lead to the discovery of novel therapeutics to target the intestinal pathology that coincides with inflammatory diseases. We utilized intestinal organoids to provide us with a physiologically relevant *in vitro* model capable of extended culture to enable direct investigation of these mechanisms in cattle. By using this model, we have established that the key inflammatory cytokines TNFα and IFNγ, but not IL-18, directly disrupt the intestinal epithelial cell cycle and tight

junction conformation, leading to increased barrier permeability. This is the first study that investigates the impact of inflammatory cytokines on gut barrier function in a bovine-specific intestinal epithelium model.

We chose to study the impact of IFN-γ, TNF-α, and IL-18 on gut barrier function in cows because of their relevance to immune function in the gut and their different cellular pathways. Elevated circulating levels of TNFα, a cytokine released by activated immune cells, especially monocytes and macrophages [28], and IFNγ, a cytokine released by T lymphocytes and specialized immune cells [27] are associated with bovine inflammatory diseases and accompanying intestinal barrier dysfunction [15, 32-35, 45]. IL-18, on the other hand, is produced by the epithelial cells themselves, and its primary function is to stimulate immune cells and induce downstream release of proinflammatory cytokines [46].

IFN-γ and TNF-α treatments, but not IL-18, disrupted intestinal barrier function as evident by the increased movement of 4kDa-dextran across the epithelial surface (Fig 3G). A larger, 70kDa-dextran displayed a mitigated effect compared to the 4kDa dextran (Fig 3G and H), showing reduced permeability to larger molecules. Accompanying the increase in permeability were morphological changes including luminal darkening and shedding of cells (Fig 2). Our findings are consistent with previous studies in other species' organoids or cell lines [12, 47, 48], but extend upon these previous findings to show the effects of specifically treating bovine intestinal epithelium with bovine inflammatory cytokines via an organoid system. Maintaining an effective barrier between the basolateral and apical sides of the epithelium is a critical role of the

intestinal epithelium, and the associated change to barrier permeability accompanying cytokine treatment indicates damage to and reduced function of the intestinal epithelial barrier.

Given the significance of tight junctions in maintaining the barrier function and the deleterious effects of IFNγ and TNFα identified in human and non-human animal cell lines [49-55], we hypothesized that IFNγ and TNFα increase intestinal epithelial permeability in cattle via the disruption of tight junctions. Tight junctions are critical structures in the regulation of paracellular permeability of small molecules, and exposure to cytotoxic compounds alters tight junctions and increases paracellular permeability [56, 57]. Downregulation of barrier-relevant tight junction proteins does not coincide with infection-induced barrier disruption in cultured epithelial cells [58]. However, the tortuosity of epithelial tight junctions is a measurable morphological trait that does coincide with a disrupted intestinal barrier [59]. Furthermore, increased cellular proliferation or inhibition of Rho kinase, and consequent inhibition of apoptosis, decrease the tortuosity in MDCK epithelial cell tight junctions [60]. Therefore, we have investigated tight junction conformation, specifically tortuosity, to further elucidate the mechanisms of permeability alteration observed in our study. Our findings show that treatment of bovine intestinal organoids with either TNFα or IFNγ does increase tight junctional tortuosity (Fig 4), consistent with tortuosity changes seen in other models of barrier disruption [59, 60], supporting a mechanistic role of tight junction conformation in bovine inflammation-induced gut barrier dysfunction. Despite the rise in tortuosity caused by cytokine treatment, there was no discernible difference in tight junction length

or width, as measured by electron microscopy coinciding with cytokine treatment (Fig 5).

While the increased movement of molecules across the paracellular pathway due to disrupted tight junctions can explain the increased gut permeability noted in vivo and in our in vitro model, we wanted to further investigate the role of cellular integrity and turnover as a potential additional factor. A healthy intestinal epithelium undergoes immense cellular turnover and completely regenerates over the course of four to five days [23], and excessive cell death may lead to barrier dysfunction and translocation of pathogens [61]. Moreover, inhibition of apoptosis ameliorates barrier dysfunction induced by *C. jejuni* infection in cultured HT-29/B6-GR/MR epithelial cells [58]. We hypothesized that cytokine treatment would negatively affect cellular turnover by reducing cellular proliferation and stimulating cell death. Treatment of bovine intestinal organoids with either TNFα or IFNγ reduced cellular proliferation as measured through immunocytochemical staining, and cell cycle analysis displayed an increase of cells in the G0/G1 phase and a reduction of cells in the G2/M phase when the organoids were treated with TNFα (Fig 6). Furthermore, IFNγ treatment also induced a rise in apoptosis (Fig 7). Altogether, whether by reducing proliferation via TNFα or IFNγ or stimulating apoptosis via IFNγ, inflammatory cytokines disrupt the cellular turnover of the epithelium in bovine intestinal organoids thus influencing the replacement of lost epithelial tissue. Our findings corroborate others that show a rise in apoptosis following cytokine or infection-induced barrier dysfunction [62-64]. One potential mechanism for the phenomena observed in our study could involve the activation of Rho GTPase via TNFα and IFNγ, which causes an increase in cell extrusions and the persistence of single cell

lesions [64, 65], and Rho kinase activation alters cytoskeletal forces and causes an increase in tight junctional tortuosity [60]. Reduced cellular turnover resulting in an altered tension on cytoskeletal actin filaments could explain the causative mechanism of increased permeability seen in our bovine intestinal organoids and would be sensible considering the reduced cellular proliferation and increased cellular death shown in our study.

Our study is not without limitations. While our organoid culture system does improve on the physiological relevance and translatability to native intestine compared to traditional cell line culture, the organoids are comprised of only intestinal epithelial cells and do not include other cell types seen in the gut such as professional immune cells and smooth muscle cells. Additionally, though our cytokine treatments are consistent with other published *in-vitro* treatments [66-69] at supraphysiologic concentrations and for relatively short periods of time, unlike chronic inflammatory conditions in-vivo which result in lower concentrations of cytokines for far longer time frames.

In conclusion, these data show that treatment with the inflammatory cytokines, TNFα or IFNγ, directly disrupts the epithelial barrier, leads to more tortuous tight junctions, and alters cellular turnover in bovine intestinal organoids. These effects were not observed when intestinal organoids were treated with IL-18. These findings further clarify the influence of systemic inflammation on the bovine gut and expand on the role of bovine intestinal organoids as a model to investigate the bovine gut and related pathologies.

Figures

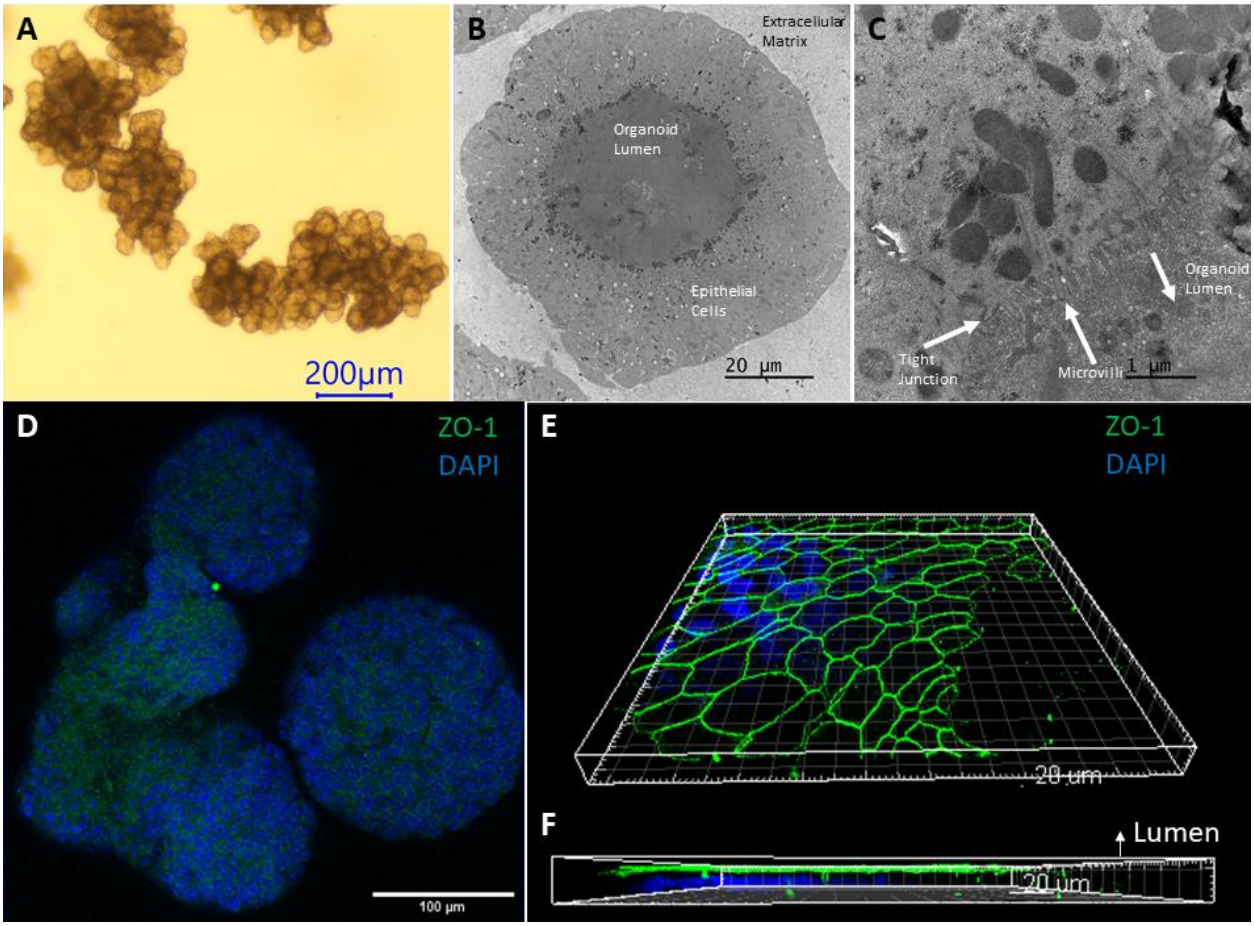

Figure 1. Bovine intestinal organoid characterization **A)** Brightfield image of a bovine enteroid using a 4x objective lens. Scale bar denotes 200µm. **B,C)** Transmission electron microscopy images of a bovine enteroid with annotated microvilli, tight junction, and lumen. **D)** Whole mount Immunocytochemical imaging of ZO-1 (Alexa Fluor 488) and DAPI using a 20x objective lens **E,F)** 3D modeling (Imaris Image Software) of ZO-1 (Alexa Fluor 488) and DAPI staining using stacked confocal images taken with a 100x objective lens, with annotated lumen, displaying the apical border of an enteroid.

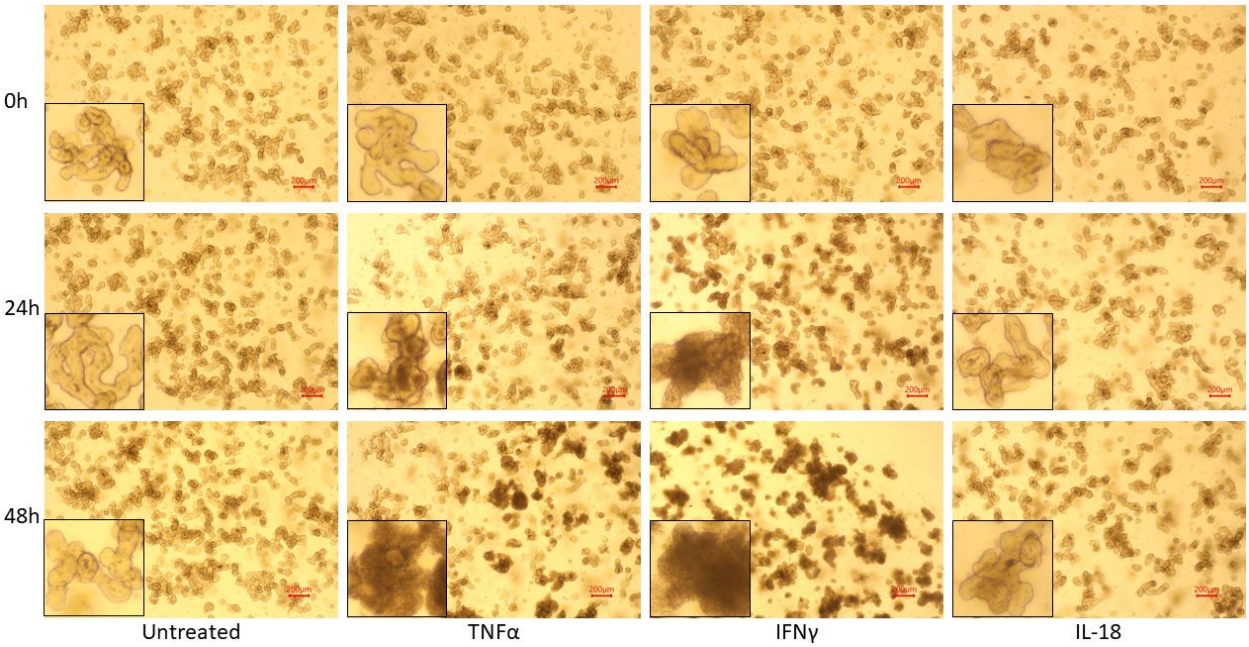

Figure 2. Morphological changes induced by cytokine treatment. Brightfield microscopy images of bovine intestinal organoids using a 4x objective lens, treated with inflammatory cytokines for 24 and 48 hours. Bottom left corners display a zoomed-in enteroid from each image. Scale bars denote 200µm.

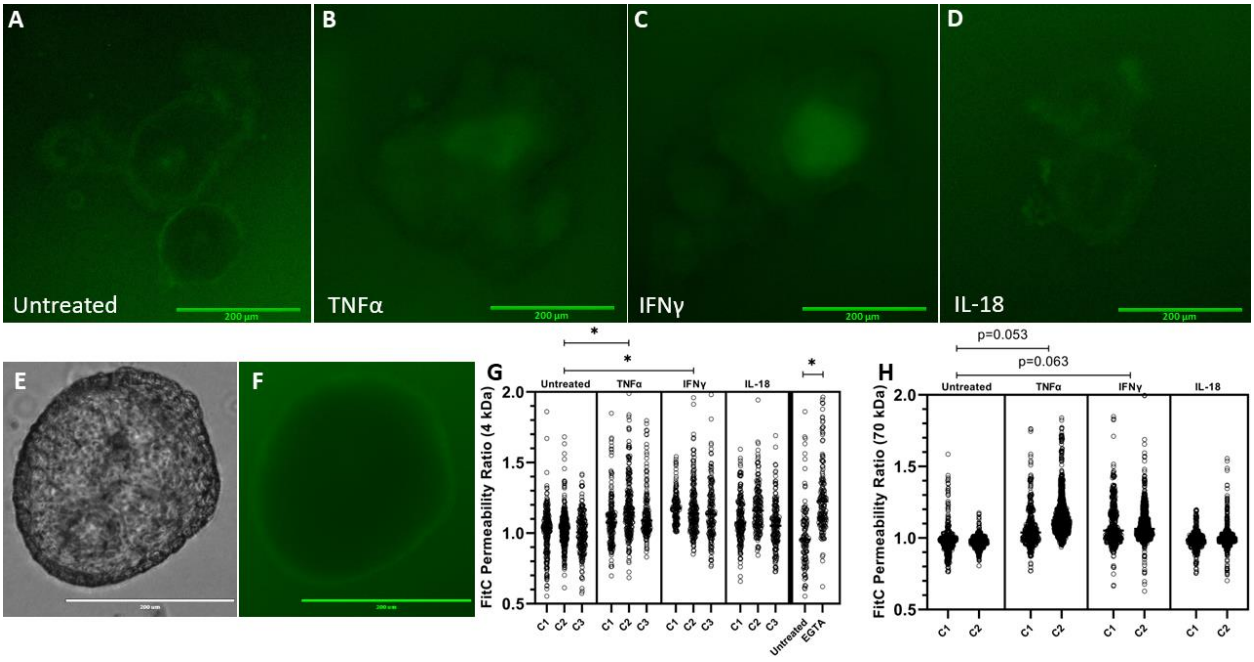

Figure 3. Cytokine treatment increases bovine intestinal organoid barrier permeability, as measured by FITC Dextran permeability. **A-D)** Representative images of bovine intestinal organoids exposed to 4kDa FITC Dextran following 24 h cytokine treatment acquired using a 10x objective lens and GFP (470/525 nm ex/em) LED light cube. Scale bars denote 200µm. **E,F)** Representative images of an untreated enteroid following 70kDa FITC Dextran exposure collected using a 20x objective lens and brightfield or GFP LED light cube. Scale bars denote 300µm. **G,H)** Luminal FITC intensity normalized to external FITC intensity following 24h cytokine treatment or two-hour treatment with 2mM EGTA as a positive control. C1, C2, and C3 indicate individual enteroid lines. Nested ANOVA (α=0.05) determined a significant effect of treatment was present for both 4kDa and 70kDa FITC Dextran (p=0.0097 and p=0.039, respectively). TNFα and IFNγ increase 4kDa FITC Dextran permeability (p=0.0257, p=0.0132, respectively) as determined by Holm-Šídák post hoc analysis. EGTA, a positive control, increases FITC Dextran permeability (p<0.0001) determined by one-tailed Mann-Whitney non-parametric test (α=0.05). Holm-Šídák post hoc analysis for 70kDa FITC Dextran displayed trending, but not significant, effects of TNFα and IFNγ treatment (p=0.052 and p=0.063, respectively).

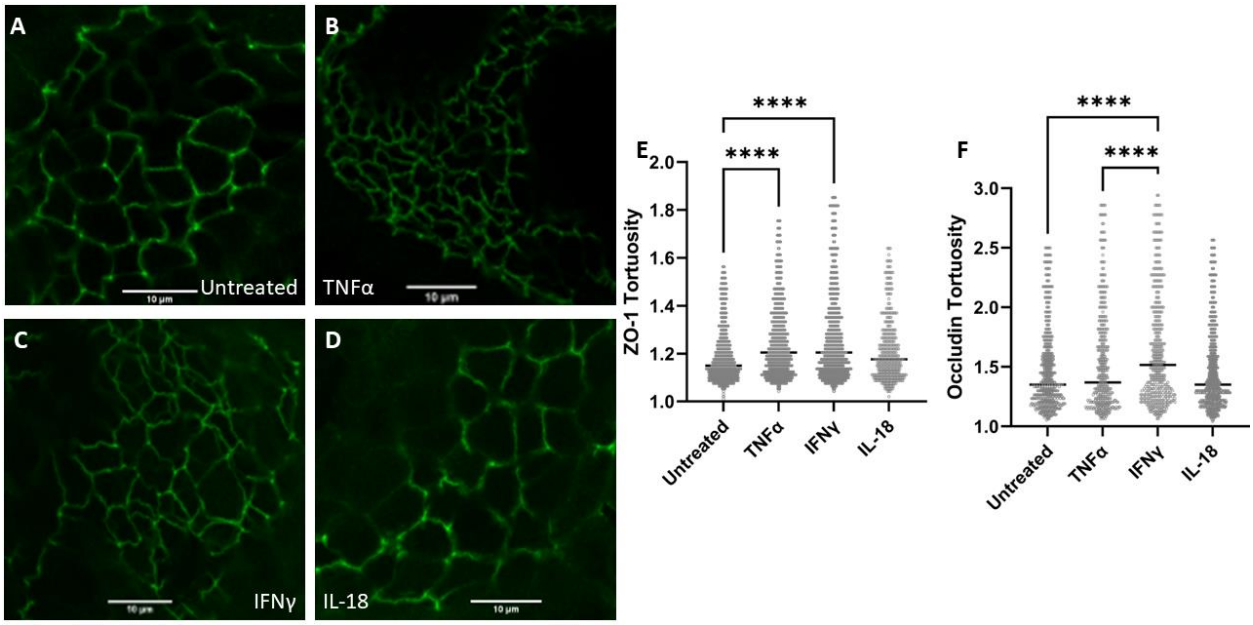

Figure 4. Cytokine treatment alters tight junction tortuosity. **A-D)** Representative ZO-1 (Alexa Fluor 488) staining of bovine intestinal organoids using a 100x objective lens following 24-hour cytokine treatment. Scale bars denote 10µm **E)** Quantification of ZO-1 tortuosity in cytokine-treated intestinal organoids. TNFα-treated bovine enteroids and IFNγ-treated bovine enteroids displayed a significant increase in junctional tortuosity ($p<0.0001$ for each treatment) determined by Kruskal-Wallis non-parametric ANOVA ($\alpha=0.05$) utilizing Dunn's post hoc analysis. **F)** Quantification of Occludin tortuosity in cytokine-treated intestinal organoids. IFNγ-treated bovine enteroids displayed a significant increase in Occludin tortuosity ($p<0.0001$) relative to all other treatments. **** denotes $p<0.0001$.

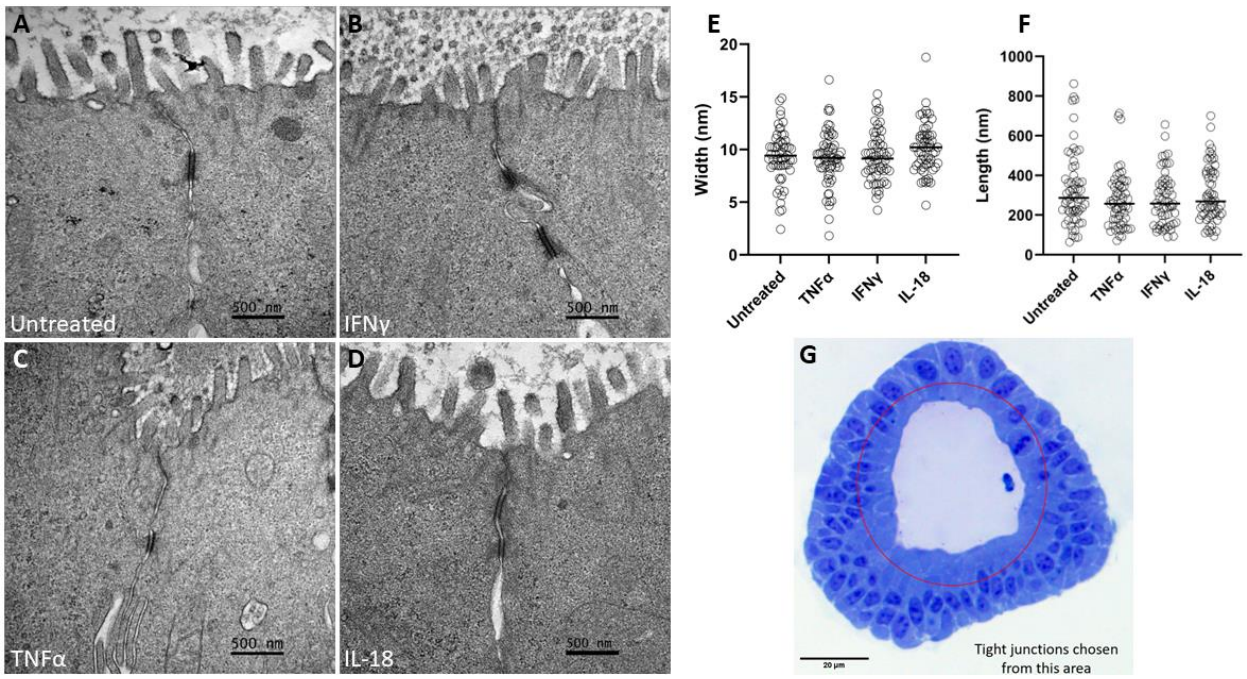

Figure 5. Cytokine treatment does not alter junctional morphology as measured by transmission electron microscopy. **A-D)** Representative TEM images of cytokine-treated intestinal organoid tight junctions. Scale bars denote 500nm. **E)** Tight junction width. **F)** Tight junction length. **G)** Light microscopy image of a bovine intestinal organoid highlighting the apical area from which tight junctions were analyzed. Scale bar denotes 20µm. Cytokine treatment did not induce a significant change in junctional length or width as determined by Kruskal-Wallis non-parametric ANOVA (α=0.05).

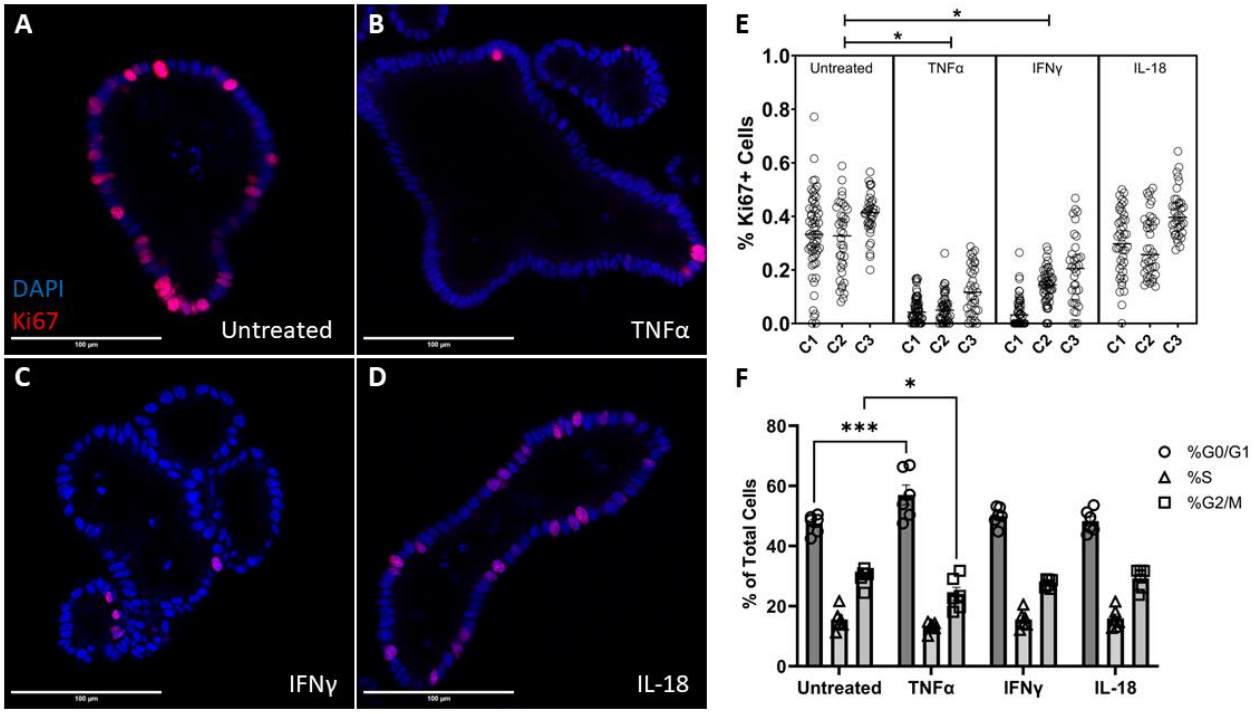

Figure 6. Cytokine treatment alters cellular proliferation. **A-D)** Representative confocal images of cytokine-treated bovine intestinal organoids stained for Ki67 (Alexa Fluor 594) and DAPI taken on a 40x objective. Scale bars denote 100µm. **E)** Percentage of proliferating cells as measured by confocal microscopy. C1, C2, and C3 indicate individual enteroid lines. **F)** Cell cycle analysis of cytokine-treated bovine intestinal organoids. TNFα and IFNγ induce a reduction in cellular proliferation (p=0.0031, p=0.0072, respectively) evidenced by nested ANOVA (α=0.05) Holm-Šídák post hoc analysis. Two-way ANOVA displays a significant interaction effect (p=0.0002) and Dunnett's multiple comparisons test show that TNFα-treatment induces a rise in the percentage of cells in the G0/G1 phase (p=0.0003) and a reduction in the percentage of cells in the G2M phase (p=0.0379). * denotes p<0.05, *** denotes p<0.001.

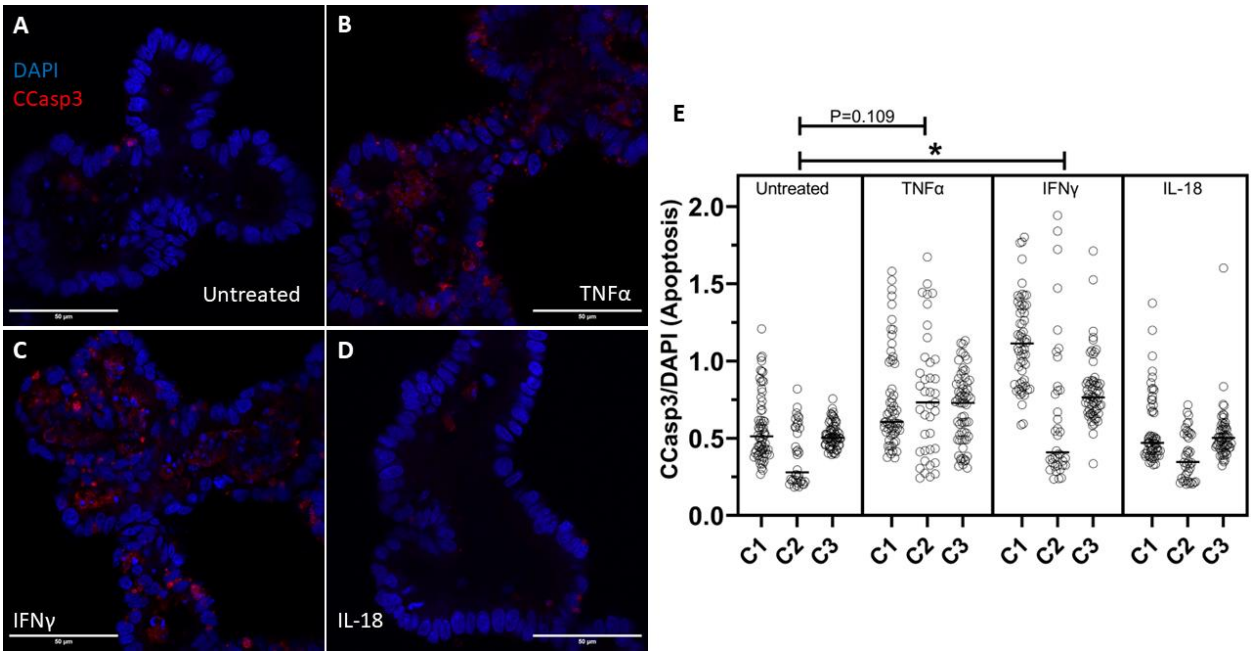

Figure 7. Cytokine treatment alters apoptosis. **A-D)** Representative confocal images of cytokine-treated bovine intestinal organoids stained for Cleaved Caspase-3 (CCasp3) (Alexa Fluor 594) and DAPI using a 63x objective lens. Scale bars denote 50µm **E)** Area of intraluminal CCasp3 normalized to DAPI measured by confocal microscopy. C1, C2, and C3 indicate individual enteroid lines. IFNγ induces a rise in apoptotic cells ($p=0.0325$) determined by nested ANOVA Holm-Šídák post hoc analysis.

Competing Interests

The authors declare no conflicts of interest. Funding for the project was provided by the USDA National Institute of Food and Agriculture as well as Marcia Rivas Memorial Funds.

References

1. Collins, J.T., A. Nguyen, and M. Badireddy, *Anatomy, Abdomen and Pelvis, Small Intestine*, in *StatPearls*. 2021: Treasure Island (FL).
2. Barrett, K.E., *New ways of thinking about (and teaching about) intestinal epithelial function.* Adv Physiol Educ, 2008. **32**(1): p. 25-34.
3. Hamilton, I., et al., *Small intestinal permeability in dermatological disease.* Q J Med, 1985. **56**(221): p. 559-67.
4. Harris, C.E., et al., *Intestinal permeability in the critically ill.* Intensive Care Med, 1992. **18**(1): p. 38-41.
5. Ukabam, S.O., R.J. Mann, and B.T. Cooper, *Small intestinal permeability to sugars in patients with atopic eczema.* Br J Dermatol, 1984. **110**(6): p. 649-52.
6. Wallaert, B., et al., *Increased intestinal permeability in active pulmonary sarcoidosis.* Am Rev Respir Dis, 1992. **145**(6): p. 1440-5.
7. Han, X., M.P. Fink, and R.L. Delude, *Proinflammatory cytokines cause NO*-dependent and -independent changes in expression and localization of tight junction proteins in intestinal epithelial cells.* Shock, 2003. **19**(3): p. 229-37.
8. Yang, R., et al., *IL-6 is essential for development of gut barrier dysfunction after hemorrhagic shock and resuscitation in mice.* Am J Physiol Gastrointest Liver Physiol, 2003. **285**(3): p. G621-9.
9. Cao, M., et al., *Amelioration of IFN-gamma and TNF-alpha-induced intestinal epithelial barrier dysfunction by berberine via suppression of MLCK-MLC phosphorylation signaling pathway.* PLoS One, 2013. **8**(5): p. e61944.
10. Nahidi, L., et al., *Differential effects of nutritional and non-nutritional therapies on intestinal barrier function in an in vitro model.* J Gastroenterol, 2012. **47**(2): p. 107-17.
11. Smyth, D., et al., *Interferon-gamma-induced increases in intestinal epithelial macromolecular permeability requires the Src kinase Fyn.* Lab Invest, 2011. **91**(5): p. 764-77.
12. Madara, J.L. and J. Stafford, *Interferon-gamma directly affects barrier function of cultured intestinal epithelial monolayers.* J Clin Invest, 1989. **83**(2): p. 724-7.
13. Aschenbach, J.R., et al., *Symposium review: The importance of the ruminal epithelial barrier for a healthy and productive cow.* J Dairy Sci, 2019. **102**(2): p. 1866-1882.
14. Liang, D., et al., *Estimating US dairy clinical disease costs with a stochastic simulation model.* J Dairy Sci, 2017. **100**(2): p. 1472-1486.
15. Pascottini, O.B., et al., *Effect of anti-inflammatory treatment on systemic inflammation, immune function, and endometrial health in postpartum dairy cows.* Sci Rep, 2020. **10**(1): p. 5236.
16. Sanz-Fernandez, M.V., et al., *Targeting the Hindgut to Improve Health and Performance in Cattle.* Animals (Basel), 2020. **10**(10).
17. Abuajamieh, M., et al., *Inflammatory biomarkers are associated with ketosis in periparturient Holstein cows.* Res Vet Sci, 2016. **109**: p. 81-85.
18. Khafipour, E., D.O. Krause, and J.C. Plaizier, *A grain-based subacute ruminal acidosis challenge causes translocation of lipopolysaccharide and triggers inflammation.* J Dairy Sci, 2009. **92**(3): p. 1060-70.

19. Koch, F., et al., *Heat stress directly impairs gut integrity and recruits distinct immune cell populations into the bovine intestine.* Proc Natl Acad Sci U S A, 2019. **116**(21): p. 10333-10338.
20. Zhang, S., et al., *Short-term feed restriction impairs the absorptive function of the reticulo-rumen and total tract barrier function in beef cattle.* J Anim Sci, 2013. **91**(4): p. 1685-95.
21. Pate, R.T., et al., *Immune and metabolic effects of rumen-protected methionine during a heat stress challenge in lactating Holstein cows.* J Anim Sci, 2021. **99**(12).
22. Luissint, A.C., C.A. Parkos, and A. Nusrat, *Inflammation and the Intestinal Barrier: Leukocyte-Epithelial Cell Interactions, Cell Junction Remodeling, and Mucosal Repair.* Gastroenterology, 2016. **151**(4): p. 616-32.
23. van der Flier, L.G. and H. Clevers, *Stem cells, self-renewal, and differentiation in the intestinal epithelium.* Annu Rev Physiol, 2009. **71**: p. 241-60.
24. Groschwitz, K.R. and S.P. Hogan, *Intestinal barrier function: molecular regulation and disease pathogenesis.* J Allergy Clin Immunol, 2009. **124**(1): p. 3-20; quiz 21-2.
25. Vancamelbeke, M. and S. Vermeire, *The intestinal barrier: a fundamental role in health and disease.* Expert Rev Gastroenterol Hepatol, 2017. **11**(9): p. 821-834.
26. Pizarro, T.T., et al., *IL-18, a novel immunoregulatory cytokine, is up-regulated in Crohn's disease: expression and localization in intestinal mucosal cells.* J Immunol, 1999. **162**(11): p. 6829-35.
27. Schroder, K., et al., *Interferon-gamma: an overview of signals, mechanisms and functions.* J Leukoc Biol, 2004. **75**(2): p. 163-89.
28. Spriggs, D.R., S. Deutsch, and D.W. Kufe, *Genomic structure, induction, and production of TNF-alpha.* Immunol Ser, 1992. **56**: p. 3-34.
29. McNair, N.N., et al., *Inflammasome components caspase-1 and adaptor protein apoptosis-associated speck-like proteins are important in resistance to Cryptosporidium parvum.* Microbes Infect, 2018. **20**(6): p. 369-375.
30. Siegmund, B., et al., *Neutralization of interleukin-18 reduces severity in murine colitis and intestinal IFN-gamma and TNF-alpha production.* Am J Physiol Regul Integr Comp Physiol, 2001. **281**(4): p. R1264-73.
31. Nowarski, R., et al., *Epithelial IL-18 Equilibrium Controls Barrier Function in Colitis.* Cell, 2015. **163**(6): p. 1444-56.
32. Cui, L., et al., *Changes in the blood routine, biochemical indexes and the pro-inflammatory cytokine expressions of peripheral leukocytes in postpartum dairy cows with metritis.* BMC Vet Res, 2019. **15**(1): p. 157.
33. El-Deeb, W.M. and S.M. El-Bahr, *Biomarkers of ketosis in dairy cows at postparturient period: acute phase proteins and pro-inflammatory cytokines.* Vet. Arhiv, 2017. **87**(4): p. 431-440.
34. Zhao, C., et al., *Inflammatory mechanism of Rumenitis in dairy cows with subacute ruminal acidosis.* BMC Vet Res, 2018. **14**(1): p. 135.
35. Kasimanickam, R.K., et al., *Associations among serum pro- and anti-inflammatory cytokines, metabolic mediators, body condition, and uterine disease in postpartum dairy cows.* Reprod Biol Endocrinol, 2013. **11**: p. 103.

36. Zachos, N.C., et al., *Human Enteroids/Colonoids and Intestinal Organoids Functionally Recapitulate Normal Intestinal Physiology and Pathophysiology.* J Biol Chem, 2016. **291**(8): p. 3759-66.
37. Derricott, H., et al., *Developing a 3D intestinal epithelium model for livestock species.* Cell Tissue Res, 2019. **375**(2): p. 409-424.
38. Hamilton, C.A., et al., *Development of in vitro enteroids derived from bovine small intestinal crypts.* Vet Res, 2018. **49**(1): p. 54.
39. Rallabandi, H.R., et al., *Evaluation of Intestinal Epithelial Barrier Function in Inflammatory Bowel Diseases Using Murine Intestinal Organoids.* Tissue Eng Regen Med, 2020. **17**(5): p. 641-650.
40. Xu, P., et al., *Intestinal organoid culture model is a valuable system to study epithelial barrier function in IBD.* Gut, 2018. **67**(10): p. 1905-1906.
41. Crakes, K.R., et al., *Fenofibrate promotes PPARalpha-targeted recovery of the intestinal epithelial barrier at the host-microbe interface in dogs with diabetes mellitus.* Sci Rep, 2021. **11**(1): p. 13454.
42. Armien, A.G., et al., *Molecular and Biological Characterization of a Cervidpoxvirus Isolated From Moose with Necrotizing Dermatitis.* Vet Pathol, 2020. **57**(2): p. 296-310.
43. Farquhar, M.G. and G.E. Palade, *Junctional complexes in various epithelia.* J Cell Biol, 1963. **17**: p. 375-412.
44. Gonschior, H., V. Haucke, and M. Lehmann, *Super-Resolution Imaging of Tight and Adherens Junctions: Challenges and Open Questions.* Int J Mol Sci, 2020. **21**(3).
45. Perez-Bosque, A., et al., *Dietary intervention with serum-derived bovine immunoglobulins protects barrier function in a mouse model of colitis.* Am J Physiol Gastrointest Liver Physiol, 2015. **308**(12): p. G1012-8.
46. Kaplanski, G., *Interleukin-18: Biological properties and role in disease pathogenesis.* Immunol Rev, 2018. **281**(1): p. 138-153.
47. Bardenbacher, M., et al., *Permeability analyses and three dimensional imaging of interferon gamma-induced barrier disintegration in intestinal organoids.* Stem Cell Res, 2019. **35**: p. 101383.
48. Onozato, D., et al., *Application of Human Induced Pluripotent Stem Cell-Derived Intestinal Organoids as a Model of Epithelial Damage and Fibrosis in Inflammatory Bowel Disease.* Biol Pharm Bull, 2020. **43**(7): p. 1088-1095.
49. Blum, M.S., et al., *Cytoskeletal rearrangement mediates human microvascular endothelial tight junction modulation by cytokines.* Am J Physiol, 1997. **273**(1 Pt 2): p. H286-94.
50. Gitter, A.H., et al., *Epithelial barrier defects in HT-29/B6 colonic cell monolayers induced by tumor necrosis factor-alpha.* Ann N Y Acad Sci, 2000. **915**: p. 193-203.
51. McKay, D.M. and P.K. Singh, *Superantigen activation of immune cells evokes epithelial (T84) transport and barrier abnormalities via IFN-gamma and TNF alpha: inhibition of increased permeability, but not diminished secretory responses by TGF-beta2.* J Immunol, 1997. **159**(5): p. 2382-90.
52. Mullin, J.M. and K.V. Snock, *Effect of tumor necrosis factor on epithelial tight junctions and transepithelial permeability.* Cancer Res, 1990. **50**(7): p. 2172-6.

53. Rodriguez, P., et al., *Tumour necrosis factor-alpha induces morphological and functional alterations of intestinal HT29 cl.19A cell monolayers.* Cytokine, 1995. **7**(5): p. 441-8.
54. Youakim, A. and M. Ahdieh, *Interferon-gamma decreases barrier function in T84 cells by reducing ZO-1 levels and disrupting apical actin.* Am J Physiol, 1999. **276**(5): p. G1279-88.
55. Al-Sadi, R., M. Boivin, and T. Ma, *Mechanism of cytokine modulation of epithelial tight junction barrier.* Front Biosci (Landmark Ed), 2009. **14**(7): p. 2765-78.
56. Madara, J.L., *Regulation of the movement of solutes across tight junctions.* Annu Rev Physiol, 1998. **60**: p. 143-59.
57. Wang, X., et al., *Exploring tight junction alteration using double fluorescent probe combination of lanthanide complex with gold nanoclusters.* Sci Rep, 2016. **6**: p. 32218.
58. Butkevych, E., et al., *Contribution of Epithelial Apoptosis and Subepithelial Immune Responses in Campylobacter jejuni-Induced Barrier Disruption.* Front Microbiol, 2020. **11**: p. 344.
59. Thaiss, C.A., et al., *Hyperglycemia drives intestinal barrier dysfunction and risk for enteric infection.* Science, 2018. **359**(6382): p. 1376-1383.
60. Lu, C.-h., et al., *Apical Actin-myosin Network Regulates the Tight Junction of Polarized Madin-Darby Canine Kidney Cells.* bioRxiv, 2021.
61. Maloy, K.J. and F. Powrie, *Intestinal homeostasis and its breakdown in inflammatory bowel disease.* Nature, 2011. **474**(7351): p. 298-306.
62. Croitoru, K. and P. Zhou, *T-cell-induced mucosal damage in the intestine.* Curr Opin Gastroenterol, 2004. **20**(6): p. 581-6.
63. Ramachandran, A., M. Madesh, and K.A. Balasubramanian, *Apoptosis in the intestinal epithelium: its relevance in normal and pathophysiological conditions.* J Gastroenterol Hepatol, 2000. **15**(2): p. 109-20.
64. T, O.C. and S. Backert, *Host epithelial cell invasion by Campylobacter jejuni: trigger or zipper mechanism?* Front Cell Infect Microbiol, 2012. **2**: p. 25.
65. Gunzel, D., et al., *Restitution of single-cell defects in the mouse colon epithelium differs from that of cultured cells.* Am J Physiol Regul Integr Comp Physiol, 2006. **290**(6): p. R1496-507.
66. Grabinger, T., et al., *Ex vivo culture of intestinal crypt organoids as a model system for assessing cell death induction in intestinal epithelial cells and enteropathy.* Cell Death Dis, 2014. **5**: p. e1228.
67. Kanai, T., et al., *Interleukin 18 is a potent proliferative factor for intestinal mucosal lymphocytes in Crohn's disease.* Gastroenterology, 2000. **119**(6): p. 1514-23.
68. Nakamura, S., et al., *Expression and responsiveness of human interleukin-18 receptor (IL-18R) on hematopoietic cell lines.* Leukemia, 2000. **14**(6): p. 1052-9.
69. Workman, M.J., et al., *Modeling Intestinal Epithelial Response to Interferon-gamma in Induced Pluripotent Stem Cell-Derived Human Intestinal Organoids.* Int J Mol Sci, 2020. **22**(1).

Chapter 4: Fenofibrate Reduces Glucose-Induced Barrier Dysfunction in Feline Enteroids

Charles K. Crawford, Aeelin Beltran, Diego Castillo, Muhammad S. Matloob, Mimoli E. Uehara, Mary L. Quilici, Veronica Lopez Cervantes, Amir Kol

Abstract

Diabetes Mellitus (DM) is an endocrine disorder that affects up to 0.7% of household cats, and 2% in some breeds. DM is associated with dysfunction of the intestinal barrier, which is comprised of a single epithelial cell layer separating the gut lumen from the body's internal environment. The barrier contains a network of tight junctions that adjoin cells and regulate paracellular movement of water and solutes. The mechanisms driving DM-associated barrier dysfunction are multifaceted, and the direct effects of hyperglycemia on the epithelium, specifically, are not fully understood. Preliminary data suggest that fenofibrate, An FDA-approved peroxisome proliferator-activated receptor-alpha (PPARα) agonist drug restores intestinal barrier dysfunction in dogs with experimentally-induced DM. We investigated the effects of hyperglycemia-like conditions on epithelial barrier function using feline intestinal organoids. We hypothesized that glucose treatment directly increases barrier permeability and alters tight junction morphology, and that fenofibrate administration can ameliorate these deleterious effects. We show that increased intracellular concentrations of glucose directly increase intestinal epithelial permeability, a deleterious effect that is mitigated by fenofibrate. Moreover, increased permeability is caused by disruption of tight junction, as evident by increased tortuosity. Finally, we found that increased junctional tortuosity and barrier permeability in hyperglycemic conditions were associated with increased Protein Kinase C-α (PKCα) activity, and that fenofibrate treatment restored PKCα activity back to baseline levels. We conclude that hyperglycemia directly induces barrier dysfunction and disruption of tight junction structure, mediated by PKCα activation in feline intestinal epithelium, which can be mitigated by fenofibrate.

Introduction

Diabetes mellitus (DM) is a metabolic disorder that results in impaired glucose homeostasis. DM is a common naturally occurring endocrine disorder in household cats (*Felis catus)* that affects up to 0.7% of cats in the United States, and incidence rates of 2% occur in highly susceptible breeds such as Burmese cats [1, 2]. DM in humans has been coined a ‘new epidemic’ and is considered one of the world’s highest priority health problems [3]. Diabetic cats can provide valuable insight into human DM in addition to veterinary care, as cats are one of few species that experiences spontaneously occurring DM that closely resembles type 2 DM in humans with glucotoxicity-induced hyperinsulinemia, obesity-induced insulin resistance, and accumulation of pancreatic islet amyloid polypeptide [4]. As such, pet cats with naturally occurring DM are a valuable translational model for DM research. Improved understanding of DM in cats holds the potential to improve veterinary healthcare outcomes while simultaneously providing insight into human DM given the shared complex pathophysiology, chronic disease manifestation, and long-term medical care diabetic people and cats share [5].

DM in cats and people is associated with multiple gastrointestinal co-morbidities collectively termed ‘diabetic enteropathy’ [6, 7]. The pathogenesis of diabetic enteropathy is complex and multifactorial and is thought to be driven by increased oxidative stress, neuroinflammation, reduced levels of nerve growth factors, structural vascular changes, and intestinal barrier dysfunction [6, 8]. The intestinal epithelium forms a selective barrier that absorbs nutrients, water, and other important molecules while simultaneously blocking the entry of pathogens and harmful substances [9]. This

barrier is wholly comprised of a layer of mucus over a monolayer of epithelial cells, followed by the lamina propria which contains immune cells [10]. The epithelial cells are adjoined by a series of protein complexes: tight junctions, adherens junctions, and desmosomes [11]. Tight junctions are comprised of transmembrane and intracellular proteins found in the apical portion of intestinal epithelial cells, and they regulate paracellular transport across the intestinal epithelium [12-15]. DM is highly associated with increased permeability of the intestinal epithelium [6, 16, 17], and DM-induced barrier dysfunction increases the risk of pathogenic entry and chronic diarrhea [18, 19]. The increased permeability involves dysregulation of paracellular transport [20]. However, the precise direct role of hyperglycemia in this process is not well understood.

Recently, intestinal barrier dysfunction has been shown to be influenced by hyperglycemia in rodent models [8, 21]. A high carbohydrate diet that induced intestinal barrier dysfunction in mice was associated with a reduction in expression of tight junctional proteins ZO-1 and occludin, but this was in conjunction with increased inflammation, making it difficult to parse the direct effects of glucose versus inflammation on epithelial tight junctions [22]. In a human intestinal epithelial cancer cell line (CACO-2), apical exposure to high glucose concentration altered tight junctional morphology as shown by increased tortuosity (the ratio of segment length and Euclidian distance between two points of a defined segment) [8, 23]. The independent effects of hyperglycemia on intestinal epithelium remain to be elucidated, especially in the context of feline DM.

To combat the effects of DM – and potentially hyperglycemia, specifically – on the intestinal epithelial barrier, one potential therapeutic agent is fenofibrate, an FDA-approved ligand of the peroxisome proliferator-activated receptor-alpha (PPARα) pathway. PPARα is a ligand-activate nuclear receptor transcription factor highly expressed in the small intestine that regulates numerous gene targets, especially related to metabolism, but can also induce non-transcriptional reductions in ion secretion [24-27]. PPARα activation improves barrier permeability, highlighting its potential use in combatting diabetic enteropathy. Downregulation of PPARα in the retina leads to increased endothelial permeability in rodents and human patients [28]. Furthermore, PPARα activation protected against induced colitis in a rodent model for inflammatory bowel disease and enhanced intestinal barrier function in rhesus macaques with chronic gut inflammation and dogs with experimentally-induced DM [23, 29, 30]. In CACO-2 cells, treatment with fenofibrate improved barrier function, reduced junctional tortuosity, and increased immunoreactive Claudin-1, a tight junctional protein, following high glucose or inflammatory cytokine exposure [23]. While PPARα activation appears to reduce intestinal barrier dysfunction, the specific mechanisms by which it may do so in DM are not fully understood. The influence of fenofibrate on Claudin-1 expression in dogs with experimentally-induced diabetes and tight junctional morphology in CACO-2 cells highlights tight junctions as a potential target [23, 30]. PPARα activation, however, reduces the concentration of the inflammatory cytokines IL-8 and TNF-α, reduces expression of apical and basolateral glucose transport proteins, and protects against oxidative stress [23, 31]. Thus, PPARα activation likely induces a complex response which attenuates intestinal barrier dysfunction. Its direct impact on

the effects of hyperglycemia on feline intestinal epithelial permeability and resultant mechanisms are unknown.

We hypothesized that hyperglycemia directly induces intestinal barrier dysfunction in diabetic cats by disrupting intestinal epithelial tight junctions. Furthermore, we hypothesized that this can be reduced by fenofibrate. To investigate this, we utilized intestinal organoids (enteroids) derived from household cat intestinal tissue, providing a relevant *in vitro* model which recapitulates native intestinal epithelium [32]. We found that hyperglycemia directly increases intestinal epithelial permeability and tight junction tortuosity, and that this effect is reduced when treated with fenofibrate. Surprisingly, mRNA expression of tight junction proteins was not altered by fenofibrate treatment. Rather, the data show that hyperglycemia increases PKCα activation, which is reduced by fenofibrate. Taken together, our data show that hyperglycemia induces intestinal barrier dysfunction in cat intestinal epithelium and highlights fenofibrate as a potential therapeutic for feline DM-induced intestinal barrier dysfunction.

Materials and Methods

Enteroid Generation: Feline intestinal enteroids were generated (Fig. S1) as previously described [33] with minor protocol modifications. Briefly, Approximately 2-3cm of feline ileum was harvested and placed in ice-cold PBS containing 100U/mL penicillin/streptomycin (Gibco) and 25µg/mL gentamicin (Thermo Fisher). The intestinal section was longitudinally cut and washed. The mucosa was separated by scraping with a glass slide. It was then minced and placed into a 50mL tube with cold PBS containing 25µg/mL gentamicin and 100U/mL penicillin/streptomycin. The tube was shaken and

then allowed to settle before the supernatant was removed. This was repeated until the supernatant was clear. Tubes containing tissue were then centrifuged for 2 minutes at 200g, the supernatant was removed, and the tissue fragments were placed in a new 50mL tube containing 0.8mM EDTA. The tissue fragments were incubated in EDTA for 30 minutes at 4°C with heavy agitation to liberate crypts. Following incubation, the tube was shaken with vigor, then centrifuged for 2 mins at 400g. The supernatant was removed and replaced with 25mL of PBS, gentamicin, and penicillin/streptomycin. The tube was shaken, allowed to settle, and the supernatant was collected and passed through a 70µm cell strainer into a new collection tube. This step was repeated twice. Tubes were centrifuged for 3 mins at 100g, the supernatant was collected and removed, and isolated crypts were reconstituted in DMEM/F12 media (Life Technologies) containing 1X B27 Supplement minus Vitamin A (Life Technologies), 25µg/mL gentamicin, and 100U/mL penicillin/streptomycin. Isolated crypts were then counted manually on a glass slide. The appropriate volume to plate 300 crypts per well was collected. Plain solution without crypts was added to reach 20µL total of crypt solution, which was combined with 30µL of Matrigel™ (Corning) per well to be plated. 50µL droplets were pipetted to create domes in the center of a well of a pre-warmed 24 well plate. These domes were incubated at 37°C for 10 mins. Following incubation to set the domes, wells were provided 720µL of growth media containing 50% L-WRN conditioned media [34, 35], 50% DMEM/F12 media, 100U/mL penicillin/streptomycin , 25µg/mL gentamicin (only for primary culture) supplemented with 10µM Y-27632 (Tocris Bioscience), 500nM Nicotinamide (Sigma), 1mM N-acetylcysteine (Sigma), 10nM Leu-Gastrin (Sigma), 1x B27-insulin (Thermo), 500nM LY2157299 (Thermo Fisher), 500nM

SB202190 (Sigma), 50ng/mL mouse recombinant EGF (Thermo), and 3μM CHIR99021 (Tocris Bioscience) (only for primary culture or post-passage). Media was changed every 3 days and organoids were passaged mechanically using a 25-gauge needle every 7-10 days.

Treatment: Four days following passage, enteroids were provided with their normal growth medium or provided with growth medium containing added glucose (final glucose concentrations of 22mM, 44mM) with or without fenofibrate (1μM, 10μM, 100μM) (Sigma) or GLUT2-selective inhibitor (1μM) (Life Chemicals) [36]. Additionally, to ensure the effects of glucose treatment were not solely due to osmotic changes, some enteroids were provided growth medium containing the inert carbohydrate, mannitol (22μM, 44μM). Enteroids were treated for 24 hours before FITC imaging, fixation, RNA extraction, or Western blot.

FITC Dextran Permeability Assay: Enteroids cultured in eight-well chamber slides (Thermo Scientific) were provided growth media containing 5μg/mL 4Kda fluorescein isothiocyanate-dextran (FITC) for 1 hour, then washed in PBS and imaged with a fluorescent microscope (EVOS M5000, Thermo Fisher). FITC fluorescent intensity inside of the enteroids (average of three data points per enteroid) was normalized to FITC intensity outside of the enteroids (average of three data points per enteroid) via image analysis software (ImageJ).

Immunofluorescence (IF) Staining: Enteroids were cultured in eight-well chamber slides for immunocytochemical staining. Media was removed and organoids were fixed in 4% paraformaldehyde for 20 minutes at room temperature. Afterward, organoids

were permeabilized in PBS containing 0.5% Triton X-100 (Sigma-Aldrich) for 20 mins at room temperature. Wells were washed in IF buffer: PBS containing 0.2% Triton X-10 and .05% Tween (Fisher Scientific). They were then blocked in IF Buffer containing 1% bovine serum albumin (Fisher Scientific) for 30 mins at room temperature. After blocking, organoids were incubated in IF buffer containing 1% bovine serum albumin with primary antibodies overnight at 4°C. Primary antibodies included ZO-1 (1A12, Invitrogen), Cleaved Caspase-3 (D175, Cell Signaling), and Ki67 (SP6, Invitrogen). Organoids were then washed in IF buffer, then incubated in IF Buffer containing 1% bovine serum albumin with secondary antibodies for 1 hour at room temperature. Organoids were washed in IF buffer, then incubated in IF buffer containing 0.1µg/mL DAPI (Thermo Fisher) for 10 mins at room temperature. The gasket of the chamber slide was then removed, one drop of ProLong Gold antifade reagent (Invitrogen) was placed into each well, and the slide was covered with a coverslip and allowed to cure for 24 hours before being placed in darkness in 4°C until imaging.

Confocal Microscopy and Image Analysis: After immunofluorescent staining for Ki67, Cleaved Caspase-3, or the tight junction protein, ZO-1, images were acquired on a TCS SP8 STED3x confocal microscope (Leica Microsystems) utilizing a 40x/1.3 oil immersion objective for Cleaved Caspase-3 (zoom 1.25) and a 63x/1.40 oil immersion objective for Ki67 (zoom 1.25) and ZO1 (zoom 3.25). ZO-1 images were processed via morphological segmentation plug-in (ImageJ) for tortuosity calculation [23, 33, 37]. The measured tortuosity was the ratio of segment length and Euclidian distance between two defined ZO-1 segment points [23].

RNA Isolation and RT-Quantitative PCR: Enteroids were collected and Matrigel was dissolved in ice-cold PBS. An RNeasy Plus Micro Kit (Qiagen) was used to extract total RNA from the enteroids, and spectrophotometry (Nanodrop, Thermo Fisher Scientific) was used to determine RNA concentration. A DNA-free DNase Treatment kit (Thermo Fisher) was used to remove gDNA and a First-strand cDNA Synthesis kit (OriGene) was used to synthesize cDNA.

A StepOnePlus Real-Time PCR System (Applied Biosystems) with PowerUp SYBR Green Master Mix (Applied Biosystems) was used for PCR amplification. *Felis catus*-specific primers were designed with Primer Blast (NCBI). Primers were validated with melting curve analysis and amplicon size confirmation via gel electrophoresis. StepOne Software v2 1 was utilized for qPCR analysis with *Felis catus* GAPDH used as an endogenous control. Primers can be found in Table S1.

Western Blot: Enteroids were collected by pipette in ice cold PBS. Matrigel was dissolved in cold PBS and removed via centrifugation and supernatant removal. Enteroid cells were lysed and protein extracted with lysis buffer (150mM NaCl, 50mM Tris base, 1% NP-40, 0.25% deoxycholic acid, 0.1% SDS) with 1% Prometheus General Protease Inhibitor Cocktail (Genesee Scientific). Protein was quantified via BCA Protein Assay kit (Thermo Fisher). 20µg of protein were loaded per well into a polyacrylamide gel (GenScript), separated by gel electrophoresis, then transferred onto a PVDF membrane (Thermo Scientific). Protein was probed with polyclonal antibodies against PKCα (Cell Signaling Technology) or phosphor-(Ser) PKC substrate (Cell Signaling Technology). Membranes were stripped and reprobed with an anti-GAPDH

monoclonal antibody (Abcam) as a loading control. Primary antibodies were diluted 1:1000. Prometheus ProSignal Femto chemiluminescent substrate (Genesee Scientific) was applied to membranes which were imaged with a KwikQuant Pro Imager (Kindle Biosciences). Densitometry analysis of bands was performed using ImageJ image analysis software.

Statistical Analysis: Experiments are separated by color and experimental data are presented as means ± SD. Data were examined for normality via Shapiro-Wilk test ($\alpha=0.05$). Comparisons of normal data were analyzed via one-way ANOVA ($\alpha=0.05$) with Holm-Šídák post hoc analysis. Comparisons of data not normally distributed were analyzed via Kruskal-Wallis non-parametric ANOVA ($\alpha=0.05$) with Dunn's post hoc analysis. Statistical significance denotation: * $p \leq 0.05$ | ** $p \leq 0.01$ | *** $p \leq 0.001$ | **** $p \leq 0.0001$

Results

Glucose treatment increases epithelial permeability in feline enteroids, which is prevented by fenofibrate

We hypothesized that hyperglycemia directly increases permeability of the feline intestinal epithelium. To test this hypothesis, we modeled hyperglycemia by exposing the basolateral surface of feline enteroids to high glucose concentrations and measured intestinal permeability using FITC labeled dextran permeability as previously described [33]. Our data show a significant increase in epithelial permeability when enteroids were exposed to 22mM and 44mM glucose ($p<0.0001$, $p<0.0001$, respectively) (Fig. 1, Fig. S2). To determine if the effects of hyperglycemia-like conditions on epithelial

permeability were driven by increased osmotic pressure, enteroids were treated with equal concentrations of the inert sugar, mannitol [38, 39]. Mannitol treatment had no effect on permeability relative to untreated enteroids. Moreover, 22mM and 44mM glucose significantly increased permeability ($p=0.0012$ and $=0.0097$, respectively) compared with its paired mannitol treatment, indicating that increased extracellular osmotic pressure was not responsible for the hyperglycemia-induced increased epithelial permeability.

To determine if increased intracellular concentrations of glucose are causing the increased intestinal epithelial permeability, we utilized a GLUT2-selective inhibitor [36] (GLUT2i, 1 μM) in conjunction with high glucose concentrations to prevent glucose entry into the epithelial cells. GLUT2i abolished the hyperglycemia-induced rise in intestinal permeability (22mM glucose, $p<0.0001$). This suggests that the intracellular increase of glucose concentration is directly driving increased permeability, though this effect was only partially reversed in the 44mM glucose-treated enteroids (Fig S2).

We hypothesized that PPARα activation would prevent this hyperglycemia-induced increase in epithelial permeability. When enteroids were exposed to hyperglycemic conditions in conjunction with PPARα agonist, fenofibrate (10μM), there was no significant increase in permeability relative to untreated enteroids. Treatment with fenofibrate significantly reduced the response to glucose ($p<0.0001$ for 22mM, $p<0.0001$ for 44mM). The data show that epithelial permeability was increased by high basolateral concentration of glucose, to mimic hyperglycemia conditions seen in DM, and this effect was prevented by GLUT2-selective inhibition or fenofibrate treatment.

Glucose treatment alters tight junction morphology, which is prevented by fenofibrate

Tight junctions regulate paracellular transport and permeability across the intestinal epithelium; we hypothesized that hyperglycemia increases intestinal permeability via an effect on tight junctions. To determine how hyperglycemia influences tight junction structure and spatial conformation we analyzed junctional tortuosity through ZO-1 immunocytochemistry and confocal microscopy image analysis. Treatment with glucose significantly increased junctional tortuosity (22mM and 44mM, $p=0.0014$ and $p<0.0001$, respectively) (Fig 2, Fig S3). Treatment with GLUT2i to block facilitated glucose transport, tight junction tortuosity was significantly reduced compared with glucose treatment alone (22mM and 44mM, $p=0.0143$ and $p=0.0024$, respectively) suggesting that increased intracellular glucose concentration directly disrupts tight junction morphology. Treatment with fenofibrate significantly decreased the effect of glucose on tight junction tortuosity ($p=0.0024$ for 22mM, $p<0.0001$ for 44mM), suggesting that fenofibrate treatment can reduce hyperglycemia-induced tight junction disruption. These data show that hyperglycemia-like conditions induce morphological changes to tight junctions that can be prevented by GLUT2-selective inhibition or fenofibrate.

Glucose treatment reduces cellular proliferation in feline enteroids but has no effect on apoptotic rate

Reduced cellular proliferation may contribute to epithelial barrier dysfunction. To investigate the effects of hyperglycemia on cellular turnover rate we utilized immunocytochemistry and confocal microscopy to analyze the proportion of Ki67-positive cells. Treatment with 44mM glucose reduced the proportion of Ki67-positive cells relative to untreated enteroids ($p=0.0032$) (Fig. 3). Treatment with fenofibrate had no significant effect on the proportion of Ki67-positive cells; enteroids treated with glucose (44mM) and fenofibrate had reduced proliferation not significantly different from enteroids treated with only glucose ($p=0.0246$). There was no significant effect of glucose (22mM) on proliferation.

We further investigated the effects of glucose on cell turnover by measurement of apoptosis using immunocytochemistry and confocal microscopy for Cleaved Caspase 3 (CCasp3) normalized to DAPI with ImageJ software analysis. There was no significant effect of treatment on normalized CCasp3 intensity (Fig. 4).

The data show that hyperglycemia-like conditions (44mM) can induce a reduction in cellular proliferation that is not affected by fenofibrate, and that these conditions do not induce a significant change in the rate of apoptosis in feline enteroids.

Glucose treatment does not alter tight junction gene transcription

To understand the mechanisms by which hyperglycemia increases intestinal permeability, and how this is improved by fenofibrate, we investigated the effects of hyperglycemic-like conditions with or without fenofibrate or GLUT2-selective inhibitor on

mRNA expression of tight junction genes via RT-qPCR. Expression of three different tight junction genes were investigated: ZO-1 (*TJP1*), Claudin 1 (*CLDN1*), and Occludin (*OCLN*). However, treatment did not alter tight junction gene expression (Fig. 5).

Glucose treatment increases PKCα activation, which is prevented by fenofibrate

We did not observe a change in tight junction gene expression; therefore, we investigated an alternative hypothesis for how glucose and fenofibrate influence intestinal permeability. Protein Kinase C-α (PKCα) activation is associated with intestinal barrier dysfunction [40, 41], and fenofibrate can non-genomically increase the activation of PKCα [42]. Therefore, we investigated PKCα protein expression and activation in our treated enteroids via western blot analysis. Western blots were performed with a PKCα antibody to investigate the effects of treatment on total PKCα protein levels (Fig 6A). Additionally, western blots were also performed with a phospho-(Ser) PKC substrate antibody; this antibody binds to PKC substrates with phosphorylated serine residues, thus indicating PKC activity (Fig 6B). Our data show no significant effect of treatment on PKCα protein expression (normalized to GAPDH) (Fig. 6C). However, there was a significant reduction in phospho-(Ser) PKC substrate protein expression (all bands within a lane averaged, normalized to GAPDH) for glucose-treated enteroids (44mM) compared to untreated enteroids ($p=0.0089$), implying an increase in PKCα activation without a change in total PKCα (Fig. 6D). When co-treated with 10μM or 100μM fenofibrate, phospho-(Ser) expression was significantly reduced compared to glucose-treated enteroids ($p=0.0492$ and $p=0.0048$, respectively) (Fig. 6D). These data suggest that PKCα activation by hyperglycemia contributes to tight junction

disruption, and that fenofibrate's non-transcriptional function as an inhibitor of PKCα mediates the counteracting of the effects of hyperglycemia.

Discussion

We sought to determine if hyperglycemia directly increases intestinal epithelial permeability, and if any glucose-induced effects may be prevented pharmacologically with the FDA-approved PPARα agonist, fenofibrate. To investigate this, we utilized stem cell-derived intestinal organoids (enteroids) to provide a model that recapitulates native feline intestinal epithelium. We further aimed to determine the effects of hyperglycemia on intestinal epithelial cells independent of inflammation, altered neuronal signaling, or smooth muscle motility that may accompany DM. Our model readily enables exposure of the basolateral side of the epithelium to glucose treatment, as is seen during hyperglycemia *in vivo*, and isolates the effects of glucose on epithelial cells from other confounding effects. With this model, we determined that glucose directly increases intestinal epithelial permeability and increases tight junctional tortuosity while increasing activation of PKCα. We also determined that treating enteroids with fenofibrate prevents glucose-induced changes to permeability and junctional tortuosity, and that fenofibrate attenuates the glucose-induced rise in PKCα activity. This is, to our knowledge, the first study to investigate the independent effects of hyperglycemia on feline intestinal permeability, elucidate the molecular mechanism of injury and highlight fenofibrate as a candidate therapeutic agent in this context.

Hyperglycemic-like conditions directly increase the permeability of the intestinal epithelium in feline enteroids as made evident by the increased entry of FITC dextran

(Fig. 1). This is consistent with previous findings of FITC dextran flux in diabetes-induced mice [8], though our data isolates the intestinal epithelium from other intestinal cellular components such as immune cells and nerves. Additionally, it has been shown that apical exposure of the human colorectal adenocarcinoma cells line, CACO-2, to high glucose concentrations increases epithelial permeability [43], which is further corroborated by our findings in feline enteroids which more closely represents a diabetic model with native intestinal epithelial cellular diversity and exposure to hyperglycemia-like conditions via the basolateral pole. We confirmed that increased extracellular osmotic pressure was not the primary cause of the hyperglycemia-induced increased epithelial permeability by incubating our enteroids with equivalent concentrations of mannitol, an inert sugar. The GLUT2 transporter is expressed on the basolateral surface of intestinal epithelial cells and, under physiological conditions, mediates absorption of glucose across the basolateral membrane. Additionally, it has been shown to facilitate retrograde entry of glucose during hyperglycemic conditions [8, 44]. We employed a GLUT2-selective inhibitor (GLUT2i) to determine if increased intracellular concentration of glucose is the cause of the observed changes in intestinal epithelial cells [36]. We found that inhibition of GLUT2 prevents the hyperglycemia-induced rise in permeability (Fig. 1). The unchanged permeability in enteroids treated with mannitol or glucose with a GLUT2i compared with our untreated controls suggests that increased intra-epithelial concentration of glucose is required for the direct effects of glucose on epithelial permeability.

Tight junctions are a critical component of epithelial barrier regulation and therefore, we aimed to investigate tight junction morphology and gene transcription to

understand potential causative mechanisms driving the hyperglycemia-induced increase in epithelial permeability. Previous studies have shown that glucose can directly alter the morphological integrity of tight junction in epithelial cell lines as measured by tortuosity [8, 23], and that increased tight junction tortuosity is associated with increased FITC dextran permeability in bovine enteroids [33]. Our study shows that hyperglycemia-like conditions induce a rise in tight junctional tortuosity, and that this rise is absent when co-treated with GLUT2i (Fig. 2). Our study corroborates the effects of glucose on tight junction morphology in other models [8, 23] and further implies the necessity of glucose entry into the epithelial cells as shown through our GLUT2i treatment. We also investigated the effects of hyperglycemia on gene expression of tight junction proteins ZO-1, Claudin 1, and Occludin. High glucose diets in mice increase FITC dextran permeability while decreasing levels of ZO-1 and Occludin, but also increase levels of inflammatory cytokines, making it difficult to parse the effects of glucose, specifically, versus inflammation [22]. We found that in the feline enteroid hyperglycemia model there was not a significant change in mRNA expression of tight junction proteins, implying that while hyperglycemia alters tight junctional morphology and epithelial permeability it does not induce changes in transcription of tight junction proteins.

Because inflammation-induced intestinal barrier dysfunction is associated with lowered cellular proliferation and increased apoptosis [33], we sought to determine the effects of glucose on cell turnover in feline enteroids. We found that 44mM glucose does reduce cellular proliferation. However, there was not a significant reduction in cell proliferation when enteroids were treated with 22mM glucose, despite an observed

increase in epithelial permeability and tight junctional tortuosity (Fig. 1, Fig. 2). The apoptotic rate in feline enteroids was not significantly changed due to hyperglycemia-like conditions. Thus, we determine that reduced cellular proliferation may play some role in glucose-induced barrier dysfunction but is not likely the primary causative mechanism driving the effects observed in our study.

In addition to determining the direct effects of glucose on intestinal epithelial permeability, we also sought to determine if hyperglycemia-induced barrier dysfunction could be prevented with the PPARα agonist, fenofibrate. Fenofibrate is an FDA-approved drug that is commonly used as a therapeutic to treat hyperlipidemia in human and veterinary patients [45, 46]. Moreover, fenofibrate abolished the increase in junctional tortuosity in an induced-diabetic dog model [23]. PPARα knockout mice display exaggerated barrier dysfunction in response to induced colitis or stress [47, 48]. However, because PPARα activation reduces inflammation induced by innate immune cells [49], it is not determined if PPARα activation by fenofibrate can protect against barrier dysfunction induced by glucose, specifically. We found that fenofibrate does diminish the glucose-induced increase in epithelial permeability (Fig. 1) and tight junction tortuosity (Fig. 2) in feline enteroids that is observed in our study. These findings corroborate previous work in other models [23, 47, 48] and additionally shows an effect of fenofibrate on glucose-induced dysfunction, specifically, in feline intestinal epithelial tissue. Work done in high-fat diet mice has shown fenofibrate to increase mRNA expression of tight junction proteins [23, 50], which was not observed in our study (Fig 5). While PPARα is a nuclear receptor that primarily functions as a transcription factor upon ligand binding and heterodimerization with retinoid X receptors

[25], it can additionally directly suppress the activation of Protein Kinase C-α (PKCα) [51].

PKCα is a serine/threonine kinase and conventional PKC that, upon activation, is translocated from the cytosol to the cell membrane and phosphorylates substrates [52]. Excessive activation of PKCα is associated with increased intestinal epithelial permeability mediated by cytoskeletal remodeling resulting in altered cell membrane shape and tight junction leakiness [40, 41, 53]. In platelets, fenofibrate is known to non-genomically reduce PKCα activation [42]. Furthermore, glucose is known to increase PKC activation through the elevated de novo synthesis of the PKC activator, diacylglycerol, caused by a buildup of glycerol-3-p resulting from increased glucose metabolism [54, 55]. Our study shows that in feline enteroids, total PKCα protein is not changed, but PKCα activation is elevated as a result of hyperglycemia-like conditions (Fig. 6). Treatment with fenofibrate in conjunction with glucose prevented the hyperglycemia-induced rise in PKCα activation (Fig 6). This would imply that one causal mechanism for hyperglycemia-induced barrier dysfunction is enhanced PKCα activity. Additionally, our study did not show a change in the mRNA expression of tight junction proteins, and PKCα is known to alter the structure of the cell membrane, resulting in elevated tight junction permeability, rather than altering tight junction protein gene expression. Finally, our study corroborates with previous work showing that fenofibrate inhibits PKCα activation without altering total PKCα protein levels [42].

Our study is not without limitations. Though our treatments are consistent with other *in vitro* studies [8, 23], we utilize supraphysiological concentrations for 24h periods

of time, while DM induces relatively lower glucose concentrations in the blood for longer periods of time [56]. Therefore, direct translations to the effects of physiological hyperglycemia are not possible. Additionally, we did not investigate the effects of GLUT2i or fenofibrate in the absence of glucose treatment. Furthermore, we only investigated the effects of treatment on the epithelial cells in our enteroid model, while other components of the intestinal barrier such as the mucosal layer or lamina propria may also be influenced by hyperglycemia, contributing to overall intestinal barrier dysfunction.

In conclusion, these data show that hyperglycemia and the downstream increase of intracellular concentrations of glucose directly disrupts the epithelial barrier, alters tight junction morphology, and increases PKCα activation in feline intestinal organoids. Additionally, these effects are diminished by the PPARα agonist, fenofibrate, in a direct and non-genomic fashion. These findings show that hyperglycemia, independent of systemic inflammation or altered neural signaling, may contribute to intestinal barrier dysfunction associated with DM in cats, and that the FDA-approved drug, fenofibrate, may serve as a potential therapeutic in this context.

Figures

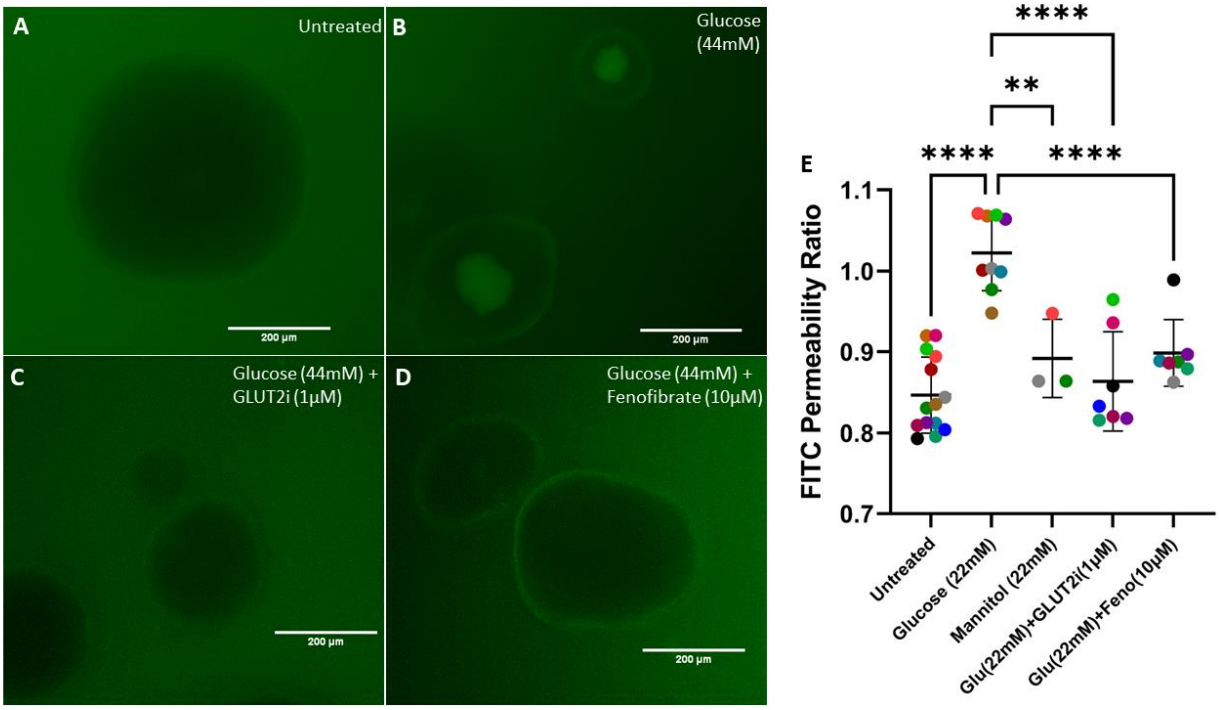

Figure 1. Glucose treatment increases feline enteroid barrier permeability measured by FITC Dextran permeability. Barrier permeability is not increased when treated with GLUT2-selective inhibitor or fenofibrate in addition to glucose. **A-D**) representative images of feline enteroids following exposure to 4kDa FITC Dextran following 24h treatment. Images are acquired with a GFP LED light cube (470/525nm ex/em). Scale bars denote 200μm. **E**) Luminal FITC intensity normalized to basolateral FITC intensity following 24h treatment with glucose, mannitol, or glucose with fenofibrate or GLUT2-selective inhibitor. One-way ANOVA (α=0.05) with Holm-Šídák post hoc analysis determined that treatment with 22mM glucose significantly increased barrier permeability ($p<0.0001$). Mannitol treatment significantly reduced enteroid permeability compared to matching concentration of glucose treatment ($p=0.0012$). Enteroids treated with glucose and 1μM GLUT2-selective inhibitor displayed significantly reduced barrier permeability compared to those treated with only glucose ($p<0.0001$). Enteroids treated with glucose and 10μM fenofibrate displayed significantly reduced permeability compared to those treated with only glucose ($p<0.0001$). Data are presented as mean ± SD with each point representing an experimental mean. Colors represent individual experiments.

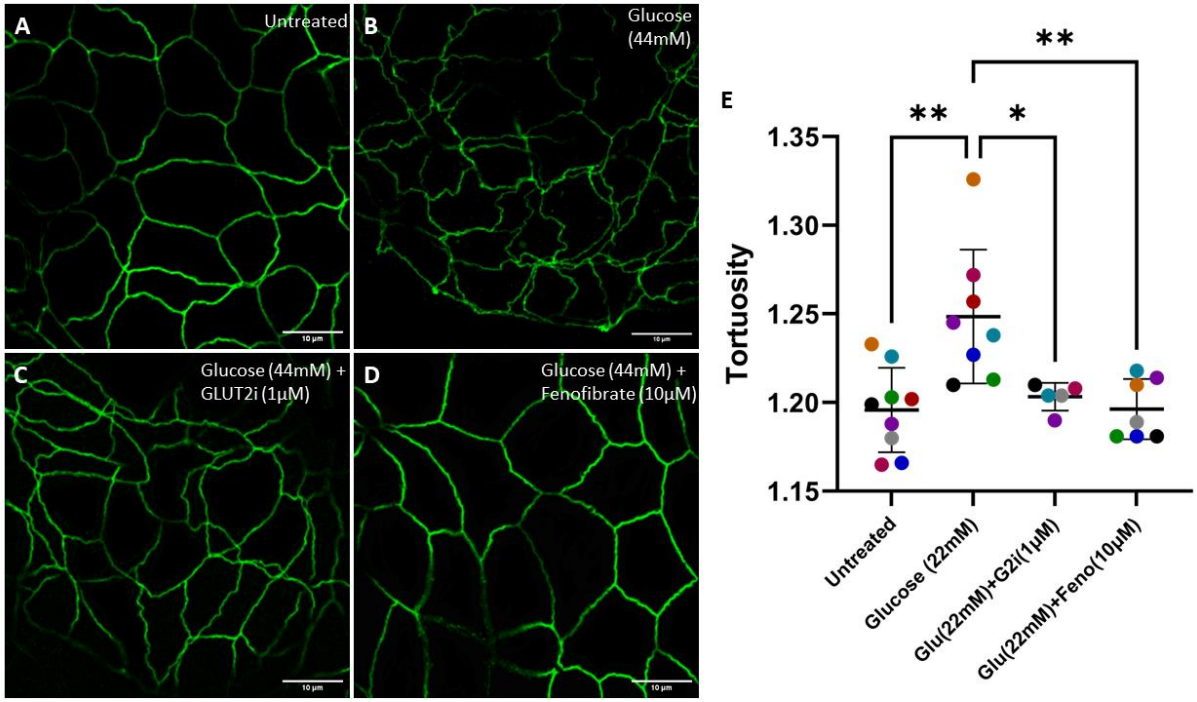

Figure 2. Glucose treatment increases tortuosity of tight junctions in feline enteroids, but not when treated in conjunction with fenofibrate or GLUT2-selective inhibitor. **A-D**) representative ZO-1 (Alexa Fluor 488) staining of feline enteroids following 24h treatment. Scale bars denote 10µm. **E**) Quantification of ZO-1 tortuosity in experimental enteroids. Treatment with 22mM glucose significantly increased ZO-1 tortuosity ($p=0.0014$) as determined by one-way ANOVA ($\alpha=0.05$) and Holm-Šídák post hoc analysis. Enteroids treated with glucose and 1µM GLUT2-selective inhibitor displayed significantly reduced ZO-1 tortuosity compared to those treated with only glucose ($p=0.0143$). Enteroids treated with 10µM fenofibrate in addition to glucose displayed significantly reduced ZO-1 tortuosity compared to those treated with only glucose ($p=0.0024$). Data are presented as mean ± SD with each point representing an experimental mean. Colors represent individual experiments.

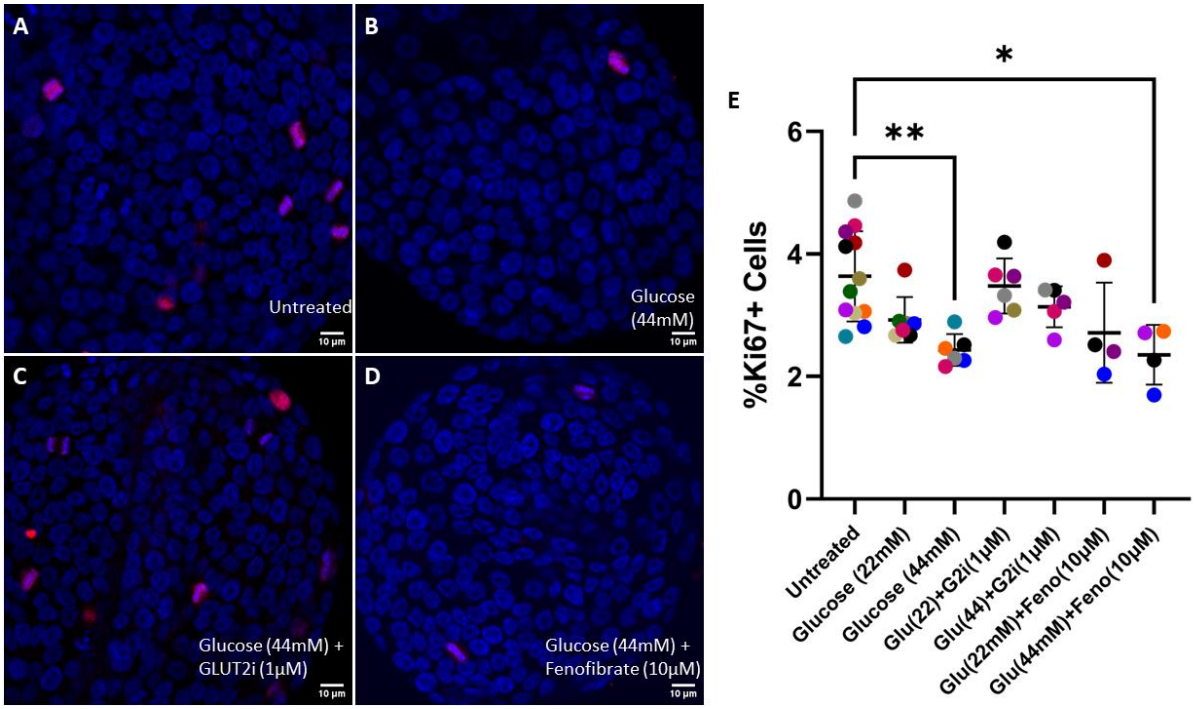

Figure 3. Glucose treatment (44mM) reduces cellular proliferation in feline enteroids. **A-D**) representative confocal images of feline enteroids stained for Ki67 (Alexa Fluor 594) and DAPI. Scale bars denote 10µm. **E**) Percentage of proliferating cells measured by confocal microscopy. Treatment with 44mM glucose with or without fenofibrate induced a significant reduction in proliferation compared to untreated enteroids (p=0.0032 without fenofibrate, p=0.0246 with fenofibrate) as determined by Kruskal-Wallis non-parametric ANOVA (α=0.05) with Dunn's post hoc analysis. Data are presented as mean ± SD with each point representing an experimental mean. Colors represent individual experiments.

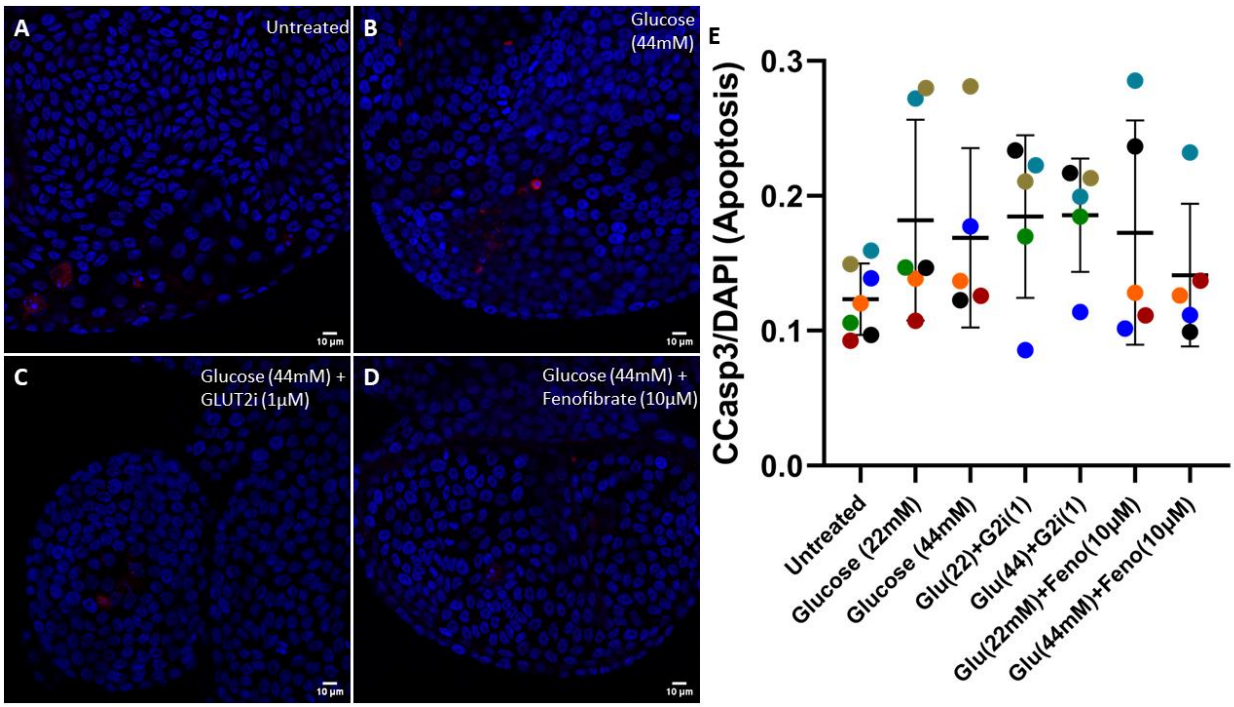

Figure 4. Glucose treatment does not alter apoptotic rate in feline enteroids. **A-D**) representative confocal images of feline enteroids stained for Cleaved Caspase-3 (Alexa Fluor 594) and DAPI. Scale bars denote 10µm. **E**) Fluorescence intensity of Cleaved Caspase-3 normalized to DAPI measured by confocal microscopy. No significant effect of treatment was detected by Kruskal-Wallis non-parametric ANOVA (α=0.05). Data are presented as mean ± SD with each point representing an experimental mean. Colors represent individual experiments.

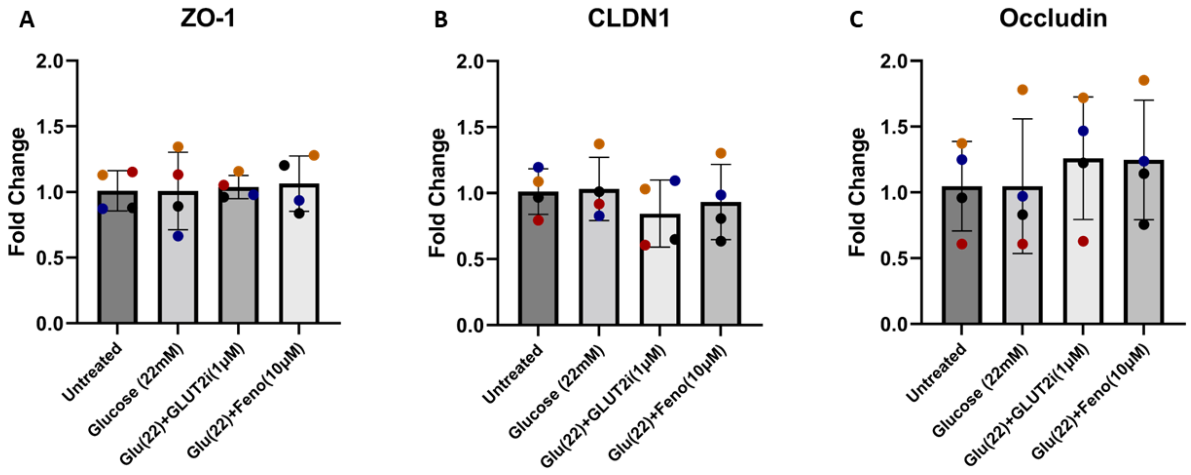

Figure 5. Glucose treatment with or without fenofibrate did not alter expression of tight junction mRNA. **A-C**) qRT-PCR analysis of mRNA expression of tight junction proteins: ZO-1, CLDN1, and Occludin. No significant treatment effect was observed as determined by one-way ANOVA (α=0.05). Data are presented as mean ± SD with each point representing mRNA expression normalized to GAPDH. Colors represent individual experiments.

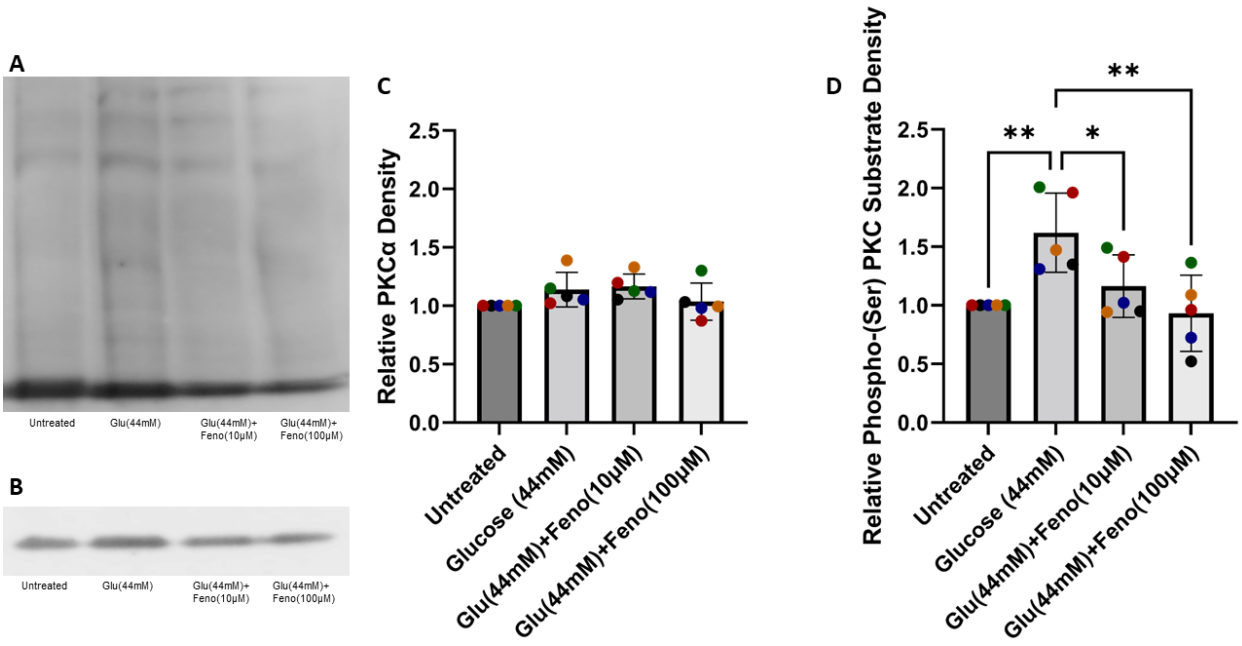

Figure 6. Glucose treatment increases PKCα activation. **A**) Representative western blot probed for phosphor-(Ser) PKC substrate antibody. **B**) Representative western blot probed for PKCα antibody. **C**) Densitometry analysis of PKCα. No significant effect of treatment was observed via one-way ANOVA (α=0.05). **D**) Densitometry analysis of phospho-(Ser) PKC substrate. Treatment induced a significant effect on phospho-(Ser) PKC substrate expression as determined by one-way ANOVA (α=0.05) (p=0.042). Holm-Šídák post hoc analysis determined that treatment with glucose (44mM) significantly increased phospho-(Ser) PKC substrate expression (p=0.0089) relative to untreated enteroids. Treatment with 44mM glucose fenofibrate (10μM or 100μM) significantly reduced phospho-(Ser) PKC substrate expression (p=0.0492 and p=0.0048, respectively). Data are presented as mean ± SD with each point representing protein expression normalized to GAPDH. Colors represent individual experiments.

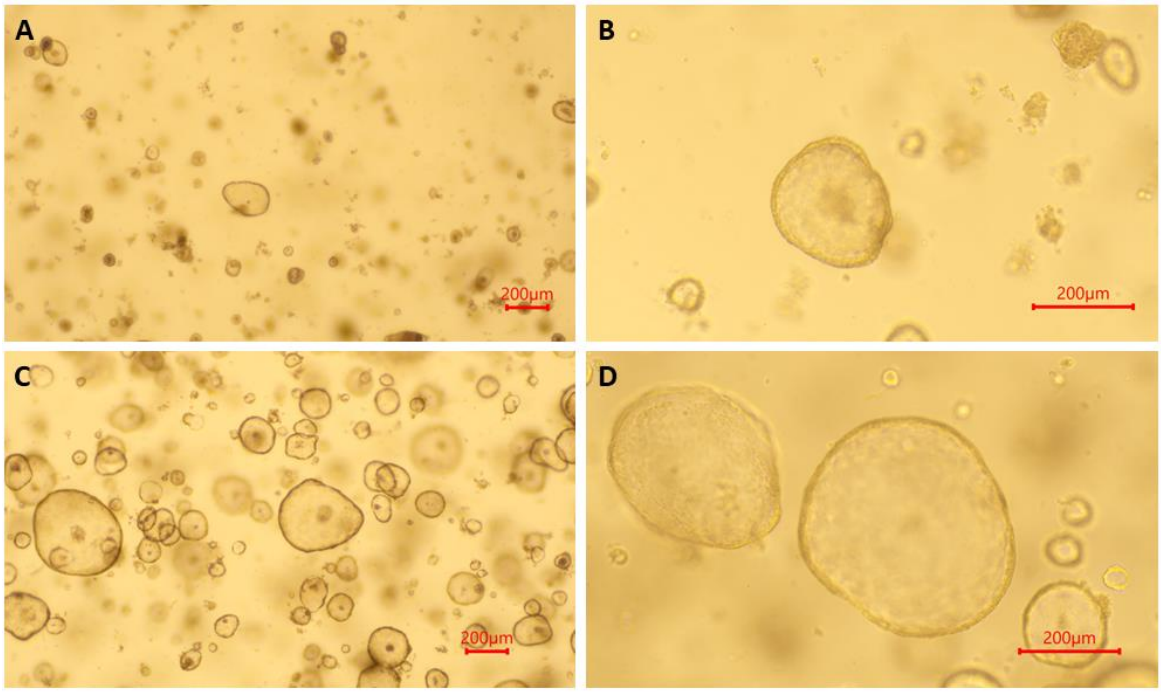

Figure S1. Feline intestinal organoids (enteroids). **A**) Brightfield image of enteroids 2 days post-passage taken with a 4x objective lens. **B**) Brightfield image of enteroids 2 days post-passage taken with a 10x objective lens. **C**) Brightfield image of enteroids 5 days post-passage taken with a 4x objective lens. **D**) Brightfield image of enteroids 5 days post-passage taken with a 10x objective lens. Scale bars denote 200µm. All images show enteroids in passage-19.

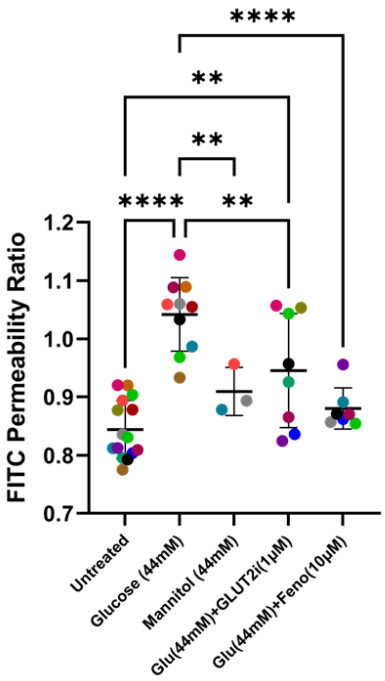

Figure S2. 44mM Glucose treatment increases feline enteroid barrier permeability measured by FITC Dextran permeability. Barrier permeability is not increased when treated with fenofibrate in addition to glucose. Luminal FITC intensity normalized to basolateral FITC intensity following 24h treatment with glucose, mannitol, or glucose with fenofibrate or GLUT2-selective inhibitor. One-way ANOVA ($\alpha=0.05$) with Holm-Šídák post hoc analysis determined that treatment with 44mM glucose with or without GLUT2-selective inhibitor significantly increased barrier permeability ($p<0.0001$ without inhibitor, $p=0.0034$ with inhibitor). Mannitol treatment significantly reduced enteroid permeability compared to matching concentration of glucose treatment ($p=0.0097$). Enteroids treated with glucose and 1μM GLUT2-selective inhibitor displayed significantly reduced barrier permeability compared to those treated with only glucose ($p=0.0097$). Enteroids treated with glucose and 10μM fenofibrate displayed significantly reduced permeability compared to those treated with only glucose ($p<0.0001$). Data are presented as mean ± SD with each point representing an experimental mean. Colors represent individual experiments.

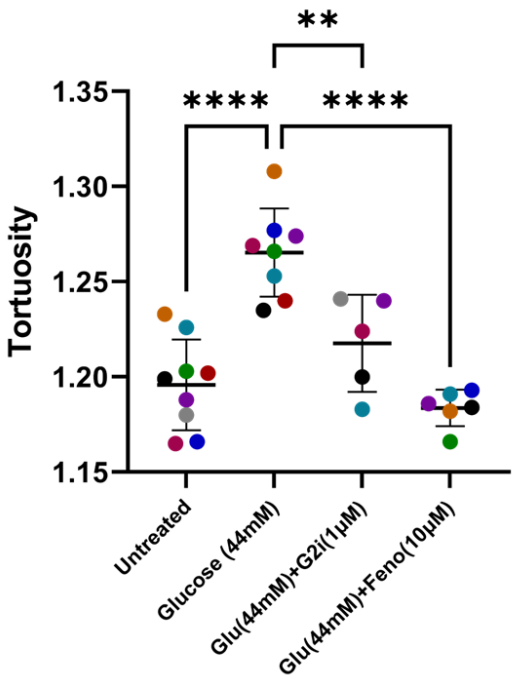

Figure S3. Glucose treatment increases tortuosity of tight junctions in feline enteroids, but not when treated in conjunction with fenofibrate or GLUT2-selective inhibitor. Quantification of ZO-1 tortuosity in experimental enteroids. Treatment with 44mM glucose significantly increased ZO-1 tortuosity ($p<0.0001$) as determined by one-way ANOVA ($\alpha=0.05$) and Holm-Šídák post hoc analysis. Enteroids treated with glucose and 1μM GLUT2-selective inhibitor displayed significantly reduced ZO-1 tortuosity compared to those treated with only glucose ($p=0.0024$). Enteroids treated with 10μM fenofibrate in addition to glucose displayed significantly reduced ZO-1 tortuosity compared to those treated with only glucose ($p<0.0001$). Data are presented as mean ± SD with each point representing an experimental mean. Colors represent individual experiments.

Table S1. Primers used for RT-qPCR

Gene	Forward Primer (5’-3’)	Reverse Primer (5’-3’)
ZO-1 (TJP1)	CAAGGTCTGCCGAGACAACA	TGCCAGGTTTTAGGATCACCG
Claudin-1 (CLDN1)	TGTCATTGGGGGTGTGACAT	AGCCAGTGAAGAGAGCCTGA
Occludin (OCLN)	CCGCGCTTGGTGTAACAGAT	TCGAACGTGCATGTCTCCAC
GAPDH	AAATTCCACGGCACAGTCAAG	TGATGGGCTTTCCATTGATGA

Acknowledgments

The authors would like to thank the soft tissue surgery service at the UC Davis William R. Pritchard Veterinary Medical Teaching Hospital for their help in obtaining intestinal tissue. We would also like to thank the Center for Companion Animal Health at UC Davis and EveryCat Health Foundation for funding this study.

References

1. Hospital, B.P., *State of Pet Health 2016 Report*, in *State of Pet Health Report*. 2016, Banfield Pet Hospital.
2. Lederer, R., et al., *Frequency of feline diabetes mellitus and breed predisposition in domestic cats in Australia.* Vet J, 2009. **179**(2): p. 254-8.
3. Kaufman, F.R., *Type 2 diabetes mellitus in children and youth: a new epidemic.* J Pediatr Endocrinol Metab, 2002. **15 Suppl 2**: p. 737-44.
4. Lutz, T.A., *Mammalian models of diabetes mellitus, with a focus on type 2 diabetes mellitus.* Nat Rev Endocrinol, 2023. **19**(6): p. 350-360.
5. Kol, A., et al., *Companion animals: Translational scientist's new best friends.* Sci Transl Med, 2015. **7**(308): p. 308ps21.
6. Meldgaard, T., et al., *Diabetic Enteropathy: From Molecule to Mechanism-Based Treatment.* J Diabetes Res, 2018. **2018**: p. 3827301.
7. Scott-Moncrieff, J.C., *Insulin resistance in cats.* Vet Clin North Am Small Anim Pract, 2010. **40**(2): p. 241-57.
8. Thaiss, C.A., et al., *Hyperglycemia drives intestinal barrier dysfunction and risk for enteric infection.* Science, 2018. **359**(6382): p. 1376-1383.
9. Barrett, K.E., *New ways of thinking about (and teaching about) intestinal epithelial function.* Adv Physiol Educ, 2008. **32**(1): p. 25-34.
10. Vancamelbeke, M. and S. Vermeire, *The intestinal barrier: a fundamental role in health and disease.* Expert Rev Gastroenterol Hepatol, 2017. **11**(9): p. 821-834.
11. Groschwitz, K.R. and S.P. Hogan, *Intestinal barrier function: molecular regulation and disease pathogenesis.* J Allergy Clin Immunol, 2009. **124**(1): p. 3-20; quiz 21-2.
12. Citi, S., et al., *Cingulin, a new peripheral component of tight junctions.* Nature, 1988. **333**(6170): p. 272-6.
13. Furuse, M., et al., *Claudin-1 and -2: novel integral membrane proteins localizing at tight junctions with no sequence similarity to occludin.* J Cell Biol, 1998. **141**(7): p. 1539-50.
14. Furuse, M., et al., *Occludin: a novel integral membrane protein localizing at tight junctions.* J Cell Biol, 1993. **123**(6 Pt 2): p. 1777-88.
15. Suzuki, T., *Regulation of the intestinal barrier by nutrients: The role of tight junctions.* Anim Sci J, 2020. **91**(1): p. e13357.
16. Kuitunen, M., et al., *Intestinal permeability to mannitol and lactulose in children with type 1 diabetes with the HLA-DQB1*02 allele.* Autoimmunity, 2002. **35**(5): p. 365-8.
17. Mooradian, A.D., et al., *Abnormal intestinal permeability to sugars in diabetes mellitus.* Diabetologia, 1986. **29**(4): p. 221-4.
18. Amar, J., et al., *Involvement of tissue bacteria in the onset of diabetes in humans: evidence for a concept.* Diabetologia, 2011. **54**(12): p. 3055-61.
19. Selby, A., et al., *Pathophysiology, Differential Diagnosis, and Treatment of Diabetic Diarrhea.* Dig Dis Sci, 2019. **64**(12): p. 3385-3393.
20. Damci, T., et al., *Increased intestinal permeability as a cause of fluctuating postprandial blood glucose levels in Type 1 diabetic patients.* Eur J Clin Invest, 2003. **33**(5): p. 397-401.

21. Francis, K.L., et al., *1357-P: Diabetic Hyperglycemia Impairs Intestinal Barrier Function in the Setting of Diet-Induced Obesity.* Diabetes, 2022. **71**(Supplement_1).
22. Do, M.H., et al., *High-Glucose or -Fructose Diet Cause Changes of the Gut Microbiota and Metabolic Disorders in Mice without Body Weight Change.* Nutrients, 2018. **10**(6).
23. Crakes, K.R., et al., *Fenofibrate promotes PPARalpha-targeted recovery of the intestinal epithelial barrier at the host-microbe interface in dogs with diabetes mellitus.* Sci Rep, 2021. **11**(1): p. 13454.
24. Bajwa, P.J., et al., *Fenofibrate inhibits intestinal Cl- secretion by blocking basolateral KCNQ1 K+ channels.* Am J Physiol Gastrointest Liver Physiol, 2007. **293**(6): p. G1288-99.
25. Braissant, O., et al., *Differential expression of peroxisome proliferator-activated receptors (PPARs): tissue distribution of PPAR-alpha, -beta, and -gamma in the adult rat.* Endocrinology, 1996. **137**(1): p. 354-66.
26. Bunger, M., et al., *Genome-wide analysis of PPARalpha activation in murine small intestine.* Physiol Genomics, 2007. **30**(2): p. 192-204.
27. Kersten, S., *Integrated physiology and systems biology of PPARalpha.* Mol Metab, 2014. **3**(4): p. 354-71.
28. Hu, Y., et al., *Pathogenic role of diabetes-induced PPAR-alpha down-regulation in microvascular dysfunction.* Proc Natl Acad Sci U S A, 2013. **110**(38): p. 15401-6.
29. Azuma, Y.T., et al., *PPARalpha contributes to colonic protection in mice with DSS-induced colitis.* Int Immunopharmacol, 2010. **10**(10): p. 1261-7.
30. Crakes, K.R., et al., *PPARalpha-targeted mitochondrial bioenergetics mediate repair of intestinal barriers at the host-microbe intersection during SIV infection.* Proc Natl Acad Sci U S A, 2019. **116**(49): p. 24819-24829.
31. de Vogel-van den Bosch, H.M., et al., *PPARalpha-mediated effects of dietary lipids on intestinal barrier gene expression.* BMC Genomics, 2008. **9**: p. 231.
32. Zachos, N.C., et al., *Human Enteroids/Colonoids and Intestinal Organoids Functionally Recapitulate Normal Intestinal Physiology and Pathophysiology.* J Biol Chem, 2016. **291**(8): p. 3759-66.
33. Crawford, C.K., et al., *Inflammatory cytokines directly disrupt the bovine intestinal epithelial barrier.* Sci Rep, 2022. **12**(1): p. 14578.
34. Miyoshi, H. and T.S. Stappenbeck, *In vitro expansion and genetic modification of gastrointestinal stem cells in spheroid culture.* Nat Protoc, 2013. **8**(12): p. 2471-82.
35. Powell, R.H. and M.S. Behnke, *WRN conditioned media is sufficient for in vitro propagation of intestinal organoids from large farm and small companion animals.* Biol Open, 2017. **6**(5): p. 698-705.
36. Schmidl, S., et al., *Identification of new GLUT2-selective inhibitors through in silico ligand screening and validation in eukaryotic expression systems.* Sci Rep, 2021. **11**(1): p. 13751.
37. Grosheva, I., et al., *High-Throughput Screen Identifies Host and Microbiota Regulators of Intestinal Barrier Function.* Gastroenterology, 2020. **159**(5): p. 1807-1823.

38. El-Remessy, A.B., et al., *High glucose-induced tyrosine nitration in endothelial cells: role of eNOS uncoupling and aldose reductase activation.* Invest Ophthalmol Vis Sci, 2003. **44**(7): p. 3135-43.
39. Young, T.K., S.C. Lee, and L.N. Tai, *Mannitol absorption and excretion in uremic patients regularly treated with gastrointestinal perfusion.* Nephron, 1980. **25**(3): p. 112-6.
40. Mullin, J.M., et al., *Increased tight junction permeability can result from protein kinase C activation/translocation and act as a tumor promotional event in epithelial cancers.* Ann N Y Acad Sci, 2000. **915**: p. 231-6.
41. Rosson, D., et al., *Protein kinase C-alpha activity modulates transepithelial permeability and cell junctions in the LLC-PK1 epithelial cell line.* J Biol Chem, 1997. **272**(23): p. 14950-3.
42. Ali, F.Y., et al., *Antiplatelet actions of statins and fibrates are mediated by PPARs.* Arterioscler Thromb Vasc Biol, 2009. **29**(5): p. 706-11.
43. Turner, J.R., et al., *Physiological regulation of epithelial tight junctions is associated with myosin light-chain phosphorylation.* Am J Physiol, 1997. **273**(4): p. C1378-85.
44. Thorens, B., *GLUT2, glucose sensing and glucose homeostasis.* Diabetologia, 2015. **58**(2): p. 221-32.
45. Forcheron, F., et al., *Mechanisms of the triglyceride- and cholesterol-lowering effect of fenofibrate in hyperlipidemic type 2 diabetic patients.* Diabetes, 2002. **51**(12): p. 3486-91.
46. Serisier, S., et al., *Fenofibrate lowers lipid parameters in obese dogs.* J Nutr, 2006. **136**(7 Suppl): p. 2037S-2040S.
47. Mazzon, E. and S. Cuzzocrea, *Absence of functional peroxisome proliferator-activated receptor-alpha enhanced ileum permeability during experimental colitis.* Shock, 2007. **28**(2): p. 192-201.
48. Mazzon, E. and S. Cuzzocrea, *Role of TNF-alpha in ileum tight junction alteration in mouse model of restraint stress.* Am J Physiol Gastrointest Liver Physiol, 2008. **294**(5): p. G1268-80.
49. Grabacka, M., et al., *The Role of PPAR Alpha in the Modulation of Innate Immunity.* Int J Mol Sci, 2021. **22**(19).
50. Wang, X., et al., *Fenofibrate Ameliorated Systemic and Retinal Inflammation and Modulated Gut Microbiota in High-Fat Diet-Induced Mice.* Front Cell Infect Microbiol, 2022. **12**: p. 839592.
51. Unsworth, A.J., G.D. Flora, and J.M. Gibbins, *Non-genomic effects of nuclear receptors: insights from the anucleate platelet.* Cardiovasc Res, 2018. **114**(5): p. 645-655.
52. Nakashima, S., *Protein kinase C alpha (PKC alpha): regulation and biological function.* J Biochem, 2002. **132**(5): p. 669-75.
53. Song, J.C., P.K. Rangachari, and J.B. Matthews, *Opposing effects of PKCalpha and PKCepsilon on basolateral membrane dynamics in intestinal epithelia.* Am J Physiol Cell Physiol, 2002. **283**(5): p. C1548-56.
54. Koya, D. and G.L. King, *Protein kinase C activation and the development of diabetic complications.* Diabetes, 1998. **47**(6): p. 859-66.

55. Lee, T.S., et al., *Activation of protein kinase C by elevation of glucose concentration: proposal for a mechanism in the development of diabetic vascular complications.* Proc Natl Acad Sci U S A, 1989. **86**(13): p. 5141-5.
56. Alt, N., et al., *Day-to-day variability of blood glucose concentration curves generated at home in cats with diabetes mellitus.* J Am Vet Med Assoc, 2007. **230**(7): p. 1011-7.